Copper Development Association
Copper Alliance

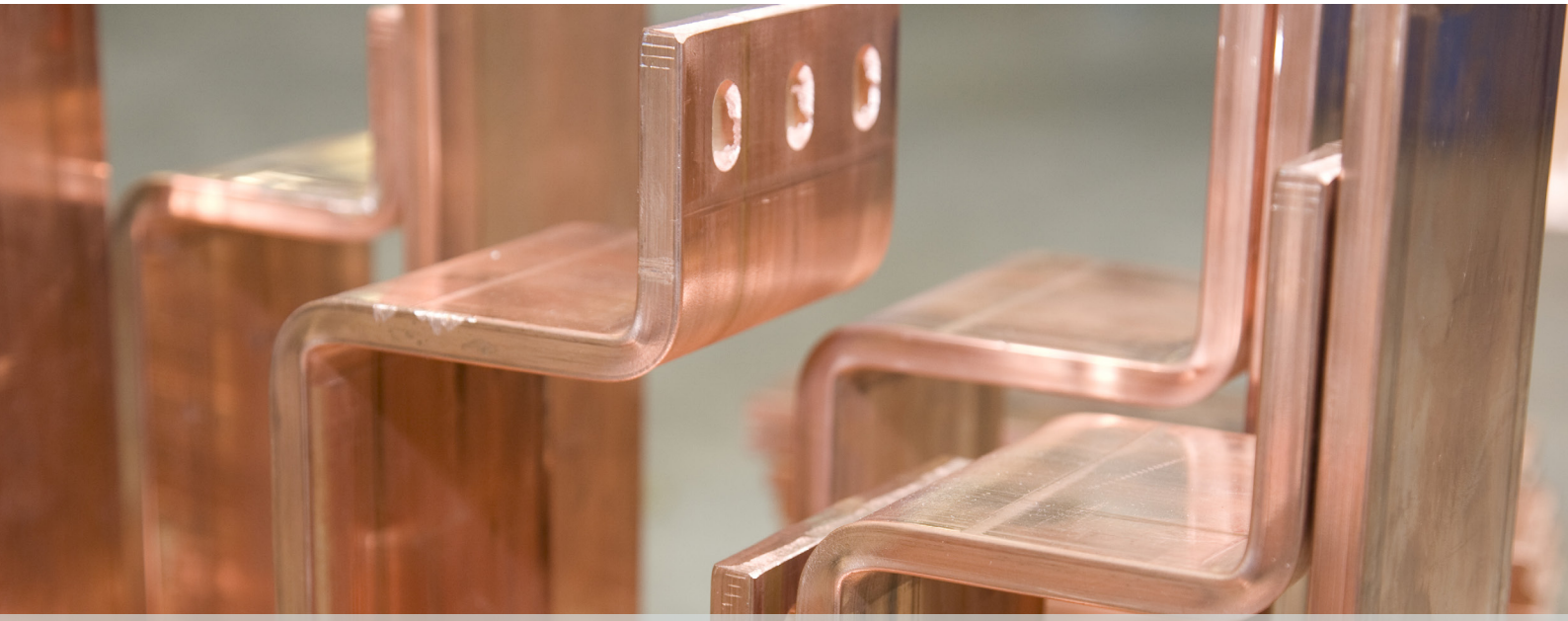

Copper for Busbars

Guidance for Design and Installation

Copper for Busbars

David Chapman & Professor Toby Norris

Copper Development Association Publication No 22

European Copper Institute Publication No Cu0201

Revised May 2014

First issued	1936
2nd-3rd revisions	1936-1950
4th revision	1950
5th revision	1952
6th-10th revisions	1954-1959
11th revision	1960
12th revision	1962
Reprinted	1964
Reprinted	1965
13th revision	1984
14th revision	1996

In this new edition the calculation of current-carrying capacity has been greatly simplified by the provision of exact formulae for some common busbar configurations and graphical methods for others. Other sections have been updated and modified to reflect current practice.

Cu **Copper Development Association**
Copper Alliance

Copper Development Association is a non-trading organisation that promotes and supports the use of copper based on its superior technical performance and its contribution to a higher quality of life. Its services, which include the provision of technical advice and information, are available to those interested in the utilisation of copper and copper alloys in all their aspects. The Association also provides a link between research and the user industries and is part of an international network of trade associations, the Copper Alliance™.

Cu **European Copper Institute**
Copper Alliance

Founded in 1996, ECI is a joint venture between the International Copper Association, Ltd (ICA), headquartered in New York, representing the majority of the world's leading mining companies, custom smelters and semi-fabricators, and the European copper industry. ECI is also part of the Copper Alliance, an international network of industry associations. Its shared mission is to work, with its members, to defend and grow markets for copper based on its superior technical performance and contributions to a higher quality of life.

David Chapman
David Chapman was the Electrical Programme Manager for Copper Development Association in the UK, where his main interests included power quality and energy efficiency. He was an author and Chief Editor of the LPQI Power Quality Application Guide.

Professor Toby Norris
Toby Norris is an electrical engineer who has worked in industry and at university. A central interest has been electromagnetic theory, especially in electric power plant and including superconductors.

Cover page picture acknowledgment:
High precision copper busbars
(Courtesy of H V Wooding Ltd)

Contents

1.0 Introduction 6
1.1 About this Guide 6
1.2 Materials for Busbars 6
1.2.1 Material Requirements 6
1.2.2 Material Choice 7
1.2.2.1 High Conductivity 7
1.2.2.1.1 Effect of Temperature on Conductivity 9
1.2.2.1.2 Effect of Cold Work on Conductivity 9
1.2.2.2 Mechanical Strength 9
1.2.2.2.1 Tensile Strength 10
1.2.2.2.2 Proof Strength 10
1.2.2.2.3 Hardness 11
1.2.2.2.4 Resistance to Softening 11
1.2.2.2.5 Creep Resistance 11
1.2.2.2.6 Fatigue Resistance 12
1.2.2.2.7 Bending and Forming 13
1.2.2.3 Connectivity 13
1.2.2.4 Maintenance 13
1.2.3 Types of High Conductivity Copper Available 14
1.2.3.1 Tough Pitch Copper, CW004A and CW005A (C101 and C102) 14
1.2.3.2 Oxygen-free High Conductivity Copper, CW008A (C103) 14
1.2.4 Available Forms 14

2.0 Current-Carrying Capacity of Busbars 15
2.1 Design Philosophy 15
2.2 Calculation of Maximum Current-Carrying Capacity 15
2.2.1 Methods of Heat Loss 15
2.2.1.1 Convection – Natural Air Cooling 16
2.2.1.2 Convection Heat Loss - Forced Air Cooling 17
2.2.1.3 Radiation 18
2.2.2 Heat Generated by a Conductor 21
2.2.2.1 Alternating Current Effects – the Factor S 22
2.2.2.1.1 Skin Effect and Skin Depth 24
2.2.2.1.2 Proximity Factor, S_p 27
2.3 Conclusion 27
2A Shape and Proximity Factors for Typical Configurations 28
2A.1 Skin and Proximity Factors for Common Busbar Shapes 28
2A.1.1 Single Solid Rods 28
2A.1.1.1 Shape Factor for Single Solid Rods 28
2A.1.1.2 Proximity Factor for Single Solid Rods 29
2A.1.2 Single Tubes 34
2A.1.2.1 Shape Factors for Single Tubes 34
2A.1.2.2 Proximity Factors for Tubes 37
2A.1.3 Single Rectangular Sections 42
2A.1.3.1 Shape Factor for Rectangular Bars 42
2A.1.3.2 Approximate Portmanteau Formula for Single Bars 45
2A.1.4 Parallel Bars 45
2A.1.4.1 Proximity Factor - Anti-parallel Currents 45
2A.1.4.2 Proximity Factor - Parallel Currents 47
2A.1.5 Three-phase Configurations 49
2A.1.5.1 Linear Plots 49
2A.1.5.2 Logarithmic Plots 53

3.0 Life Cycle Costing 56
3.1 Introduction 56
3.1.1 The Future Value of Money – Net Present Value 56
3.1.1.1 Monthly Payments 59
3.1.2 Loading 60
3.1.3 Lifetime 60
3.1.4 Sensitivity Analysis 60
3.2 Application to an Electrical Installation 60
3.2.1 Installation Design 61
3.2.2 Installation Costs 61
3.2.3 Recurring Costs 61
3.2.3.1 Maintenance Costs 61
3.2.3.2 Energy 61
3.2.4 End of Life Costs 68
3.3 Conclusion 68

4.0 Short-Circuit Effects 69
4.1 Introduction 69
4.2 Short-Circuit Heating of Bars 69
4.3 Electromagnetic Stresses 70
4.3.1 Estimating the Forces Between Parallel Sets of Bars 72
4.3.1.1 Round Bars 72
4.3.1.1.1 Triangular Array 73
4.3.1.1.2 In-Line Array 74
4.3.1.2 Bars of Rectangular Section 74
4.4 Mounting Arrangements 76
4.4.1 Maximum Permissible Stress 76
4.4.1.1 Moment of Inertia 77
4.4.2 Deflection 78
4.4.3 Natural Frequency 78

5.0 Busbar Profiles 79
5.1 Introduction 79
5.2 Reasons for Using Profiles 79
5.2.1 Skin Effect Reduction 79
5.2.2 Weight and Cost Saving 79
5.2.3 Integrated Fixings and Mountings 80
5.2.4 Retention of Intellectual Integrity 80
5.3 Economics of Profiles 80
5.4 Practical Profiles 80
5.4.1 Manufacturing Process 80
5.4.1.1 EN 13605 80
5.4.1.1.1 Straightness, Flatness and Twist 82
5.4.2 Design for Manufacturing 84
5.4.2.1 Wall Thickness 84
5.4.2.2 Avoid Sharp Corners 84
5.4.2.3 Symmetry 84
5.4.2.4 Be Compact 85
5.4.2.5 Avoid Deep Narrow Channels 85
5.4.2.6 Avoid Hollow Chambers 85
5.4.3 Functional Design 85

Contents

5.5 Electrical Design Considerations ... 85
5.5.1 Skin Effect ... 85
5.5.2 Thermal Dissipation ... 86
5.5.3 Jointing and Mounting ... 87
5.5.4 Short Circuit Performance - Moment of Inertia ... 88
5.6 Calculation of Moment of Inertia of Complex Sections ... 88

6.0 Jointing of Copper Busbars ... 90
6.1 Introduction ... 90
6.2 Busbar Jointing Methods ... 90
6.3 Joint Resistance ... 91
6.3.1 Streamline Effect ... 92
6.3.2 Contact Resistance ... 94
6.3.2.1 Condition of Contact Surfaces ... 94
6.3.2.2 Effect of Pressure on Contact Resistance ... 94
6.4 Bolting Arrangements ... 98
6.4.1 Joint Efficiency ... 99
6.5 Clamped Joints ... 101
6.6 Degradation Mechanisms ... 101
6.6.1 Oxidation ... 101
6.6.2 Corrosion ... 102
6.6.3 Fretting ... 102
6.6.4 Creep and Stress Relaxation ... 102
6.6.5 Thermal Expansion ... 102
6.7 Conclusion ... 102

Annex: Coatings ... 103
A1.0 Introduction ... 103
A2.0 Reasons for Coating ... 103
A2.1 Coating to Provide Electrical Insulation ... 103
A2.2 Coating to Inhibit Corrosion ... 103
A2.2.1 Metal Coatings ... 103
A2.2.2 Non-Metallic Coatings ... 103
A2.3 Coating to Increase Current Rating ... 103
A2.4 Coating for Cosmetic Purposes ... 104
A2.5 Coating to Improve Joint Performance ... 104
A3.0 Methods of Coating ... 104
A3.1 Factory Application Methods ... 104
A3.1.1 Extrusion ... 104
A3.1.2 Powder Coating ... 105
A3.2 On-Site Application Methods ... 105
A3.2.1 Heat-Shrinkable Sleeve ... 105
A3.2.2 Painting ... 105
A3.2.2.1 Alkyd Paints ... 105
A3.2.2.2 Two-Part Epoxy ... 105
A4.0 Inspection and Maintenance ... 105

Tables & Figures

Tables

Table 1 Properties of Typical Grades of Copper and Aluminium 7
Table 2 Properties of 100% IACS Copper ... 7
Table 3 Implied Properties of 100% IACS Copper ... 8
Table 4 Comparison of Creep Properties of HC Copper and Aluminium ... 12
Table 5 Comparison of Fatigue Properties of HC Copper and Aluminium ... 12
Table 6 Minimum Bend Radius of HC Copper ... 13
Table 7 Self-extinguishing Arcs in Copper and Aluminium Busbars ... 13
Table 8 Discount Factors for Various Discount Rates ... 57
Table 9 Maximum Working Current for a Range of Busbar Sizes ... 62
Table 10 Resistance and Power Loss at 500 Amps ... 62
Table 11 Energy Cost Per Metre for Various Widths of Copper Bars at 500 A Load ... 63
Table 12 Present Value (€) per Metre of Bar ... 67
Table 13 Power Factor and Peak Current ... 71
Table 14 Tolerances for Dimensions *b* and *h* for b_{max} or h_{max} <20:1 ... 82
Table 15 Tolerances for Dimensions *b* and *h* for b_{max} or $h_{max} \geq 20:1$ ... 82
Table 16 Thickness Tolerances ... 82
Table 17 Coefficient for Twist Tolerance ... 84
Table 18 Maximum Sizes of Profile According to Two Manufacturers ... 84
Table 19 Nut Factors for Different States of Lubrication ... 96
Table 20 Proof Strength and Coefficient of Thermal Expansion for Copper and Typical Bolt Materials ... 96
Table 21 Typical Thread Characteristics ... 97
Table 22 Typical Busbar Bolting Arrangements ... 99

Figures

Figure 1 Effect of small concentrations of impurities on the resistivity of copper ... 8
Figure 2 Effect of cold rolling on mechanical properties and hardness of high conductivity copper strips ... 10
Figure 3 Typical creep properties of commercially pure copper and aluminium ... 12
Figure 4 Heat dissipation by convection from a vertical surface for various temperature rises above ambient ... 16
Figure 5 Convection loss from typical bar sections ... 17
Figure 6 Heat dissipation by radiation from a surface assuming relative emissivity of 0.5 and surroundings at 30°C ... 18
Figure 7 Radiation loss from typical bar sections ... 19
Figure 8 Convection and radiation losses at various temperatures ... 20
Figure 9 Total heat losses for a single bar of various heights against temperature rise ... 20
Figure 10 Total heat losses for each bar of a parallel pair of various heights against temperature rise ... 21

Figure 11 Parameter p versus cross-sectional area in mm^2 for typical copper at 80°C 23
Figure 12 Resistivity of typical HC copper (101.5% IACS) as a function of temperature 25
Figure 13 Skin depth of typical HC copper (101.5% IACS) at 50 Hz, 60 Hz, 400 Hz as a function of temperature 25
Figure 14 dc resistance of typical HC Copper (101.5% IACS) versus area at 20°C and 80°C 26
Figure 15 Plots of shape factor versus γ 29
Figure 16 Factor A for round bars as a function of γ 30
Figure 17 Proximity factor, Sp, for single phase systems with parallel round bars 31
Figure 18 Mean proximity factors for flat arrangement of round bars carrying balanced three phase currents 32
Figure 19 Mean proximity factors for delta arrangement of round bars carrying balanced three phase currents 33
Figure 20 Shape factor for tubes 35
Figure 21 Shape factor for tubes with low values of shape factor 35
Figure 22 Shape factor for tubes 36
Figure 23 The shape factor computed from the Bessel function formula using $\sqrt{(f/r_{dc})}$ as the frequency parameter 36
Figure 24 Shape factor as a function of the ratio, $g=\frac{\text{wall thickness } t}{\text{skin depth } \delta}$ 37
Figure 25 Factor A versus $\beta = t/a$ for values of $g = t/\delta$ 38
Figure 26 Proximity factor for single phase tubes as function of the factor A for values of $\eta=s/2a=s/d$ 38
Figure 27 Proximity factor for single phase tubes 39
Figure 28 Factor A for proximity loss factor as a function of $g = t/\delta$ for various values of $\beta = t/a$ 40
Figure 29 Proximity factor, S_p, for round bars at various spacings designated by η 41
Figure 30 R_{ac}/R_{dc} as a function of the parameter $\sqrt{f}/R_{dc}$ 43
Figure 31 R_{ac}/R_{dc} as a function of the parameter $\sqrt{f}/R_{dc}$ 43
Figure 32 Shape factor, R_{ac}/R_{dc}, as a function of the parameter $\sqrt{f}/R_{dc}$ 44
Figure 33 Shape factor versus $2b/\delta$ for various values of b/a . 44
Figure 34 Plots of the shape ratio $\frac{R_{ac}}{R_{dc}}$ versus the ratio $\frac{s}{a}$ for various values of $\sqrt{\frac{f}{R_{dc}}}$ for anti-parallel currents 47
Figure 35 Shape factor $S = \frac{R_{ac}}{R_{dc}}$ as a function of the separation s for various values of $\sqrt{\frac{f}{R_{dc}}}$ with R_{dc} in μΩ/m and f in Hz 49
Figure 36 Linear plots of R_{ac}/R_{dc} versus p where $p \approx 1{\cdot}5853\sqrt{\frac{f}{R_{dc}}}$ with R_{dc} in μΩ/m and f in Hz 52
Figure 37 Quasi logarithmic plots of R_{ac}/R_{dc} versus p where $p \approx 1{\cdot}5853\sqrt{\frac{f}{R_{dc}}}$ with R_{dc} in μΩ/m and f in Hz 55
Figure 38 Power loss versus width for 6.3 mm thick copper bars 63
Figure 39 Cost of energy loss per metre versus width for 6.3 mm thick copper bars 64
Figure 40 Total cost per metre versus bar width for 5000 hours operation at 500 A 64
Figure 41 Total cost per metre of bar versus bar width for a range of operating times 65
Figure 42 Total cost per metre against current density for a range of operation times 66
Figure 43 Estimated working temperature versus width of bar (mm) for 500 A load 66
Figure 44 Cost per metre (€) against bar width for a) 20 000 hours operation without discount and b) 2000 hours per year for 10 years at 5% discount 67
Figure 45 Short-circuit current waveform 71
Figure 46 Three phase system with spacings D (mm), (a) triangular array (b) inline array 73
Figure 47 Factor K for calculating the force between two bars of rectangular section 75
Figure 48 Form factor K_b. (a) low values of a/b (long sides facing each other) (b) high values of a/b 75
Figure 49 Typical copper profiles 79
Figure 50 A non-typical profile indicating the dimensions used in the standard 81
Figure 51 Measurement of straightness 83
Figure 52 Measurement of flatness 83
Figure 53 Measurement of twist 83
Figure 54 Profile cross-section showing mounting lugs and slots for bolt-head 85
Figure 55 R_{ac}/R_{dc} as a function of the parameter $\sqrt{f}/R_{dc}$ with f in Hz and R_{dc} in μΩ/m 86
Figure 56 Thermal image of two profiles under load 87
Figure 57 Hole-free joints 87
Figure 58 Calculation of moment of inertia of a complex shape 88
Figure 59 Parameters used in the calculation of moment of inertia of each element 89
Figure 60 A typical bolted joint 90
Figure 61 A simple clamped joint 90
Figure 62 A riveted joint 91
Figure 63 A soldered joint 91
Figure 64 A welded joint 91
Figure 65 An overlapped joint 91
Figure 66 Streamline effect in overlapped joints 92
Figure 67 Bolt placement in overlapped joints 93
Figure 68 Overlap joint between bars with angled ends 93
Figure 69 The effect of pressure on the contact resistance of a joint 95
Figure 70 Possible bolting techniques for copper busbars 98
Figure 71 Joint with a longitudinal slot 98

Disclaimer

1.0 Introduction

David Chapman

1.1. About this Guide

Busbars are used within electrical installations for distributing power from a supply point to a number of output circuits. They may be used in a variety of configurations ranging from vertical risers, carrying current to each floor of a multi-storey building, to bars used entirely within a distribution panel or within an industrial process.

The issues that need to be addressed in the design of busbar systems are:

- Temperature rise due to energy losses
- Energy efficiency and lifetime cost
- Short-circuit current stresses and protection
- Jointing methods and performance
- Maintenance.

This book provides the information needed to design efficient, economic and reliable busbar systems.

In any electrical circuit some electrical energy is lost as heat which, if not kept within safe limits, may impair the long term performance or the safety of the system. For busbar systems, the maximum working current is determined primarily by the maximum tolerable working temperature, which is, in turn, determined by considerations such as safety, the retention of mechanical properties of the conductor, compatibility with mounting structures and cable connections. '2.0 Current-Carrying Capacity of Busbars' discusses how to estimate the working current and temperature.

A higher working temperature means that energy is being wasted. Designing for lower energy loss requires the use of more conductor material but results in more reliable operation due to the lower working temperature and, because the cost of lifetime energy losses is far greater than the cost of first installation, lower lifetime costs. The process of assessing the life cycle cost of a busbar system is described in '3.0 Life Cycle Costing'.

Because of the large currents involved, short circuit protection of busbar systems needs careful consideration. The important issues are the temperature rise of the busbar during the event and the magnitude of the forces generated by the high current, which may cause deformation of the bars and the failure of mountings. The design of the mounting system is an important factor and one that is becoming more important with the increase in harmonic currents, which can trigger mechanical resonances in the busbar. '4.0 Short-Circuit Effects' discusses these issues.

It is usually necessary to joint busbars on site during installation and this is most easily accomplished by bolting bars together or by welding. For long and reliable service, joints need to be carefully made with controlled torque applied to correctly sized bolts. A properly designed and implemented joint can have a resistance lower than that of the same length of plain bar. The design of efficient joints is discussed in '6.0 Jointing'.

The remainder of this Introduction presents reference material giving mechanical and electrical properties of copper that are required for design purposes.

1.2 Materials for Busbars

1.2.1 Material Requirements

To achieve a long and reliable service life at the lowest lifetime cost, the conductor material needs the following properties:

- Low electrical and thermal resistance
- High mechanical strength in tension, compression and shear
- High resistance to fatigue failure
- Low electrical resistance of surface films
- Ease of fabrication
- High resistance to corrosion
- Competitive first cost and high eventual recovery value.

This combination of properties is best met by copper. Aluminium is the main alternative material, but a comparison of the properties of the two metals shows that, in nearly all respects, copper is the superior busbar material.

1.2.2 Material Choice

Busbars are generally made from either copper or aluminium. For a complete list of mechanical properties and compositions of copper used for busbars, see BS EN 13601: 2013 Copper rod, bar and wire for electrical purposes. Table 1 below gives a comparison of some electrical and mechanical properties. It can be seen that for conductivity and strength, high conductivity (HC) copper is far superior to aluminium. The only disadvantage of copper is its higher density, which results in higher weight. The greater hardness of copper compared with aluminium gives it better resistance to mechanical damage, both during erection and in service. Copper bars are also less likely to develop problems in clamped joints due to cold metal flow under the prolonged application of a high contact pressure. The higher modulus of elasticity of copper gives it greater beam stiffness compared with an aluminium conductor of the same dimensions. The temperature variations encountered under service conditions require a certain amount of flexibility to be allowed for in the design. The lower coefficient of linear expansion of copper reduces the degree of flexibility required.

Table 1 – Properties of Typical Grades of Copper and Aluminium

Property (at 20°C)	Copper (C101)	Aluminium (1350)	Units
Electrical conductivity (annealed)	101	61	% IACS
Electrical resistance (annealed)	17.2	28.3	nΩ mm
Temperature coefficient of resistivity	0.0039	0.004	per °K
Thermal conductivity	397	230	W/m°K
Specific heat	385	900	J/kg °K
Coefficient of expansion	17×10^{-6}	23×10^{-6}	per °K
Tensile strength (annealed)	200-250	50-60	N/mm^2
Tensile strength (half hard)	260-300	85-100	N/mm^2
0.2% proof strength (annealed)	50-55	20-30	N/mm^2
0.2% proof strength (half hard))	170-200	60-65	N/mm^2
Elastic modulus	116-130	70	kN/mm^2
Density	8910	2700	kg/m^2
Melting point	1083	660	°C

1.2.2.1 High Conductivity

The electrical properties of HC copper were standardised in 1913 by the International Electrotechnical Commission, which defined the International Annealed Copper Standard (IACS) in terms of the following properties at 20°C:

Table 2 – Properties of 100% IACS Copper

Volume conductivity, σ_v	58 MS/m
Density, d	8890 kg/m^3
Temperature coefficient of resistance, α	0.00393/°C

It follows from the first two of these values that:

Table 3 – Implied Properties of 100% IACS Copper

Volume resistivity, ρ_v (= $1/\sigma_v$)	1.7241 mΩcm
Mass conductivity, σ_m (= σ_v / d)	6524 Sm²/kg
Mass resistivity, ρ_m (= $1/\sigma_m$)	153.28 μΩkg/m²

These values correspond to 100% IACS. Since that time, processing technology has improved to the point where routine day-to-day-production HC copper can reach a conductivity of 102% IACS or even higher. It has become normal practice to express the conductivity of all electrical alloys, including aluminium, in terms of IACS.

Aluminium has a lower conductivity than copper (61% IACS), so an equivalent resistance conductor would have a cross-sectional area which is a factor of 1.6 times greater than one made from copper. Taking into account the difference in density, the aluminium conductor would have half the weight of copper. Copper will therefore allow a more compact installation and, in many systems, space considerations are of greater importance than weight. Greater weight may make installation slightly more difficult but, since the electromagnetic stresses set up in the bar are usually more severe than the stress due to its weight, the mounting design is largely unaffected.

Although busbar systems should normally be designed for lowest lifetime cost – which means a lower working temperature to reduce waste energy costs – the ability of copper to maintain its mechanical properties at higher temperatures provides extra capacity and safety during short circuit conditions. Copper also allows the use of higher peak operating temperatures in special circumstances.

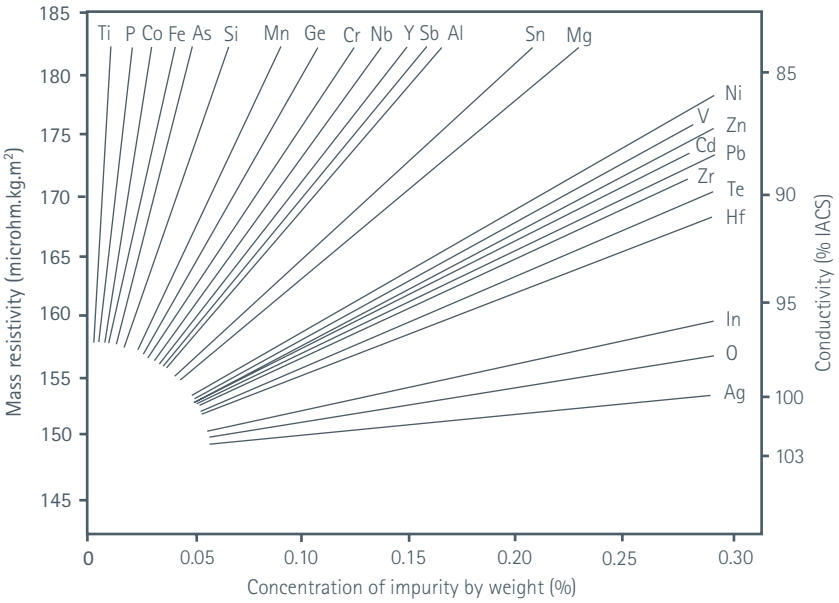

Figure 1 – Effect of small concentrations of impurities on the resistivity of copper

The degree to which the electrical conductivity is affected by an impurity depends largely on the element present, as illustrated in Figure 1. For example, the presence of only 0.04% phosphorus reduces the conductivity of HC copper to around 80% IACS. Normally, the purest copper is used for bulk conductors. In particular, oxygen-free copper is usually specified, not only for its high conductivity but also because it can be welded without the risk of hydrogen embrittlement.

When enhanced mechanical properties - such as increased strength or wear resistance - are required, a silver-bearing (up to 0.12%) copper can be used at the expense of a small increase in resistivity. Many other electrical alloys are available, but they are intended for special purposes, such as contacts or terminals, and are not used as bulk conductors.

1.2.2.1.1 Effect of Temperature on Conductivity

Conductivity varies with temperature so it is important that the correct value is used for the actual working temperature. The resistance of a copper conductor at temperatures up to 200°C can be calculated from:

$$R = R_{20}(1+\alpha_{20}\Delta T)$$

where:

R_{20}	is the conductor resistance at a temperature of 20°C, in Ω
α_{20}	is the temperature coefficient of resistance at 20°C, per K. α = 0.0039 for copper
$\Delta T = T_k - 20$	is the temperature difference, in degrees K
T_k	is the final temperature, in K.

Note that α is temperature dependent; the value given will yield sufficiently accurate results up to 200°C. An alternative equation, which gives sufficiently accurate results for engineering purposes over a wide temperature range, is:

$$R = R_{20}\left(\frac{T}{T_{20}}\right)^{1.16} = R_{20}\left(\frac{T}{293}\right)^{1.16}$$

where:

R	is the resistance at temperature T
R_{20}	is the resistance at 20°C (293°K)
T	is the temperature in °K, i.e. temperature in °C + 273.

1.2.2.1.2 Effect of Cold Work on Conductivity

The conductivity of copper is decreased by cold working and may be 2 to 3% less in the hard drawn condition than when annealed. Thus standards for hard drawn HC copper products should stipulate a minimum conductivity requirement of 97% IACS compared with 100% IACS for annealed products.

An approximate relationship between tensile strength of cold worked copper and its increase in electrical resistivity is:

$$P = F/160$$

where:

P	is % increase in electrical resistivity of cold worked copper over its resistivity when annealed
F	is tensile strength, N/mm².

1.2.2.2 Mechanical Strength

The mechanical strength of the busbar material is important to ensure that the material is not deformed during transport and assembly, does not sag over an extended working life at maximum temperature, does not creep under pressure leading to loosened joints and does not permanently distort under short circuit loads.

The mechanical properties are influenced by the production processes employed. Most busbar materials will have been extruded and drawn resulting, typically, in a 'half-hard' material. The effect on the mechanical properties of cold work by rolling (to reduce the thickness) is shown in Figure 2. Cold working of the material has the effect of raising the tensile strength, proof strength and hardness, but reducing its elongation.

1.2.2.2.1 Tensile Strength

In the 'as-cast' condition, HC copper has a tensile strength of 150-170 N/mm². The changes in structure brought about by hot working raise the tensile strength to the order of 200-220 N/mm².

The maximum tensile strength obtainable in practice depends on the shape and cross-sectional area of the conductor. The larger the cross-sectional area of a conductor the lower its tensile strength, since the amount of cold work that can be applied is limited by the reduction in area which can be achieved.

For the usual sizes of busbar conductors in the hard-condition, tensile strengths from 250 N/mm² up to 340 N/mm² can be obtained depending on the cross-sectional area.

1.2.2.2.2 Proof Strength

The 'proof strength' is the stress required to produce a defined amount of permanent deformation in the metal and is a valuable guide to its mechanical properties. Proof strength is defined as the stress at which a non-proportional elongation equal to a specified percentage (usually 0.2%) of the original gauge length occurs.

As with the tensile strength, the proof strength varies with the amount of cold work put into the material (see Figure 2).

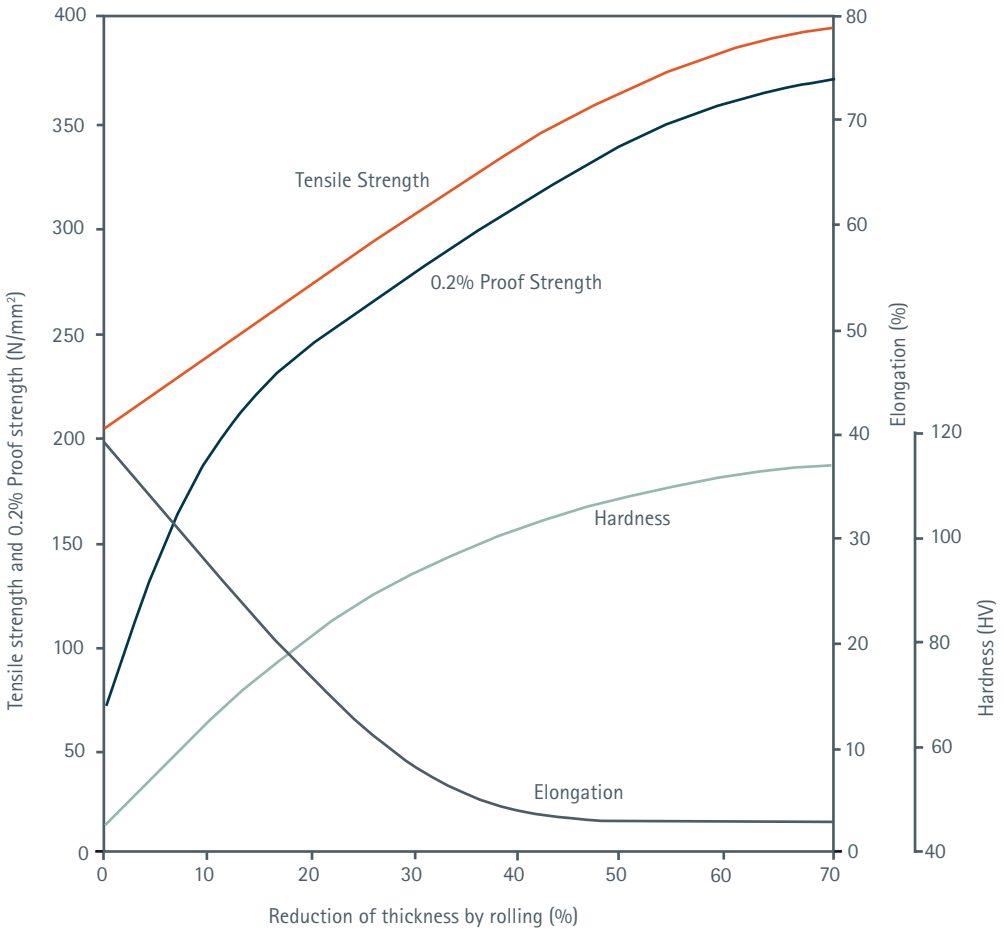

Figure 2 – Effect of cold rolling on mechanical properties and hardness of high conductivity copper strips

1.2.2.2.3 Hardness

Standards applicable to busbar conductors do not specify hardness measurement as part of the testing requirements. It can however be more quickly and easily carried out than a tensile test and is therefore convenient as a guide to the strength of a conductor. The results have to be used with discretion for two reasons:

- Unlike ferrous materials, the relationship between hardness and tensile strength is not constant (see Figure 2).
- A hardness test is usually only a measurement of the outer skin of the material tested. If the conductor is of large cross-sectional area and has received a minimum amount of cold work, the skin will be harder than the underlying metal. Consequently, variations in hardness may be obtained dependent on where the measurement is made in relation to its cross-section.

As a guide, typical hardness figures of the temper range of conductors supplied are:

Annealed	(O)	60 HV max
Half-hard	(½H)	70-95 HV
Hard	(H)	90 HV min.

1.2.2.2.4 Resistance to Softening

It is well known that the exposure of cold worked copper to elevated temperatures results in softening and mechanical properties typical of those of annealed material. Softening is time and temperature dependent and it is difficult to estimate precisely the time at which it starts and finishes. It is usual therefore to consider the time to 'half-softening', i.e. the time taken for the hardness to fall by 50% of the original increase in hardness caused by cold reduction.

In the case of HC copper, this softening occurs at temperatures above 150°C. It has been established experimentally that such copper would operate successfully at a temperature of 105°C for periods of 20-25 years, and that it could withstand short-circuit conditions as high as 250°C for a few seconds without any adverse effect.

If hard drawn conductors are required to retain strength under operating conditions higher than normal, the addition of small amounts of silver at the melting and casting stage produces alloys with improved resistance to softening. The addition of 0.06% silver raises the softening temperature by approximately 100°C without any significant effect on its conductivity, at the same time appreciably increasing its creep resistance.

1.2.2.2.5 Creep Resistance

Creep, another time and temperature dependent property, is the non-recoverable plastic deformation of a metal under prolonged stress. The ability of a metal to resist creep is of prime importance to design engineers.

From published creep data, it can be seen that high conductivity aluminium exhibits evidence of significant creep at ambient temperature if heavily stressed. At the same stress, a similar rate of creep is only shown by high conductivity copper at a temperature of 150°C, which is well above the usual operating temperature of busbars.

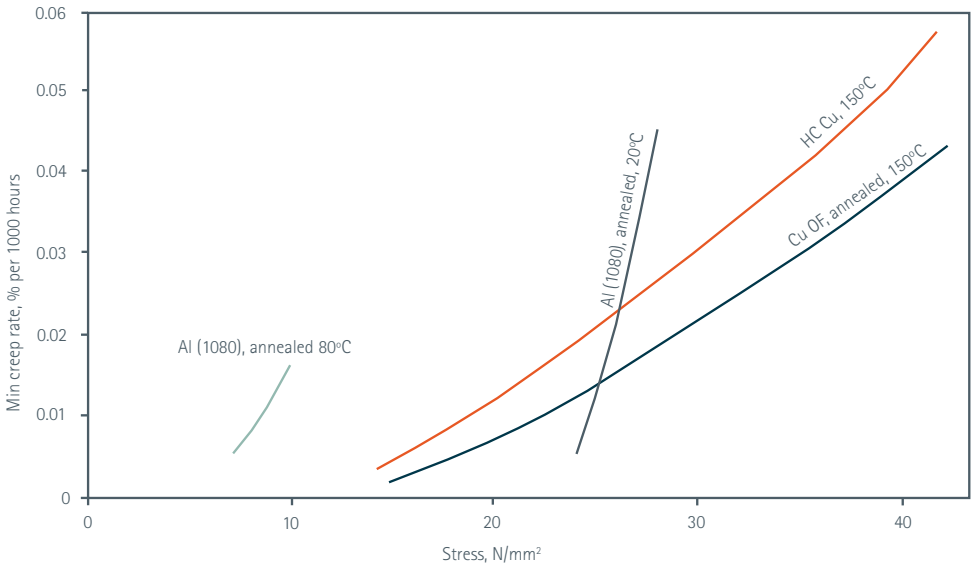

Figure 3 – Typical creep properties of commercially pure copper and aluminium

Table 4 – Comparison of Creep Properties of High Conductivity Copper and Aluminium

Material	Testing Temp (°C)	Min Creep Rate (% per 1000h)	Stress (N/mm²)
Al (1080) annealed	20	0.022	26 *
HC Cu annealed	150	0.022	26 *
Cu-0.086% Ag 50% c.w.	130	0.004	138
Cu-0.086% Ag 50% c.w.	225	0.029	96.5
			* Interpolated from Figure 3

The creep resistance of oxygen-free HC copper is better than that of tough pitch HC copper. This is due to the very small amounts of impurities which remain in solid solution in oxygen-free copper, but which are absorbed in the oxide particles in tough pitch copper. Some typical observations are shown in Figure 3. Tough pitch copper creeps relatively rapidly under low stress at 220°C. The addition of silver to both oxygen-free and tough pitch coppers results in a significant increase in creep resistance.

1.2.2.2.6 Fatigue Resistance

Fatigue is the mechanism leading to fracture under repeated or fluctuating stresses. Fatigue fractures are progressive, beginning as minute cracks which grow under the action of the stress. As the crack propagates, the load bearing area is reduced and failure occurs by ductile fracture before the crack develops across the full area.

Table 5 – Comparison of Fatigue Properties of High Conductivity Copper and Aluminium

Material		Fatigue Strength (N/mm²)	No of Cycles x 10^6
HC Aluminium	annealed	20	50
	half-hard (H8)	45	50
HC Copper	annealed	62	300
	half-hard	115	300

Conditions for such failures can be set up in a busbar system rigidly clamped for support and then subjected to vibrating conditions. Where higher stresses or working temperatures are to be allowed for, copper containing small amounts of silver (about 0.1%) is used. The creep resistance and softening resistance of copper-silver alloys increase with increasing silver content.

In the conditions in which high conductivity aluminium and copper are used, either annealed (or as-welded) or half-hard, the fatigue strength of copper is approximately double that of aluminium. This gives a useful reserve of strength against failure initiated by mechanical or thermal cycling.

1.2.2.2.7 Bending and Forming

The high conductivity coppers are ductile and, in the correct temper, will withstand severe bending and forming operations. As a general guide to bending, copper in the half-hard or hard temper will bend satisfactorily round formers of the following radii:

Table 6 – Minimum Bend Radius of High Conductivity Copper

Thickness (t)	Minimum Bend Radius
Up to 10 mm	1 t
11-25 mm	1.5 t
26-50 mm	2 t

Material of thicknesses greater than 50 mm is not normally bent; however, it is possible to do so by localised annealing prior to bending.

1.2.2.3 Connectivity

The surface of copper naturally oxidises, forming a thin hard layer on the surface which normally prevents further oxidation. This oxide film is conductive (under busbar conditions where it is sandwiched between two copper electrodes) so it does not affect the quality of bolted or clamped joints. On the other hand, exposed aluminium surfaces rapidly form a hard insulating film of aluminium oxide, which makes jointing very difficult and can lead to long term reliability problems. Terminals, switch contacts and similar parts are nearly always produced from copper or a copper alloy. The use of copper for the busbars to which these parts are connected therefore avoids contacts between dissimilar metals and the inherent jointing and corrosion problems associated with them.

1.2.2.4 Maintenance

The higher melting point and thermal conductivity of copper reduce the possibility of damage resulting from hot spots or accidental flashovers in service. If arcing occurs, copper busbars are less likely to support the arc than aluminium. Table 7 shows that copper can self-extinguish arcs across smaller separations, and at higher busbar currents. This self-extinguishing behaviour is related to the much larger heat input required to vaporise copper than aluminium.

Table 7 – Self-extinguishing Arcs in Copper and Aluminium Busbars

	Copper	Aluminium
Minimum busbar spacing, mm	50	100
Maximum current per busbar, A	4500	3220

Copper liberates considerably less heat during oxidation than aluminium and is therefore much less likely to sustain combustion in the case of accidental ignition by an arc. The large amounts of heat liberated by the oxidation of aluminium in this event are sufficient to vaporise more metal than was originally oxidised. This vaporised aluminium can itself rapidly oxidise, thus sustaining the reaction. The excess heat generated in this way heats nearby materials, including the busbar itself, the air and any supporting fixtures. As the busbar and air temperatures rise, the rates of the vaporisation and oxidation increase, so accelerating the whole process. As the air temperature is increased, the air expands and propels hot oxide particles. The busbar may reach its melting point, further increasing the rate of oxidation and providing hot liquid to be propelled, while other materials, such as wood panels, may be raised to their ignition temperatures. These dangers are avoided by the use of copper busbars.

Finally, copper is an economical conductor material. It gives long and reliable service at minimum maintenance costs and, when an installation is eventually replaced, the copper will have a high recovery value. Because of its many advantages, copper is still used worldwide as an electrical conductor material despite attempts at substitution.

1.2.3 Types of High Conductivity Copper Available

1.2.3.1 Tough Pitch Copper, CW004A and CW005A (C101 and C102)

Coppers of this type, produced by fire-refining or remelting of electrolytic cathode, contain a small, deliberate addition of oxygen which scavenges impurities from the metal. The oxygen is present in the form of fine, well-distributed cuprous oxide particles only visible by microscopic examination of a polished section of the metal. Typical oxygen contents of these coppers fall in the range 0.02-0.05%. Between these limits the presence of the oxygen in this form has only a slight effect on the mechanical and electrical properties of the copper. It can, however, give rise to porosity and intergranular cracks or fissures if the copper is heated in a reducing atmosphere, as can happen during welding or brazing. This is a result of the reaction of the cuprous oxide particles with hydrogen and is known as 'hydrogen embrittlement'. Provided a reducing atmosphere is avoided, good welds and brazes can be readily achieved.

1.2.3.2 Oxygen-free High Conductivity Copper, CW008A (C103)

In view of the above remarks, if welding and brazing operations under reducing conditions are unavoidable, it is necessary to use a different (and more expensive) grade of high conductivity copper which is specially produced for this purpose. This type of copper, known as 'oxygen-free high conductivity copper', is normally produced by melting and casting under a protective atmosphere. To obtain the high conductivity required it is necessary to select the best raw materials. The result is a high purity product containing 99.95% copper. This enables a conductivity of 100% IACS to be specified even in the absence of the scavenging oxygen.

1.2.4 Available Forms

HC copper conductors are obtainable in bar, strip, rod or tube form. For busbar applications, the most common forms supplied are bar, rod or tube and these are normally supplied in the hard condition. In this condition they offer greater stiffness, strength and hardness and have a better surface finish. Because of the practical difficulty of straightening uncoiled hard material, it is normally supplied in straight lengths, coiled material being limited to the smaller sizes.

The maximum length of material available with the advent of continuous casting methods is dependent on the capability of the supplier's plant.

2.0 Current-Carrying Capacity of Busbars

David Chapman & Professor Toby Norris

2.1 Design Philosophy

The current-carrying capacity of a busbar is limited by the maximum acceptable working temperature of the system, taking into account the properties of the conductor material, the materials used for mounting the bars and the limitations of any cables (including their insulation) or devices connected to the bars.

There are two design limits; the maximum permitted temperature rise, as defined by switchgear standards, and the maximum temperature rise consistent with lowest lifetime costs - in the vast majority of cases, the maximum temperature dictated by economic considerations will be rather lower than that permitted by standards.

National and international standards, such as British Standard BS 159 and American Standard ANSI C37.20, give maximum temperature rises as well as maximum ambient temperatures. For example, BS 159:1992 stipulates a maximum temperature rise of 50°C above a 24 hour mean ambient temperature of up to 35°C, and a peak ambient temperature of 40°C. Alternatively, ANSI C37.20 permits a temperature rise of 65°C above a maximum ambient of 40°C, provided that silver-plated (or acceptable alternative) bolted terminations are used. If not, a temperature rise of 30°C is allowed.

These upper temperature limits were chosen to limit the potential for surface oxidation of conductor materials and to reduce the mechanical stress at joints due to cyclic temperature variations. In practice these limitations on temperature rise may be relaxed for copper busbars if suitable insulation materials are used. A nominal rise of 60°C or more above an ambient of 40°C is allowed by EN 60439-1:1994 provided that suitable precautions, such as plating, are taken. EN 60439-1:1994 states that the temperature rise of busbars and conductors is limited by the mechanical strength of the busbar material, the effect on adjacent equipment, the permissible temperature rise of insulating materials in contact with the bars and the effect on apparatus connected to the busbars. In practice, this last consideration limits the maximum working temperature to that of the insulation of cables connected to the bar – typically 90°C or 70°C.

Running busbars at a high working temperature allows the size of the bar to be minimised, saving material and initial cost. However, there are good reasons to design for a lower working temperature.

- A higher maximum temperature implies a wider variation in temperature during the load cycle, which causes varying stress on joints and supports as the bars expand and contract. Eventually, this may lead to poor joint performance and decreased reliability.
- In some cases it is difficult to remove heat from busbar compartments, resulting in ancillary equipment operating in an elevated ambient temperature.
- High temperatures indicate high energy losses. Lowering the temperature by increasing the size of the conductor reduces energy losses and thereby reduces the cost of ownership over the whole lifetime of the installation. If the installation is designed for lowest lifetime cost, the working temperature will be far below the limit set by standards and the system will be much more reliable.

2.2 Calculation of Maximum Current-Carrying Capacity

In engineering terms, the current rating for a busbar depends on the choice of working temperature. The bar is heated by the power dissipated in it by the load current flowing through the resistance, and cooled by radiation to its surroundings and convection from its surfaces. At the working temperature, the heat generation and loss mechanisms, which are highly temperature and shape dependent, are balanced.

2.2.1 Methods of Heat Loss

The heat generated in a busbar can only be dissipated in the following ways:

- Convection
- Radiation
- Conduction

In most cases, convection and radiation heat losses determine the current-carrying capacity of a busbar system. In a simple busbar, conduction plays no part since there is no heat flow along a bar of uniform temperature. Conduction need only be taken into account where a known amount of heat can flow into a heat sink outside the busbar system, or where adjacent parts of the system have differing cooling capacities. Conduction may be important in panel enclosures.

These cooling mechanisms are highly non-linear; doubling the width of a bar does not double the convection loss of a bar. The proportion of heat loss by convection and radiation depends on the conductor size, with the portion attributable to convection normally being greater for a small conductor and less for larger conductors.

2.2.1.1 Convection – Natural Air Cooling

The heat dissipated per unit area by convection depends on the shape and size of the conductor and its temperature rise above ambient temperature. This value is usually calculated for still air conditions but can be increased greatly if there is forced air-cooling. Where outdoor busbar systems are concerned, calculations should always be treated as in still (i.e. without wind effect) air unless specific information is given to the contrary.

The following formulae estimate the convection heat loss from a surface in W/m² in free air:

For vertical surfaces:

$$W_v = \frac{7.66\theta^{1.25}}{L^{0.25}}$$

For horizontal surfaces:

$$W_h = \frac{5.92\theta^{1.25}}{L^{0.25}}$$

For round tubes:

$$W_c = \frac{7.66\theta^{1.25}}{d^{0.25}}$$

where:

θ is temperature rise, °C
L is height or width of surface, mm
d is diameter of tube, mm.

Figure 4 shows the heat loss from a vertical surface (W_V) for various temperature rises plotted against surface height.

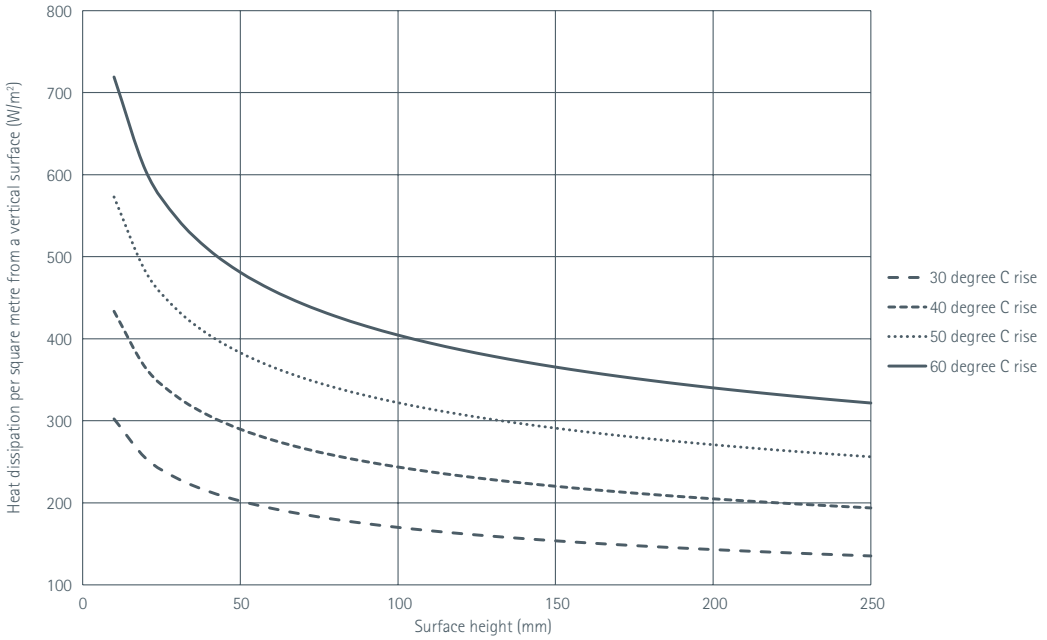

Figure 4 – Heat dissipation by convection from a vertical surface for various temperature rises above ambient

Figure 5 indicates which formula should be used for various conductor geometries.

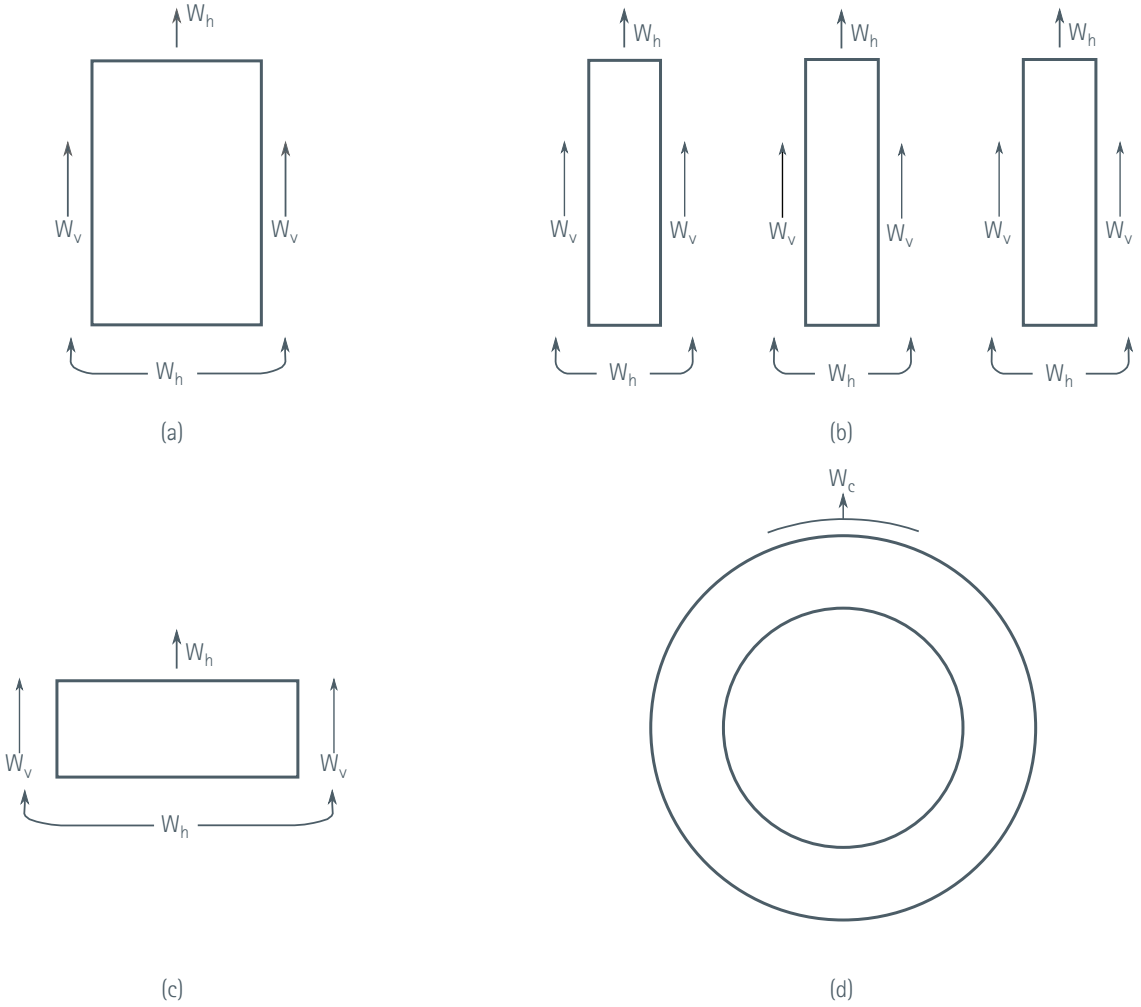

Figure 5 – Convection loss from typical bar sections

Comparing diagrams (a) and (b) and assuming a similar cross-sectional area, it can be seen that the heat loss from arrangement (b) is much larger, provided the gap between the bars is not less than the thickness of each bar.

2.2.1.2 Convection Heat Loss – Forced Air Cooling

If the air velocity over the busbar surface is less than 0.5 m/s, the above formulae for W_V, W_h and W_C apply. For higher air velocities the following may be used:

$$W_a = 120\sqrt{v} \times A\theta$$

where:

W_a is heat lost per unit length from bar, W/m
v is air velocity, m/s
A is surface area per unit length of bar, m²/m
θ is temperature rise, °C.

2.2.1.3 Radiation

The rate at which heat is radiated from a body to its surroundings is proportional to the difference between the fourth power of their absolute temperatures and the relative emissivity between the body and its surroundings. Emissivity describes how well a material radiates heat with a perfect radiator (a black body) having a value of unity and a perfectly reflecting surface a value of zero.

Since the amount of radiation depends on the temperature of the bar and its surroundings, bars in enclosed spaces may lose very little heat by radiation. Note that radiation in a particular direction will be influenced by the temperature and condition of any target surface.

The relative emissivity is calculated as follows:

$$e = \frac{\varepsilon_1 \varepsilon_2}{(\varepsilon_1 + \varepsilon_2) - (\varepsilon_1 \varepsilon_2)}$$

where:

e is relative emissivity
ε_1 is absolute emissivity of body 1
ε_2 is absolute emissivity of body 2

Typical emissivity values for copper busbars in various surface conditions are:

Bright metal	0.10
Partially oxidised	0.30
Heavily oxidised	0.70
Dull non-metallic paint	0.90

The rate of heat loss by radiation from a bar (W/m²) is given by:

$$W_r = 5.70 \times 10^{-8} \times e(T_1^4 - T_2^4)$$

where:

e is relative emissivity
T_1 is absolute temperature of body 1, K
T_2 is absolute temperature of body 2, K (i.e. ambient temperature of the surroundings)

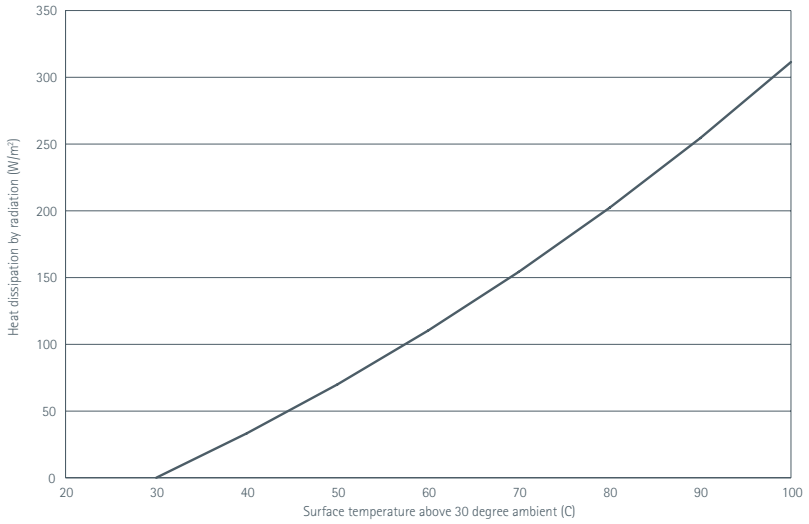

Figure 6 – Heat dissipation by radiation from a surface assuming relative emissivity of 0.5 and surroundings at 30°C

Figure 6 shows the heat loss from a surface against surface temperature. The diagrams in Figure 7 define the effective surface areas for radiation from conductors of common shapes and arrangements. Note that there is no heat loss by radiation from opposing busbar faces since the temperatures are approximately equal.

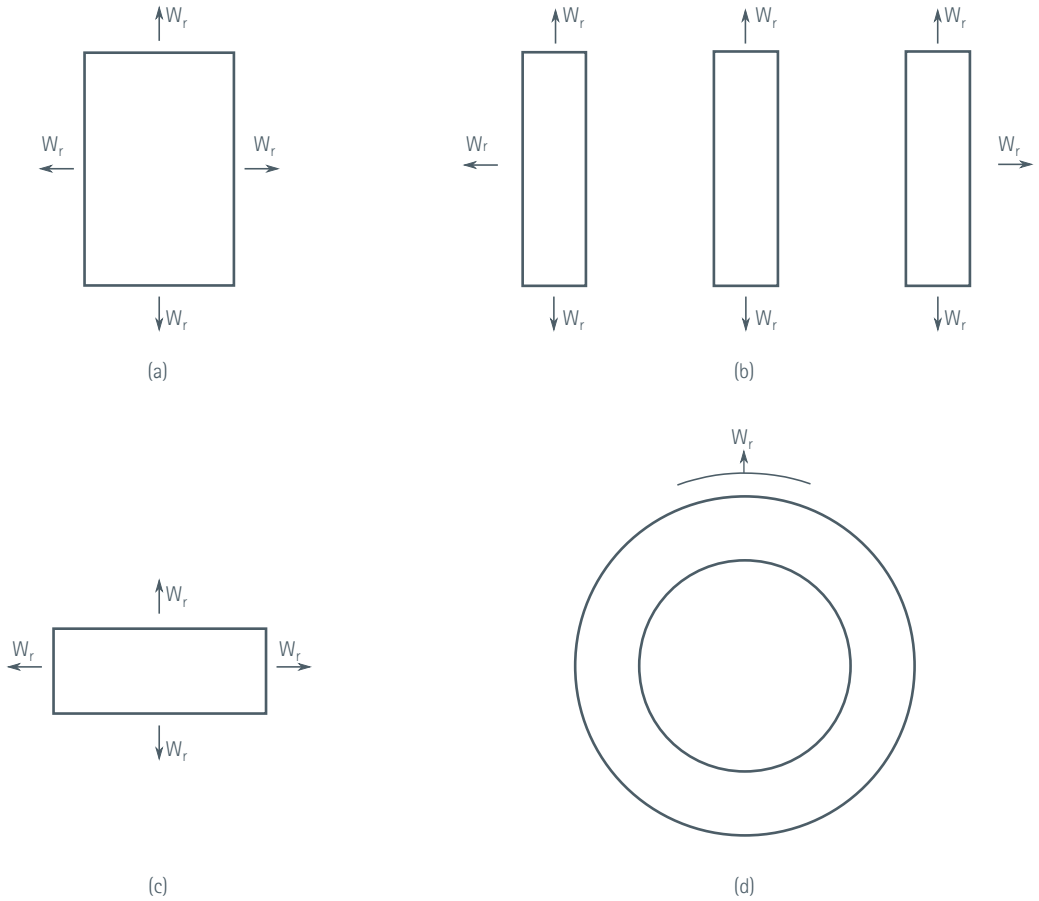

Figure 7 – Radiation loss from typical bar sections

The ratio of heat dissipated by convection and radiation varies considerably according to the height of the surface and the temperature rise, with radiation becoming less important for smaller bars and lower temperature rises. Figure 8 combines the data from Figure 4 and Figure 6 with the radiation dissipation levels, which are independent of surface height, shown as horizontal bars on the right.

In some countries it is common practice to attempt to increase emissivity to improve the dissipation by radiation by treating the surface of busbars, for example by painting them black. Since the natural emissivity of a copper bar that has been in use for even a short time will be above 0.5 and probably approaching 0.7, the benefit of increasing it to 0.9, although positive, will be small. On the negative side, the paint layer acts as an insulator, reducing the efficiency of the convection process. In general, painting will give little increase and possibly a reduction in the current-carrying capacity of a busbar for a given working temperature. Painting may be worthwhile for very wide bars (where convection is less effective) operating at large temperature rises (where radiation is more effective).

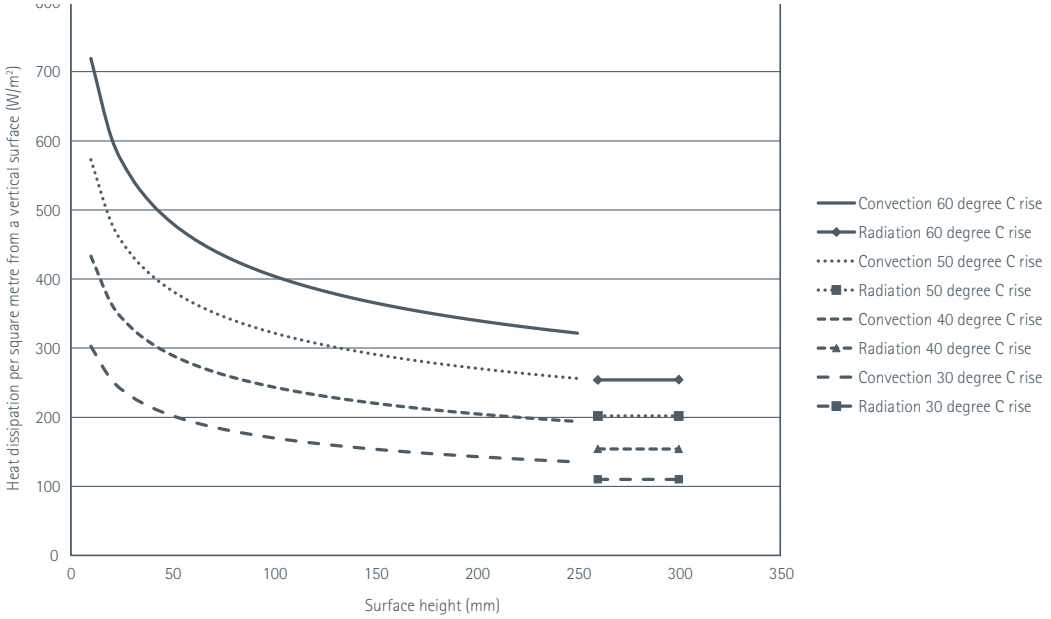

Figure 8 – Convection and radiation (right) losses at various temperatures

The plots given so far have been in terms of power dissipated per unit area of surface; for engineering purposes it is the heat dissipation per unit length which is of interest. Figure 9 and Figure 10 show the heat dissipation from the major surfaces of single and parallel vertically mounted bars. The relatively small contribution of the horizontal surfaces is ignored in these plots. These plots may be useful in determining a starting point for detailed calculation using the formulae previously given.

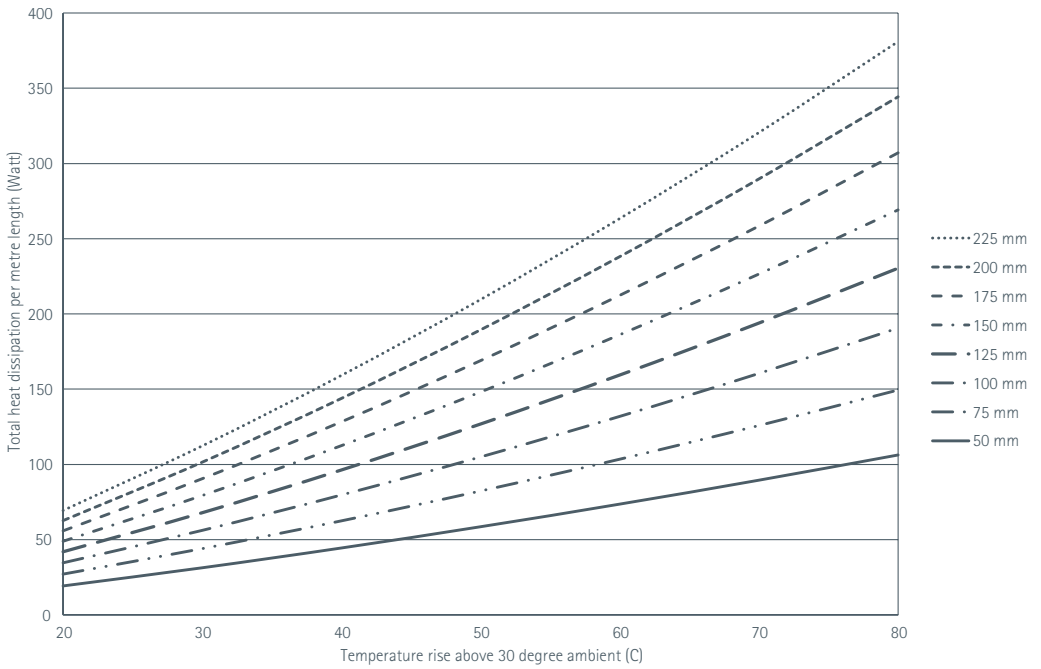

Figure 9 – Total heat losses for a single bar of various heights against temperature rise

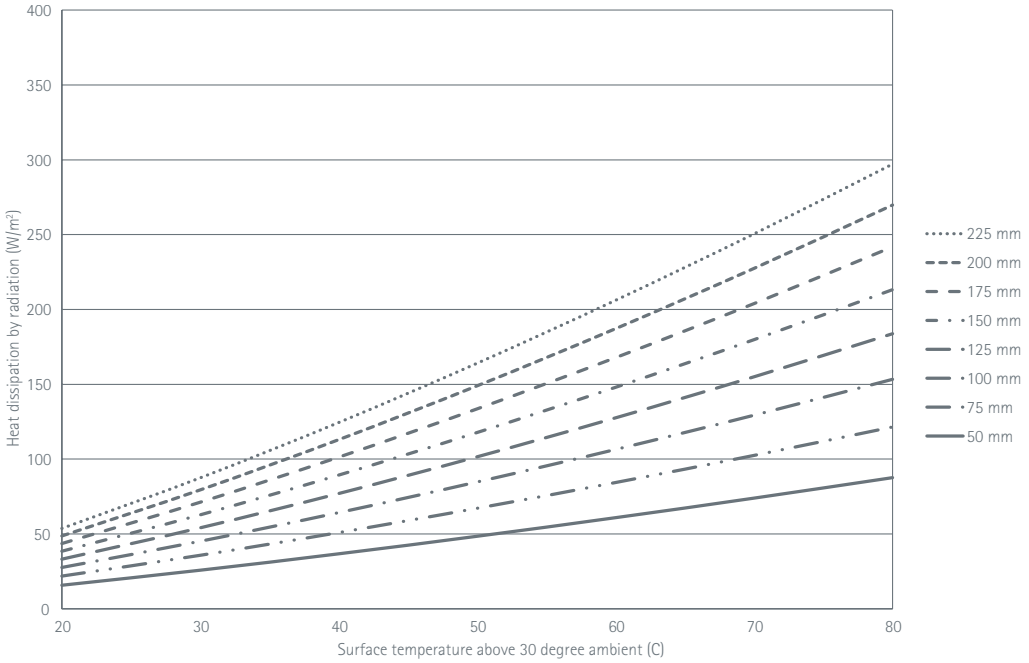

Figure 10 – Total heat losses for each bar of a parallel pair of various heights against temperature rise

2.2.2 Heat Generated by a Conductor

The rate at which heat is generated per unit length of a conductor carrying a direct current is the product I^2R watts, where I is the current flowing in the conductor and R is the resistance per unit length. In the case of dc busbar systems, the value for the resistance can be calculated directly from the resistivity of the copper or copper alloy at the expected working temperature. Where an ac busbar system is concerned, the resistance is increased because current density is increased near the outer surface of the conductor and reduced in the middle; this is called skin effect. Eddy currents induced by magnetic fields arising from currents in nearby conductors increase losses further; this is called proximity effect. The calculation of these effects is discussed later; for the present, a correction factor, S, is used.

The power dissipated in the conductor is

$$P = I^2 \times R_0 \times S$$

where:

P is the power dissipated per unit length
I is the current in conductor
R_0 is the dc resistance per unit length at the working temperature
S is the correction factor for shape and proximity.

The process of sizing a busbar is one of iteration. Starting from an arbitrary size and the desired working temperature, the heat power loss from the surface of a one-metre section can be calculated. The electrical power loss for the one-metre section can also be calculated. If the electrical power dissipated is higher than the heat dissipation, the bar is too small; the size should be increased and the calculations repeated until a close match is obtained. Note that the value of resistivity used in the calculation must be corrected for the working temperature and the value of S (the correction for shape and proximity factors) must be recalculated for each size. A very approximate starting point is to assume an average current density of 2 A/mm² in still air and iterate either up or down.

2.2.2.1 Alternating Current Effects – the Factor *S*

The factor *S*, introduced above, is the product of the factors due to skin effect, S_k, and proximity factor, S_p. Accurate determination of skin and proximity effects is complex and generally requires finite element analysis. In this publication results are presented as curves and, where possible, 'portmanteau formulae' in the form of polynomials or ratios of polynomials valid over a given range of an independent variable such as the scaling factor, *p*, described below. Most of these formulae were found by curve fitting to data computed by finite element analysis. The portmanteau formulae do not always reflect satisfactorily a physical explanation and are usually very inaccurate outside the given range. They are normally accurate to within ±1% within the stated range unless otherwise noted.

The graphs are plotted from the computed data. To make them readable, scaling factors and quasi-logarithmic scales are used.

The **resistance/frequency** parameter scaling factor combines frequency, resistivity and size. For a busbar configuration of given shape or relative proportions, the ac resistance and inductance may be expressed as a function of a ratio of frequency to dc resistance. Two forms of the scaling factor are used in terms of either

(a) The parameter, *p*, defined as

$$p = \sqrt{2}\mu_0\sqrt{\frac{f}{R_{dc}}} \approx 1.585\sqrt{\frac{f}{R_{dc}}}$$

where:

f is frequency in Hz
R_{dc} is dc resistance in μΩ/m

also

$$p = \sqrt{\frac{2}{\pi}}\frac{\sqrt{A}}{\delta} \approx 0.8\frac{\sqrt{A}}{\delta}$$

where:

A is the cross-sectional area
δ is the skin depth

The area A and the skin depth must be in comparable units. Thus if δ is in mm then *A* must be in mm^2.

Sometimes $\sqrt{\frac{f}{R_{dc}}}$ is used as the scaling parameter.

The parameter *p* is chosen since it appears widely in the literature on the subject. The plots for different cross-sectional shapes give clearer curves when using *p* rather than, say, p^2.

For $p \leq 0.5$ the resistance is little different from the dc resistance. R_{ac} is proportional to p^4 for low values of *p* and so proportional to the square of the frequency but, at higher values beyond $p = 5$, the resistance becomes linear with *p*, i.e. proportional to the square root of frequency. If efficiency is a concern, then *p* will normally be substantially less than 5 and more likely to be in the range 0 to 2. Figure 11 shows how *p* varies with cross-sectional area at a selection of frequencies for copper at 80°C.

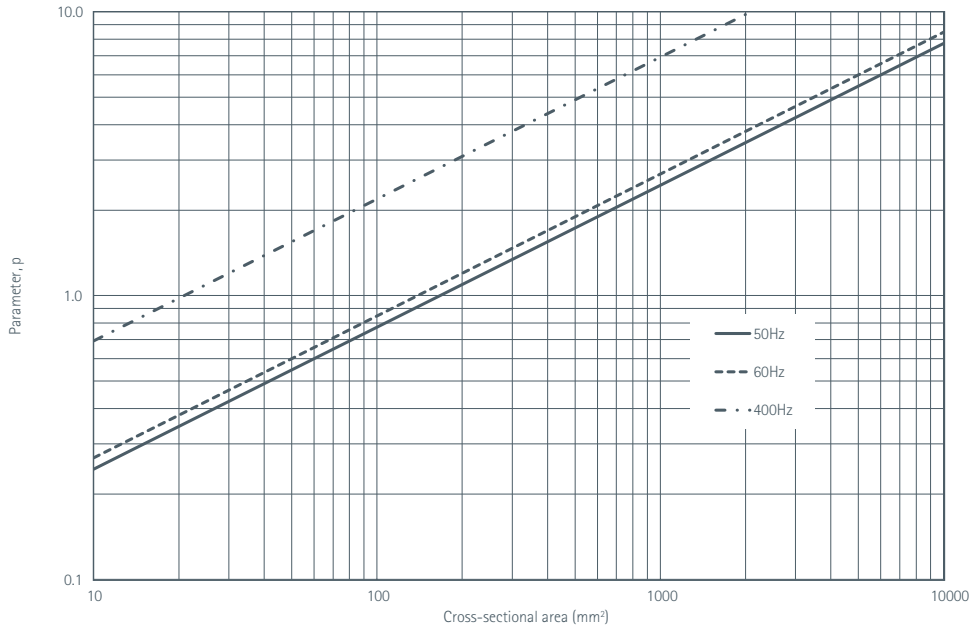

Figure 11 – Parameter *p* versus cross-sectional area in mm² for typical copper at 80˚C

In some of the plots the scaling factor may be expressed simply as $\sqrt{\frac{f}{R_{dc}}}$ or in terms of γ.

(b) The ratio γ, defined as

$$\gamma = \frac{Leading\ dimension}{\delta, skin\ depth}$$

This can often give a physical idea of the effect of size of a conductor as, for example, for round bars where $\gamma = \frac{d}{\delta}$ and d is the bar diameter. For low losses $\gamma \leq 1$ is desirable.

For a given busbar geometry, the values of γ and p are proportional to each other.

Quasi logarithmic scales: The resistance ratio or shape factor, $S = R_{ac} / R_{dc}$, approaches unity at low frequencies. In some graphs the logarithm of (S–1) is plotted against the independent variable such as scaling parameter, p. This method shows the approach to unity in more detail. However, the values on the S scale are labelled as the actual values of S and not of (S–1). Such plots typically go down to S = 1.01 as covering a useful range.

Busbar configuration: The choice of busbar configuration will depend on many factors. Round bars, tubes, strips or channels are common. Factors to be taken into consideration include frequency and the presence of harmonics, cost of materials, degree of compactness sought, cooling arrangements, magnetic mechanical forces and cost of support structures, inductance and, for longer bars, capacitance.

From Figure 11 it will be seen that, for $p < 2$, the cross-sectional area of bars is limited to 400 mm². At a typical current of 2 A mm^{-2} this is a current of 800 A. The effective ac resistance may be reduced by:

1. Using two bars per phase separated by a suitable distance along their length. This possibility is discussed for some shapes in later sections.
2. Using multiple bars for a phase and transposing them along the length of the bar
3. Interleaving phases but then the design becomes more detailed.

2.2.2.1.1 Skin Effect and Skin Depth

Current flowing in the inner parts of a conductor produces a magnetic field inside the conductor that circulates around the axis of the conductor. This alternating magnetic field induces an electric field that drives currents in such a way that the current in the centre of the conductor is reduced while the current in the outer parts is increased. These induced recirculating currents are referred to as **eddy currents.** The overall result is that the current density is highest near the surface and falls off towards the interior.

A measure of the extent of the fall off (and so of the effect of the ac nature) is the **skin depth,** sometimes called **the depth of penetration,** and usually given the symbol δ.

$$\delta = \sqrt{\frac{\rho}{\pi \mu_0 f}} = \sqrt{\frac{2\rho}{\mu_0 \omega}}$$

where:

ρ is resistivity of conductor material, Ω m
μ_0 is permeability of free space, $4\pi\ 10^{-7}$ H/m
f is frequency, Hz
δ is skin depth, m

Or, in alternative units,

$$\delta = \frac{50}{\pi}\sqrt{\frac{\rho}{f}} \approx 15.915\sqrt{\frac{\rho}{f}}$$

where:

ρ is resistivity of conductor material, nΩ m
f is frequency, Hz
δ is skin depth, mm

Hence, for copper at 20°C (ρ = 17 nΩ m),

$$\delta \approx \frac{65.6}{\sqrt{f}}$$

≈ 9.27 mm at 50Hz
≈ 8.46 mm at 60 Hz
≈ 3.28 mm at 400 Hz

About 85% of the current is carried in a layer of thickness equal to the skin depth in conductors that are much thicker than the skin depth. In such thick conductors the resistance is as if the current flowed with uniform current density in a layer of thickness equal to the skin depth.

Figure 12 shows how the resistivity of a typical grade of copper varies with temperature and Figure 13 shows how the skin depth varies with temperature at typical power frequencies.

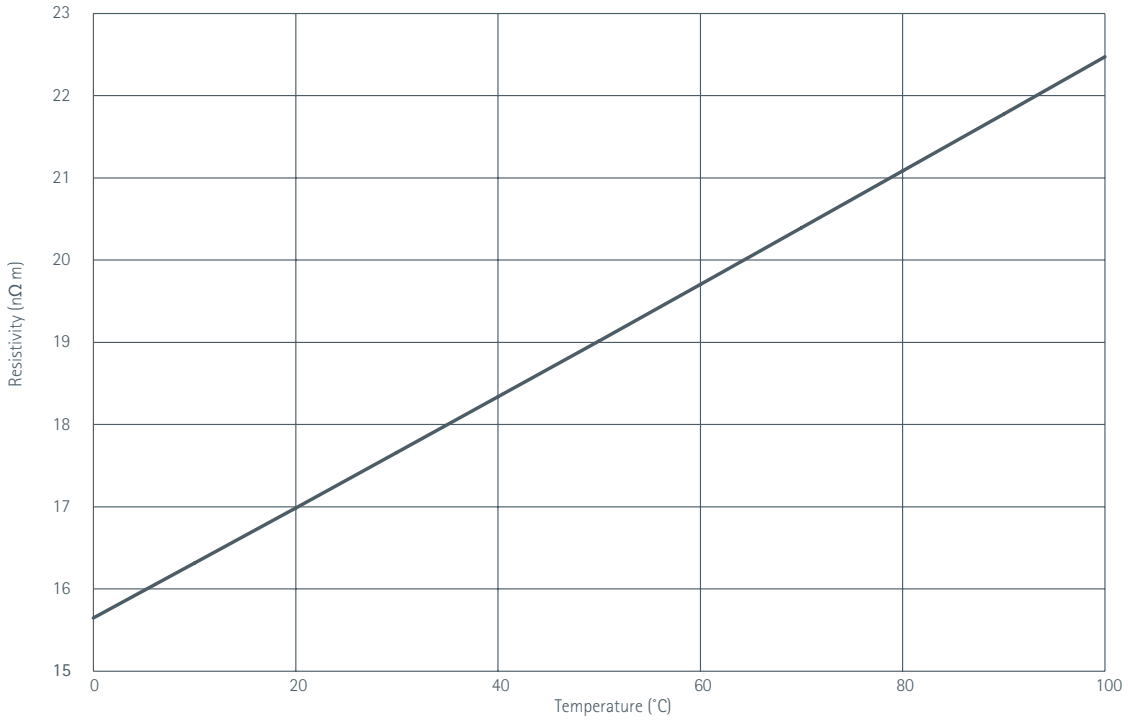

Figure 12 – Resistivity of typical HC copper (101.5% IACS) as a function of temperature. Note 10nΩ m = 1μΩ cm

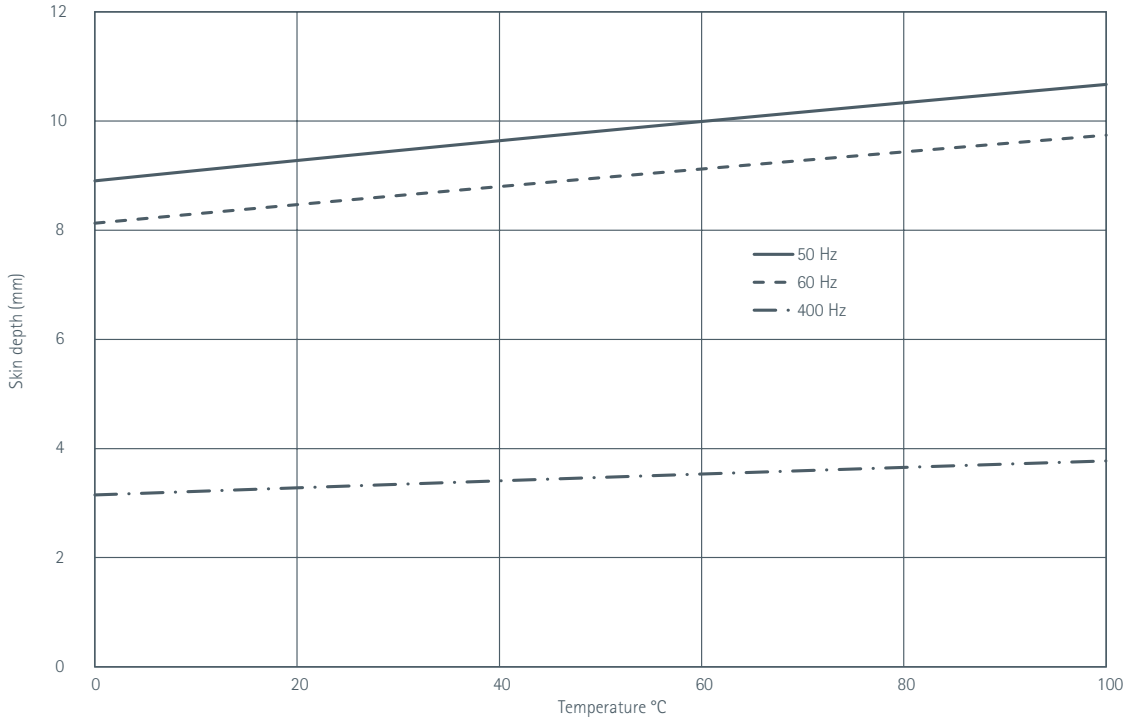

Figure 13 – Skin depth of typical HC copper (101.5% IACS) at 50 Hz, 60 Hz and 400 Hz as a function of temperature

If the dimensions of the bar are larger than about half the skin depth, then ac effects will be important. In such a case, the extra thickness may increase the losses rather than reduce them, but only slightly.

A useful measure of the ac effect in determining the ac resistance of a bar is the **Shape Factor**, *S*, defined as

$$S = \frac{R_{ac}}{R_{dc}}$$

where:

R_{dc} is the dc resistance
R_{ac} is the ac resistance

thus,

$$R_{dc} = \frac{\rho}{A}$$

where:

R_{dc} is resistance, Ω/m
A is cross-section, m^2
ρ is resistivity, Ω m

or,

$$R_{dc} = \frac{1000\rho}{A}$$

where:

R_{dc} is resistance, μΩ/m or mΩ/km
A is cross-section, mm^2
ρ is resistivity, nΩ m

and

$$R_{ac} = S\,R_{dc}$$

Although computing the bar resistance is straightforward, Figure 14 is given either as a check or for approximate estimation.

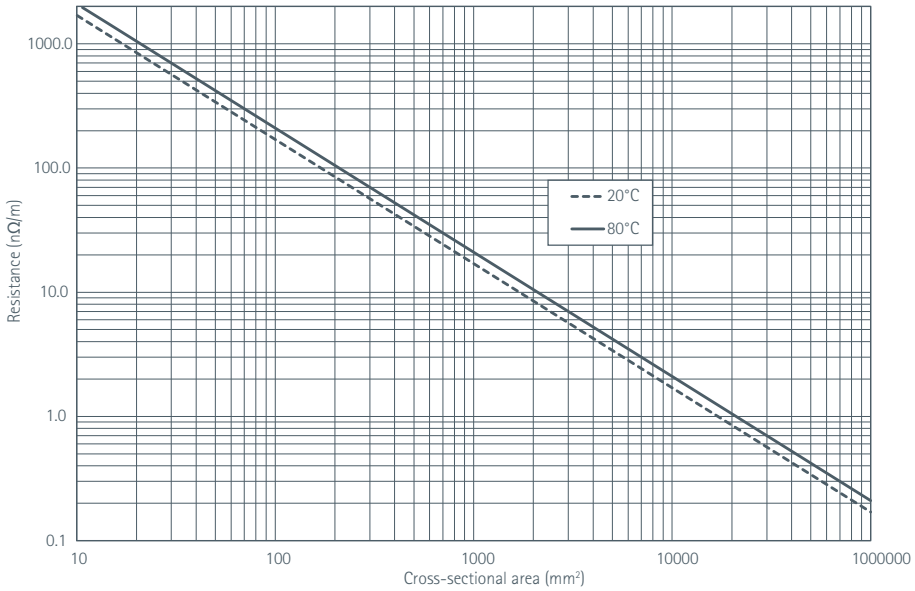

Figure 14 – dc resistance of typical HC Copper (101.5% IACS) versus area at 20°C and 80°C

One would hope in any design that the shape factor, *S*, would be not much more than unity.

The determination of the shape factor is a principal feature of this section.

The power, *P*, dissipated as heat in a bar carrying current, *I*, is then

$$P = S\, R_{dc} I^2$$

$$P = S\, \frac{\rho}{A}\, I^2$$

where:

P	is the power dissipated per metre length, W/m
R_{dc}	is the resistance per metre length, Ω/m
S	is shape factor
ρ	is resistivity, Ω m
A	is cross-sectional area, m^2

or

$$P = 1000\, S\, R_{dc} I^2$$

$$P = 1000\, S\, \frac{\rho}{A}\, I^2$$

where:

P	is the power dissipated per metre length, mW/m
R_{dc}	is the resistance per metre length, μΩ/m; mΩ/km
S	is shape factor
ρ	is resistivity, nΩ m
A	is cross-sectional area, mm^2.

The precise calculation of eddy current in conductors of general shape requires finite difference or other numerical computational procedures. These procedures require extensive programme writing or access to one of the commercially available programmes and practice in its use. However, for some common configurations there are exact (if complicated) formulae, while for others there are simpler approximations and graphical methods. These are given in '2A Shape and Proximity Factors for Typical Configurations'.

2.2.2.1.2 Proximity Factor, S_p

With conductors in parallel there are also eddy current mechanisms and further current redistribution in a conductor caused by magnetic fields arising from currents in neighbouring conductors. This is the **proximity effect**.

In the case of a single bar, the eddy current mechanism tends to drive current to flow in outer regions of the bar.

In the case of adjacent conductors carrying anti-parallel currents, the effect is to draw current flow towards the facing surfaces of the bars. For round bars or tubes which are carrying anti-parallel currents there is an increase in the current density at those parts of the bar that face each other, so losses are higher. For closely spaced parallel strips with their long sides facing each other, there is still a concentration of current near the ends of the strips, but overall the current is more uniformly distributed across the width and overall losses can be reduced.

The proximity factor is sometimes expressed as S_p so that the effective resistance, R_{ac}, as given by:

$$\frac{R_{ac}}{R_{dc}} = S\, S_p$$

In section 2A, which gives charts and equations for common busbar shapes and arrangements, the shape and proximity factors are given either separately as S and S_p or combined together as R_{ac}/R_{dc}.

2.3 Conclusion

The design of a busbar system for a particular duty is quite a complex issue. It requires an iterative approach to arrive at a size and disposition that delivers the energy efficiency levels appropriate to the duty factor of the application while ensuring good reliability and safety.

2A Shape and Proximity Factors for Typical Configurations

2A.1 Skin and Proximity Factors for Common Busbar Shapes

2A.1.1 Single Solid Rods

2A.1.1.1 Shape Factor for Single Solid Rods

For a rod of radius *a* calculate γ:

$$\gamma = \frac{a}{\delta}$$

where δ is skin depth.

Substituting for δ,

$$\gamma = 2\sqrt{\frac{\pi}{10}}\sqrt{\frac{f}{R_{dc}}} \approx 1.121\sqrt{\frac{f}{R_{dc}}}$$

where:

f is frequency, Hz
R_{dc} is resistance in μΩ/m

then,

$$\gamma = \frac{1}{\sqrt{2}}\, p \approx 0.707\, p$$

S_p can be calculated from the following approximate formulae:

for γ < 1.98:

$$S_p \approx 1 + \frac{5\gamma^4}{240 + 4\gamma^4}$$

Error is <0.02% if γ < 1.68; <0.1% if γ < 1.98

for γ > 3.9:

$$S_p \approx \frac{2\gamma + 1}{2} + \frac{3}{32\gamma}$$

Error is <0.8% if γ > 3.9, <0.2% if γ > 5

In the intermediate range 1.6 < γ < 3.9 the following formula is within 0.2%:

$$S_p \approx 0.84 - 0.13\gamma + 0.22\gamma^2 - 0.0246\gamma^3$$

Errors lie between -0.2 % and + 0.15 %.

Computations using the formulae may be checked by comparison with the graphs in Figure 15. These graphs might also be used directly for approximate working.

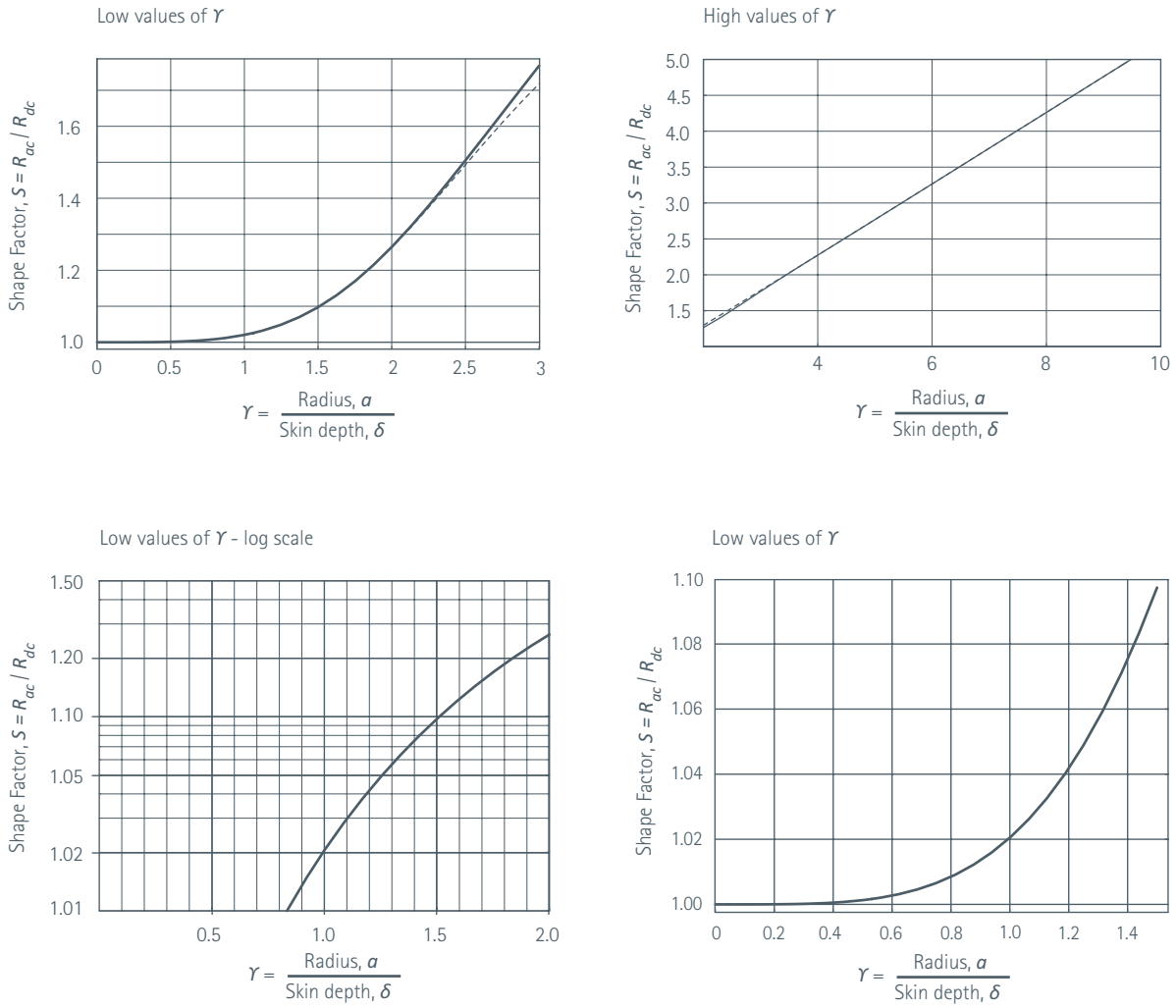

Figure 15 – Plots of shape factor versus γ. In the upper left-hand figure, for low values of γ, the dotted line shows the exact formula and the solid line the given approximation. The difference is scarcely discernable.

2A.1.1.2 Proximity Factor for Single Solid Rods

For the round bar calculate η,

$$\eta = \frac{s}{2a}$$

where:

s is the spacing of the centres
a is the bar radius.

Then the proximity factor, for $\eta > 2$

$$S_p = \frac{1}{\sqrt{1 - \frac{A}{\eta^2}}}$$

$\eta > 2$ means that the minimum space between the opposing curved faces is greater than the bar diameter.

The factor A in the above equation is a function of $\gamma = \frac{a}{\delta}$ and approximately for $\gamma < 2$

$$A = \frac{\gamma^4(1 - 0.128\gamma^2)}{5.705 + 1.88\gamma^2}$$

This relationship is plotted in Figure 16.

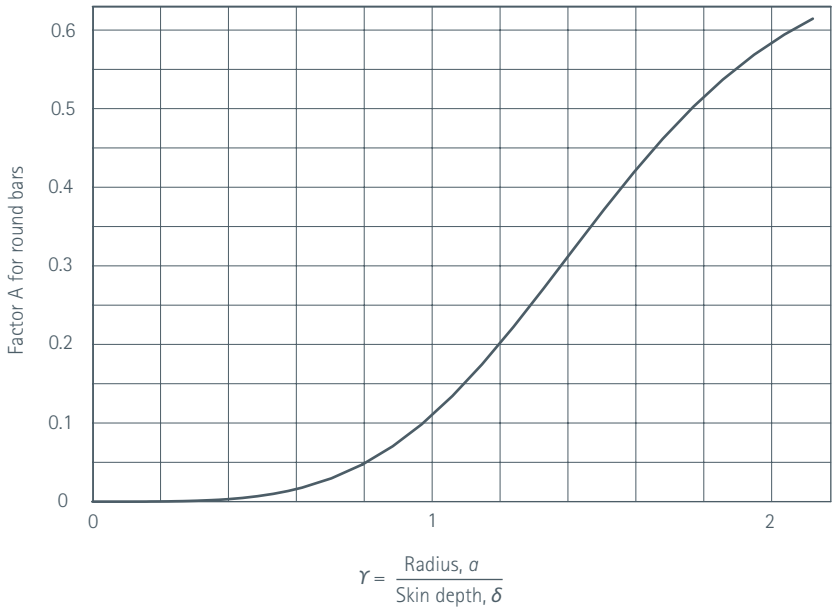

Figure 16 – Factor *A* for round bars as a function of γ

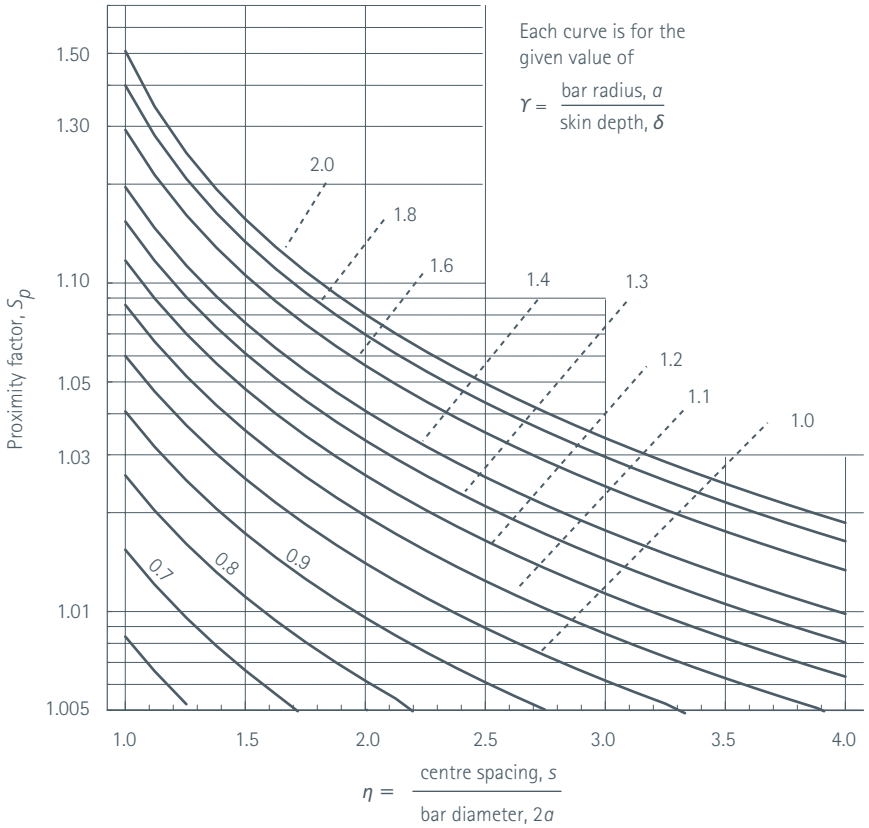

Figure 17 – Proximity factor, *Sp*, for single phase systems with parallel round bars

For three phase systems calculate μ:

$$\mu = \frac{A(\gamma)}{\eta^2}$$

where:

$$\eta = \frac{s}{2a}$$

Then for a triangular arrangement of three phase busbars,

$$S_{p\,triangular} \approx S_p\left(1 + \frac{\mu}{4} - \frac{5\mu^2}{24} - \frac{3\mu^8}{8}\right)$$

And for a flat arrangement the average proximity factor is

$$S_{p\,flat} \approx S_p\left(1 + \frac{\mu}{4} - \frac{\mu^2}{8} + \frac{5\mu^8}{24}\right)$$

The factors are plotted in Figure 18 and Figure 19.

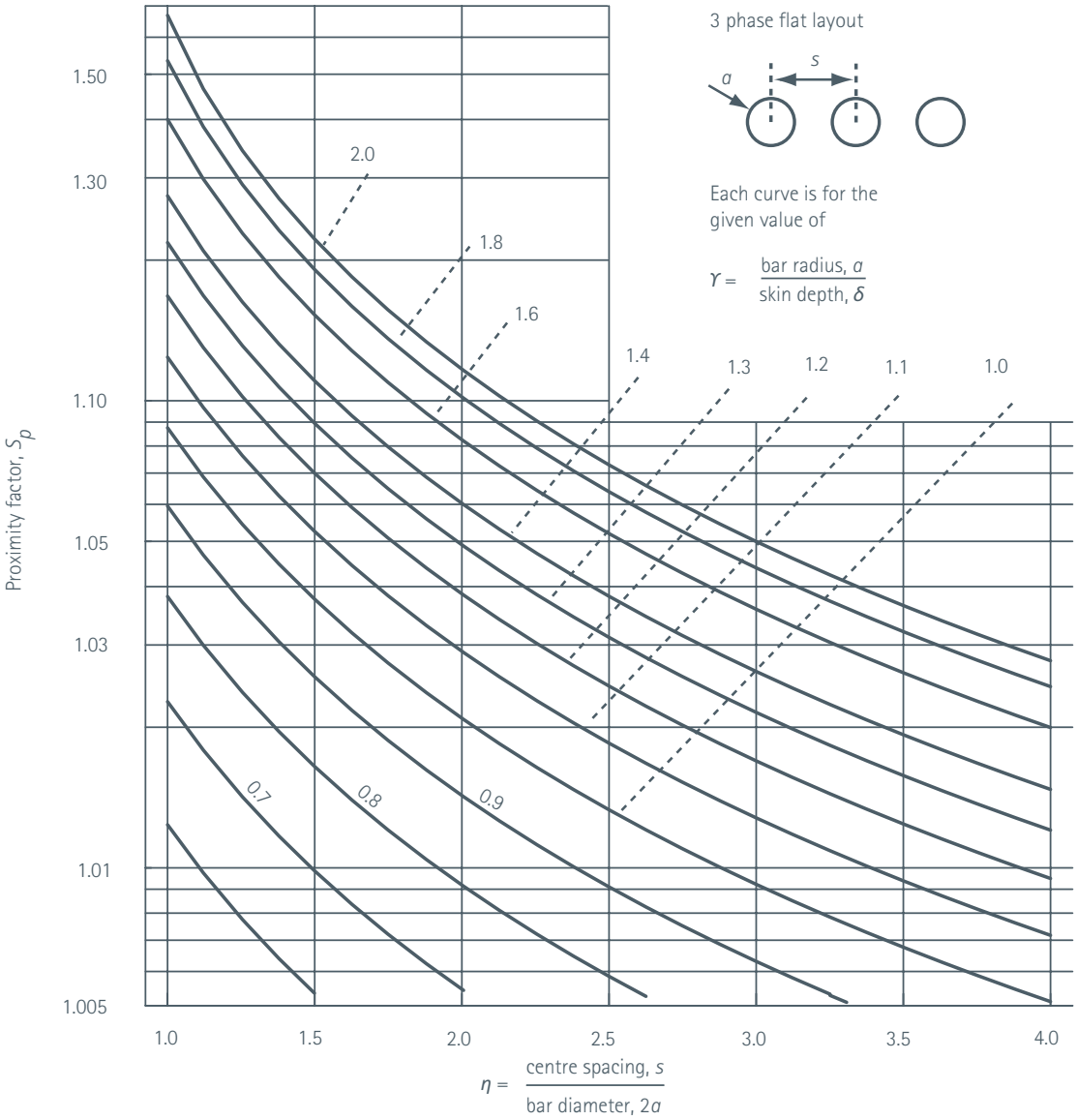

Figure 18 – Mean proximity factors for flat arrangement of round bars carrying balanced three phase currents

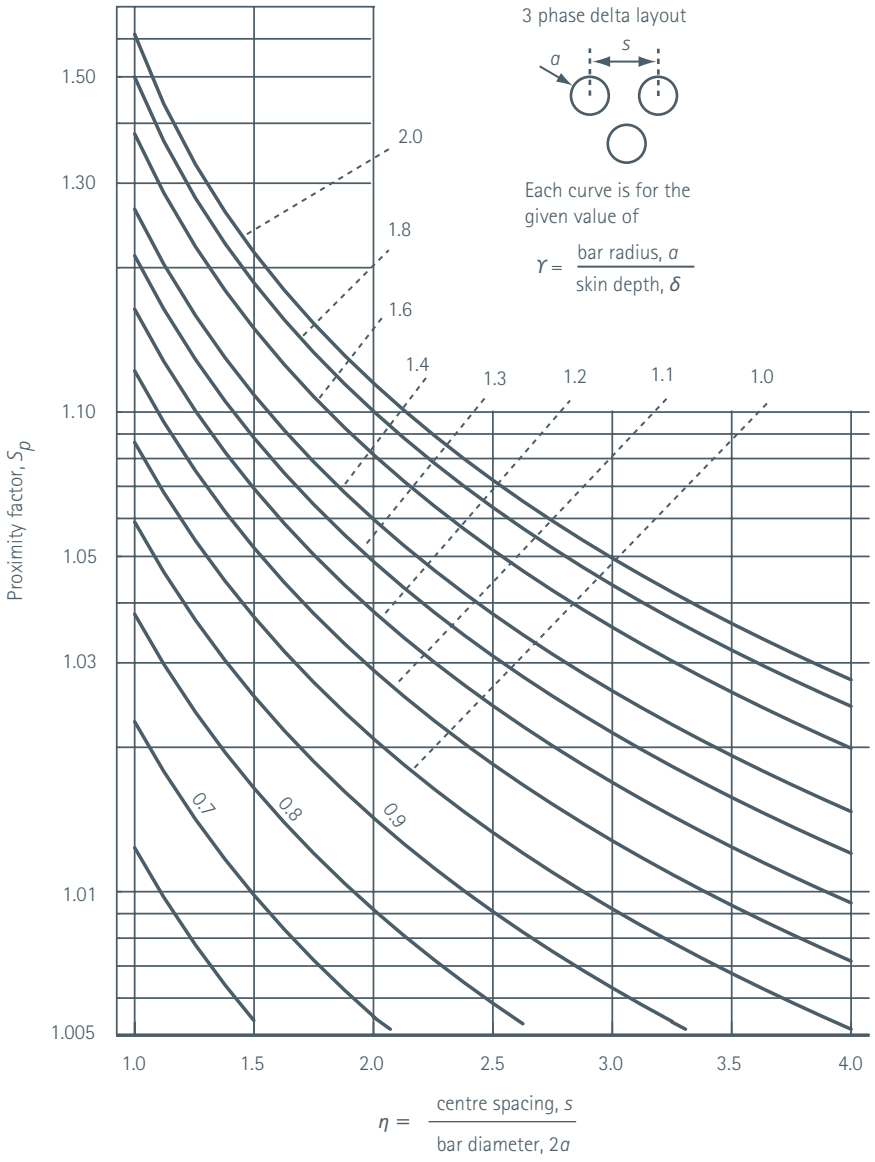

Figure 19 – Mean proximity factors for delta arrangement of round bars carrying balanced three phase currents

2A.1.2 Single Tubes

2A.1.2.1 Shape Factors for Single Tubes

Calculate parameters g and β as:

$$g = \frac{t}{\delta}$$

and

$$\beta = \frac{t}{a}$$

where:

a is radius
δ is skin depth
t is wall thickness

The units for a, δ and t must be the same.

The approximate formula for S is

$$S \approx 1 + A(g)\left\{1 - \frac{\beta}{2} - \beta^2 B(g)\right\}$$

where A and B are given by:

for $g < 1.6$:

$$A(g) = \frac{28g^4}{315 + 12g^4}$$

$$B(g) = \frac{56}{211 + 4g^4}$$

for $1.59 < g < 3.9$:

$$A(g) = -1.22 + 1.07g$$

$$B(g) = \frac{1827 - 300g}{3005 + 1555g}$$

for $g > 3.9$:

$$A(g) = g - 1$$

$$B(g) = \frac{3}{8g - 5}$$

Figures 20 to 24 show plots of shape factor for various tube sizes.

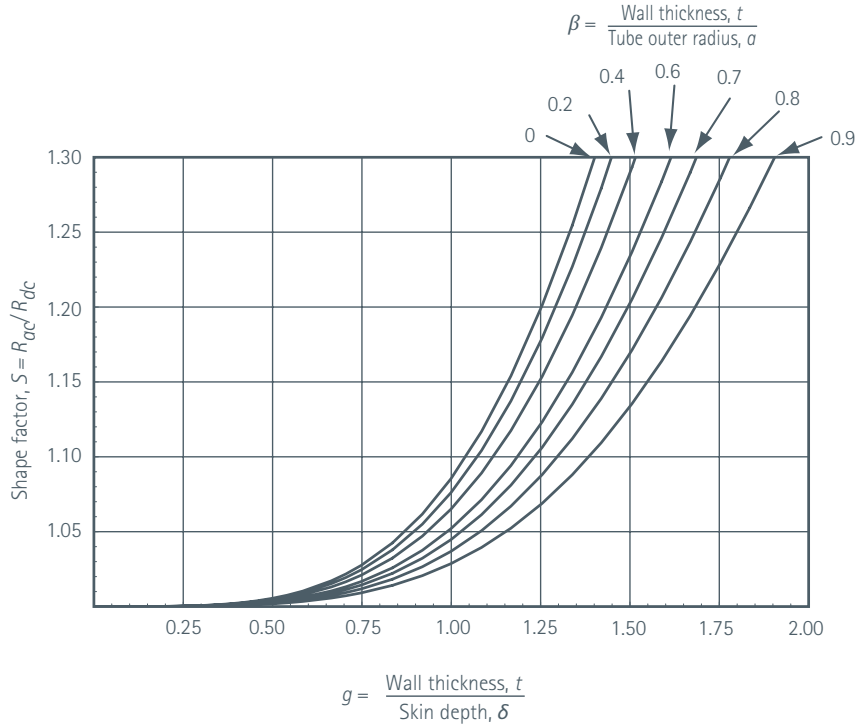

Figure 20 – Shape factor for tubes

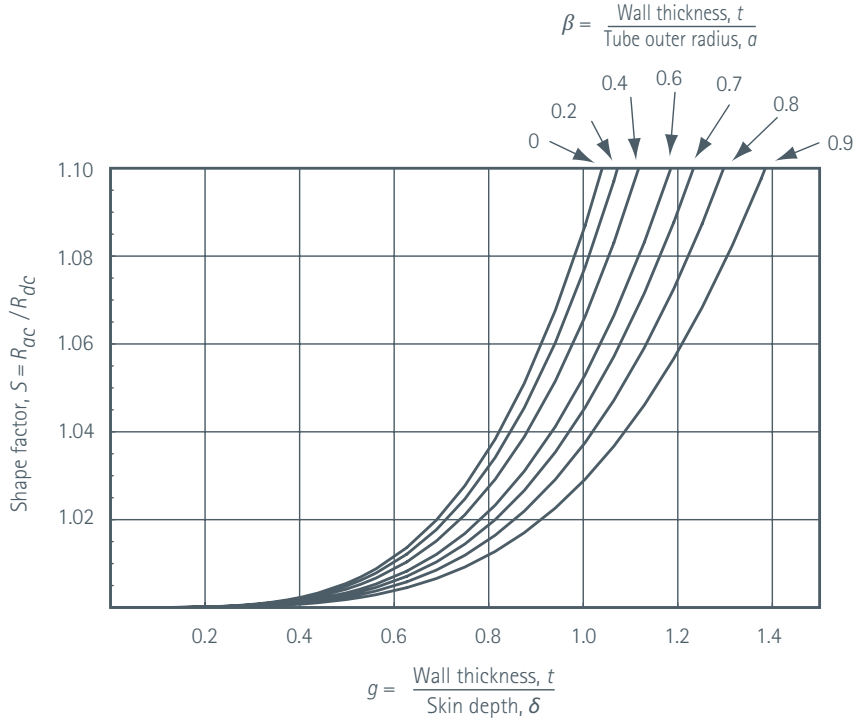

Figure 21 – Shape factor for tubes with low values of shape factor

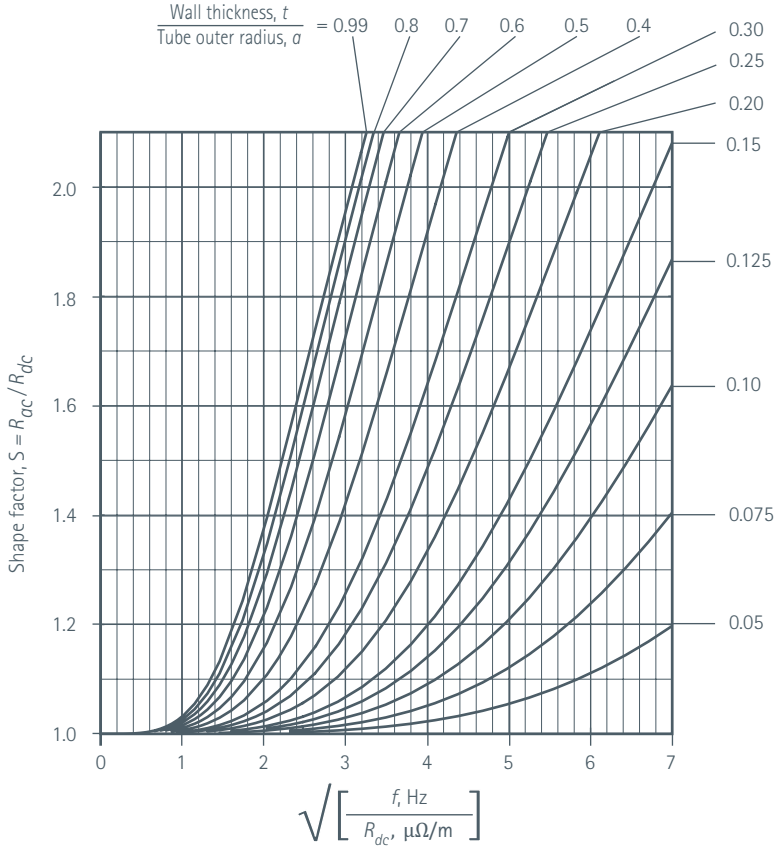

Figure 22 – Shape factor for tubes

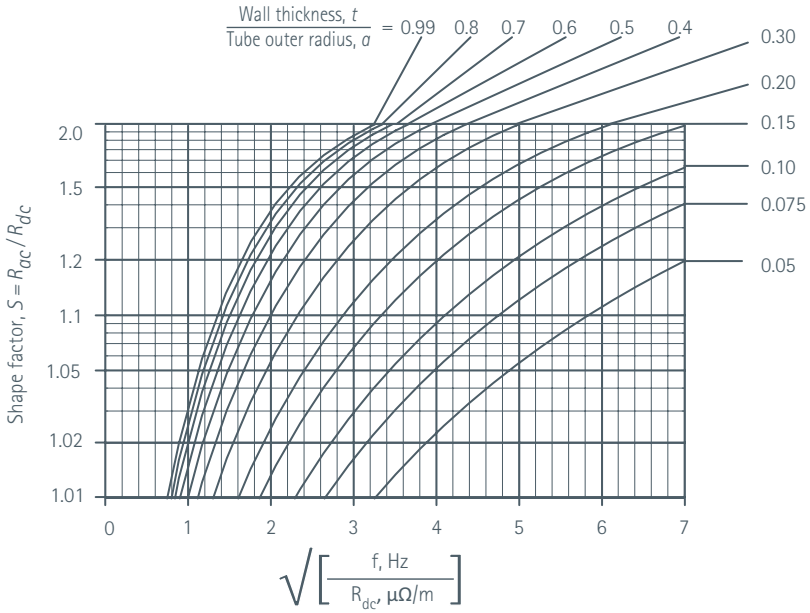

Figure 23 – The shape factor computed from the Bessel function formula using $\sqrt{(f/r_{dc})}$ as the frequency parameter

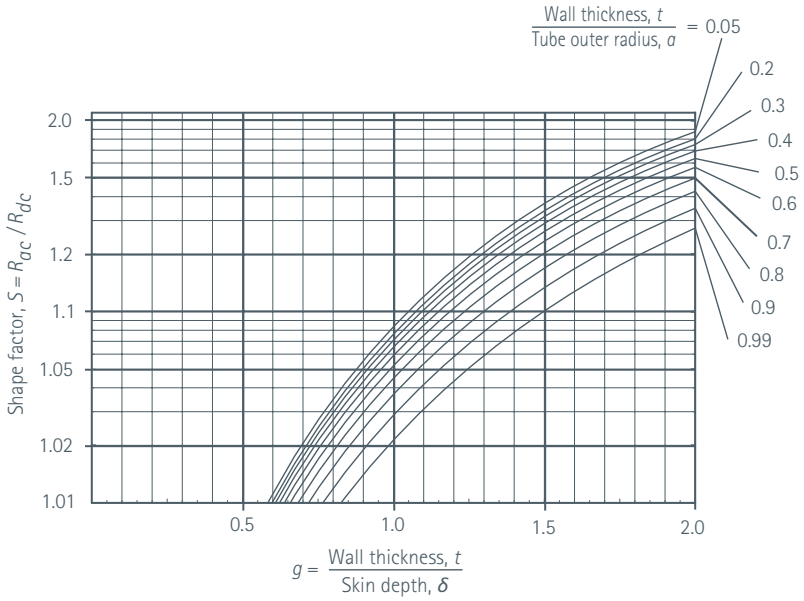

Figure 24 – Shape factor as a function of the ratio, $g = \frac{wall\ thickness\ t}{skin\ depth\ \delta}$

2A.1.2.2 Proximity Factors for Tubes

As for the round bar calculate η,

$$\eta = \frac{s}{2a}$$

where:

s is the spacing of the centres
a is the bar radius.

For **moderate to large** spacings, i.e. for $\eta > 2$,

$$S_p = \frac{1}{\sqrt{1 - \frac{A}{\eta^2}}}$$

with the factor A now given by

$$A = a(x) + p(x)\left[1 - \gamma_A^2 - \frac{(1-\gamma_A)x^3}{400 + x^3}\right]$$

where:

$$x = \sqrt{2}\ \gamma\ \gamma_a$$

$$\gamma_A = \sqrt{b(2-\beta)}$$

$$\gamma = \frac{a}{\delta}$$

$$a(x) \approx \frac{x^4\,(1 - 0.064x^2)}{22.8 + 3.76x^2}$$

$$p(x) \approx \frac{x^4(1 - 0.134x^2)}{25 + 3.973x^2}$$

NOTE: The factor *a(x)* is not the same as the radius *a*. '*a(x)*' is a term normally adopted in the literature and *a* and *a(x)* are unlikely to be confused once the difference is established.

For the single phase case we have Figure 25 which plots the factor *A* against β = t/a. This factor *A* is then used in Figure 26 to find S_p, the proximity factor for values of η=*s/2a=s/d*.

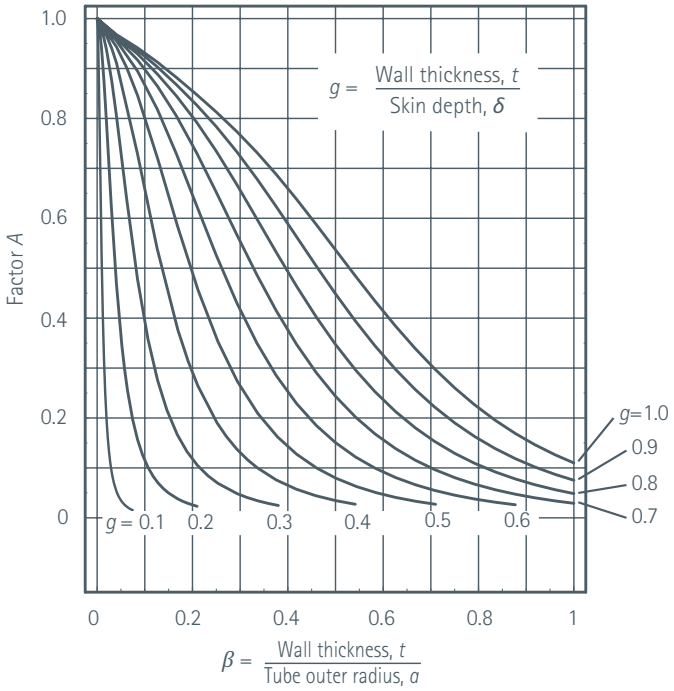

Figure 25 – Factor *A* versus β = *t/a* for values of *g* = *t*/δ

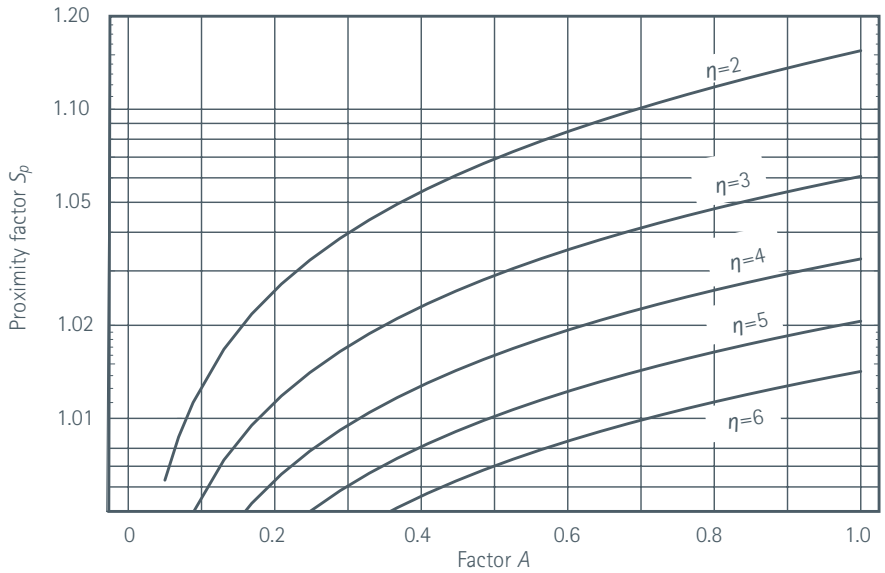

Figure 26 – Proximity factor for single phase tubes as function of the factor *A* for values of η=*s/2a=s/d*

These graphs may be combined into a joint chart as in Figure 27.

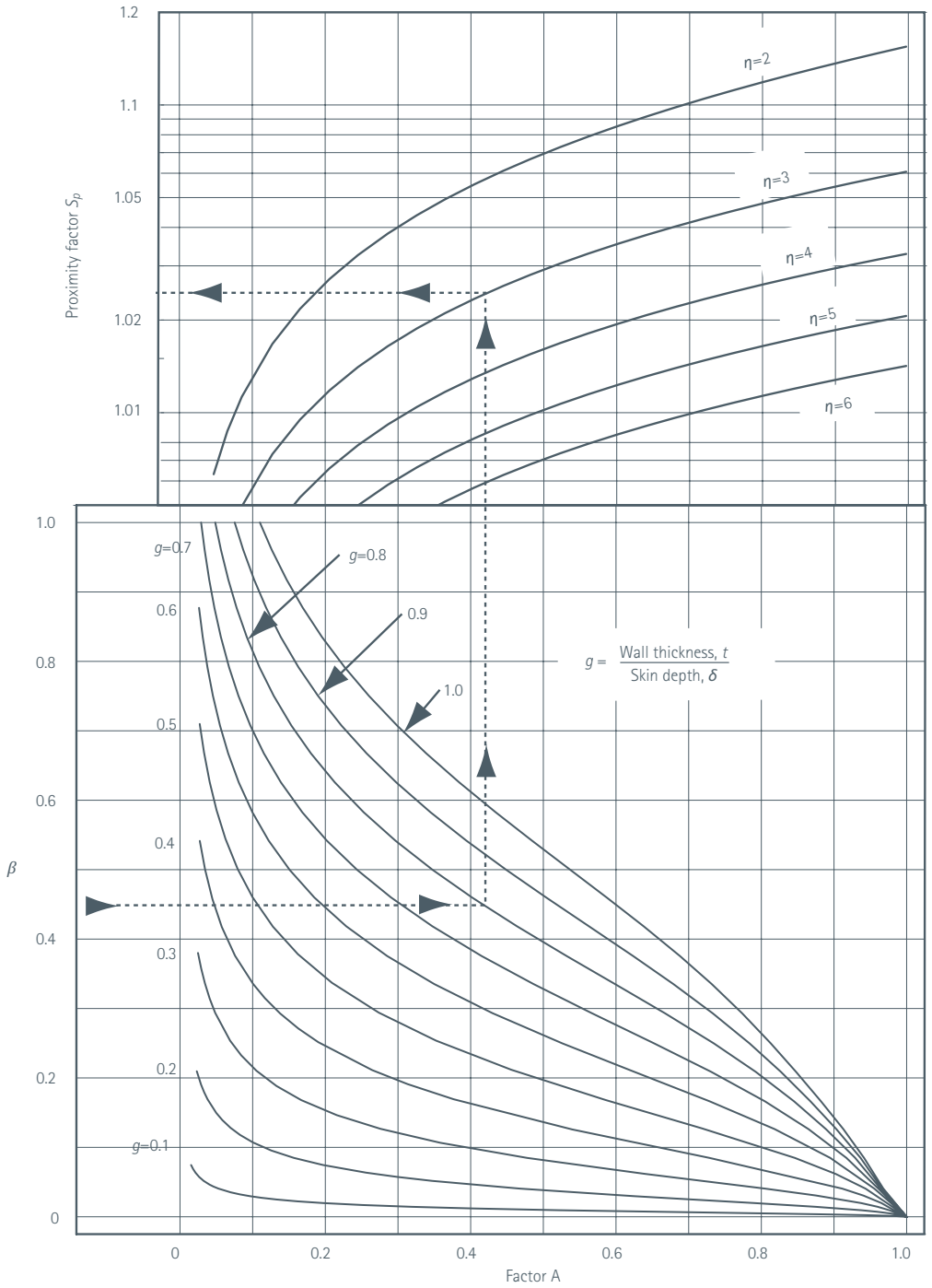

Figure 27 – Proximity factor for single phase tubes. $\beta = t/a$, $g = t/\delta$ and $\eta = s/2a = s/d$ with t = wall thickness, a = radius, d = diameter, δ = skin depth

The chart is used by starting with the value of β on the vertical axis of the lower plot, drawing a horizontal line to the curve for the value of g to obtain the value of the factor A. Next, draw a line vertically to the upper plot to intersect the line for the value of η. Finally move horizontally to the left to read of the proximity coefficient, S_p, from the vertical axis of the upper plot. In the illustrated case, $\beta = 0.45$, $g \approx 0.8$, $A \approx 0.42$, $\eta = 3$ and $S_p = 1.025$.

For low values of the parameter *A*, and when *g* is small, the charts just described are not very accurate. Thus Figure 28 and Figure 29 may be used in these circumstances.

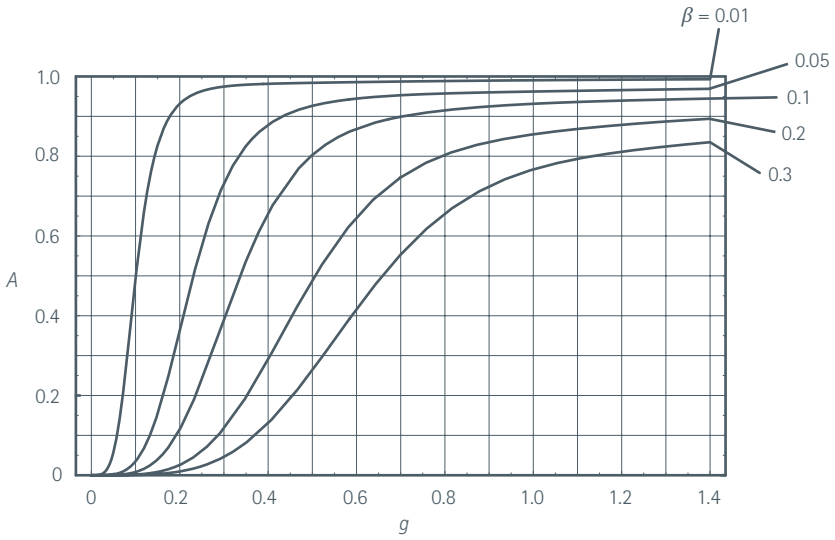

Figure 28 – Factor A for proximity loss factor as a function of $g = t/\delta$ for various values of $\beta = t/a$

The formula just derived applies to a single phase system with two parallel conductors. For three phase systems calculate μ:

$$\mu = \frac{A}{\eta^2}$$

where:

$$\eta = \frac{s}{2a}$$

Then for a triangular arrangement of three phase busbars

$$S_{ptriangular} \approx S_p\left(1 + \frac{\mu}{4} - \frac{5\mu^2}{24} - \frac{3\mu^8}{8}\right)$$

And for a flat arrangement the average proximity factor is

$$S_{pflat} \approx S_p\left(1 + \frac{\mu}{4} - \frac{\mu^2}{8} + \frac{5\mu^8}{24}\right)$$

For **small** spacings, i.e. for $\eta < 2$, the approximate formulae are rather bulky but the chart given in Figure 29 can be used.

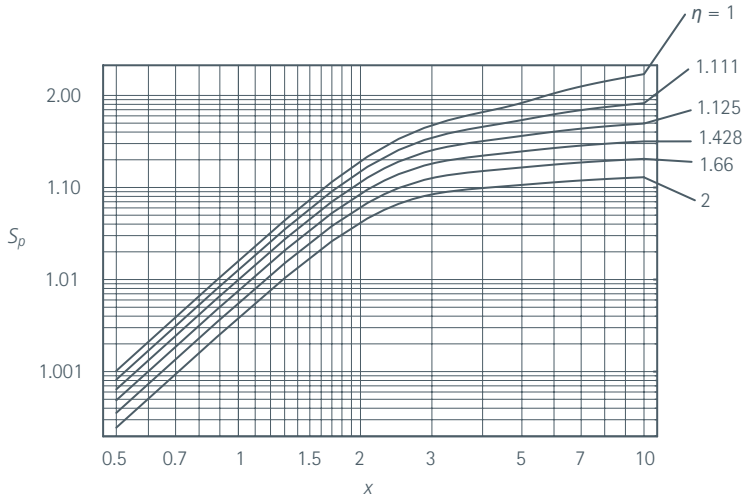

Figure 29 – Proximity factor, S_p, for round bars at various spacings designated by η as defined in the figure

The parameter *x* is given by:

$$x = \sqrt{2}\,\frac{a}{\delta}\,\sqrt{\beta(2-\beta)}$$

where:

δ is skin depth

a is tube radius

and

$$\beta = \frac{t}{a}$$

where:

t is the tube wall thickness.

Also, in SI units,

$$x = \frac{2\pi\mu_0 f}{R_{dc}}$$

with

R_{dc} in μΩ/m and

f in Hz

$$x = \frac{\sqrt{8}}{10}\pi\sqrt{\frac{f}{R_{dc}}} \approx 0.89\sqrt{\frac{f}{R_{dc}}} \approx \frac{1}{1.125}\sqrt{\frac{f}{R_{dc}}}$$

2A.1.3 Single Rectangular Sections

We consider here first single bars of rectangular cross-section which might be called strips or even straps. In subsections we consider single phases divided into two strips, separated from each other and carrying currents in the same direction. This leads to reduced losses. Then we consider a pair of bars carrying anti-parallel currents to form a single phase circuit. Finally, we consider three phase arrangements of bars carrying balanced positive phase sequence currents.

A portmanteau formula is given for a single bar, but not for the other arrangements, since none are available. The reason for the dearth is partly because it requires two or more parameters to describe the shape. Thus, resort must be made to graphs or detailed computation using a fairly complicated programme.

2A.1.3.1 Shape Factor for Rectangular Bars

There are no analytic formulae for this case. Resort must be made to numerical methods such as finite elements, finite differences or current simulation, i.e. particle elements.

Recollect that the parameter p is defined as:

$$p = \sqrt{2}\mu_0 \sqrt{\frac{f}{R_{dc}}} \approx 1.585 \sqrt{\frac{f}{R_{dc}}}$$

where:

f is frequency in Hz
R_{dC} is dc resistivity in μΩ/m

and

$$p = \sqrt{\frac{2}{\pi}} \frac{\sqrt{A}}{\delta} \approx 0.8 \frac{\sqrt{A}}{\delta}$$

where:

A is the cross-sectional area
δ is the skin depth

The area A and the skin depth must be in comparable units. Thus if δ is in mm then A must be in mm^2.

The following plots are of shape factor for strips of different cross-sectional proportions.

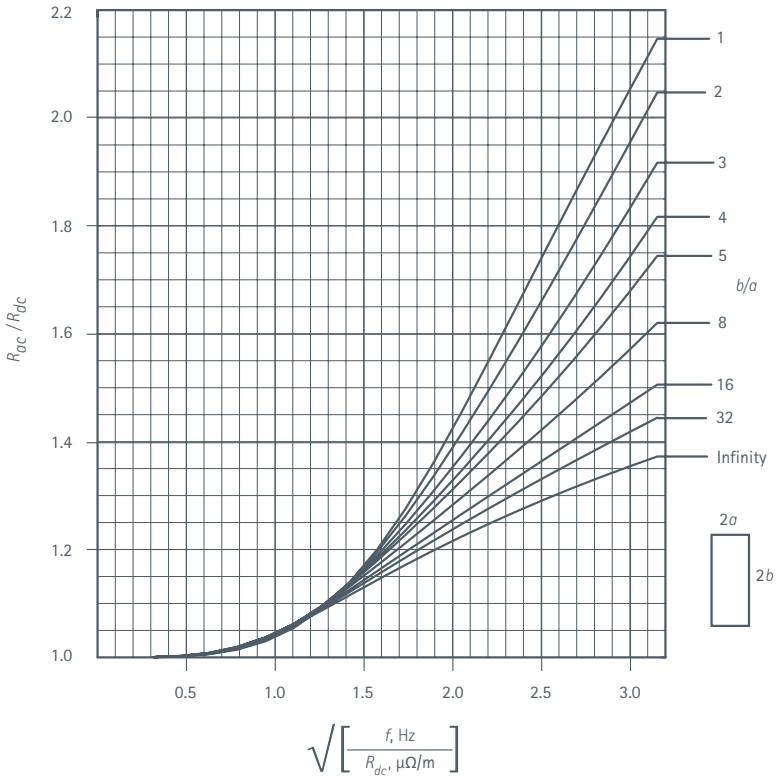

Figure 30 – R_{ac}/R_{dc} as a function of the parameter $\sqrt{f}/R_{dc}$

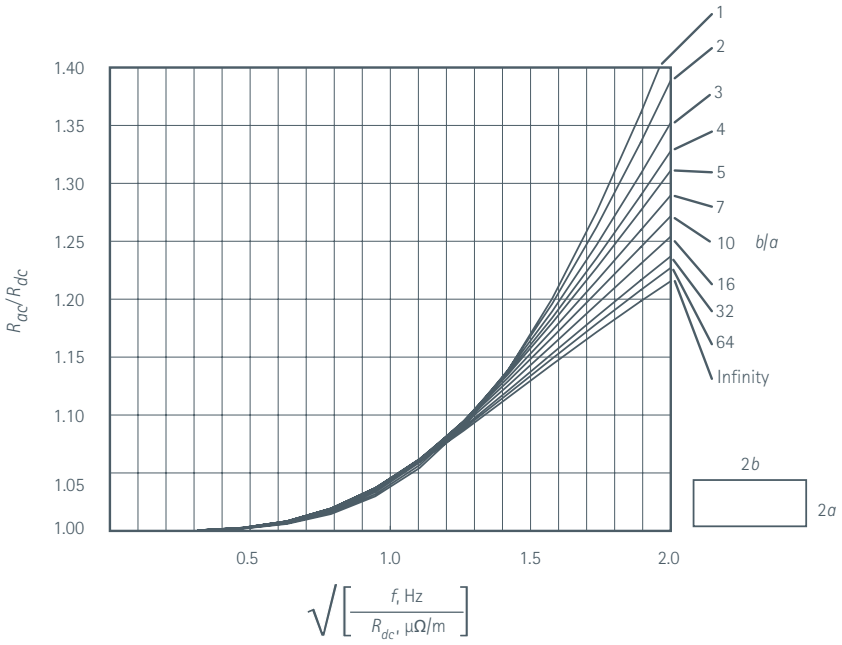

Figure 31 – R_{ac}/R_{dc} as a function of the parameter $\sqrt{f}/R_{dc}$. The range of the parameter is narrower than in the previous figure

At low values of p the curves for the different aspects ratios cross, as illustrated in Figure 32.

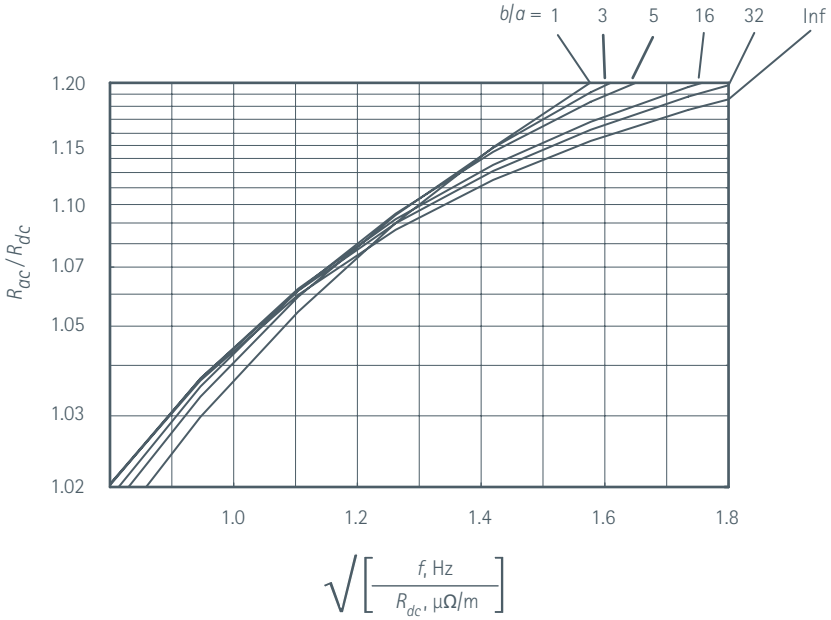

Figure 32 – Shape factor, R_{ac}/R_{dc}, as a function of the parameter $\sqrt{f}/R_{dc}$. Note the logarithmic scale for the shape factor and that the lines for constant b/a cross.

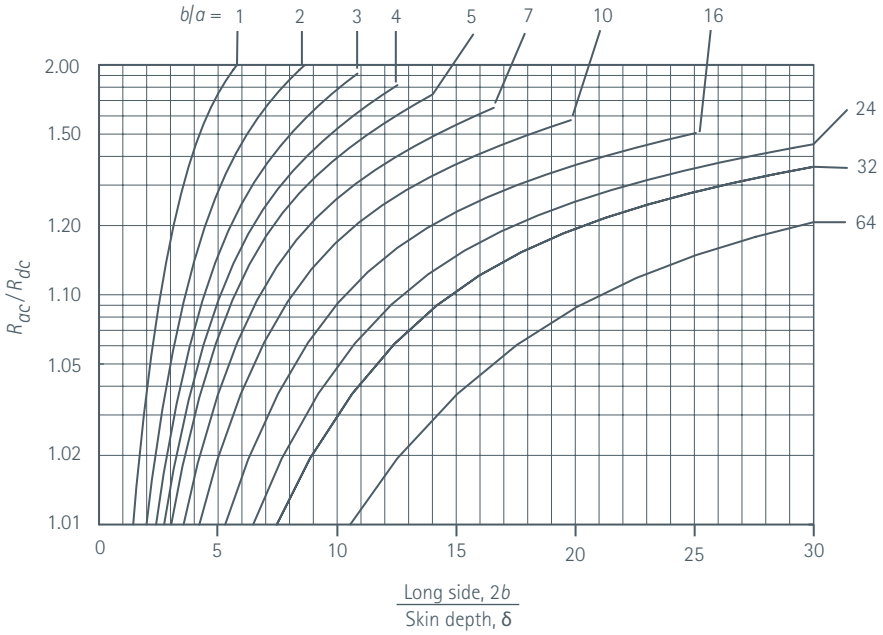

Figure 33 – Shape factor versus $2b/\delta$ for various values of b/a

For values of $\sqrt{(f/R_{dc})} < 1.25$ the thin sectioned bar has a slightly higher shape factor than the square conductor, whereas for higher values a thin shape gives a lower shape factor. For copper at 20˚C with $\rho = 17$ nΩ m the transitional cross-sectional area is about 500 mm^2; i.e. in old units, about 1 sq in. One may, however, prefer a thin strip of say 6 mm by 80 mm, which is more readily cooled because it has a larger vertical flat face. The increase in losses is of the order of one percent.

2A.1.3.2 Approximate Portmanteau Formula for Single Bars

An approximate formula which was made by curve fitting is:

$$S = \frac{R_{ac}}{R_{dc}} = 1 + \frac{a_s p^4}{1 + b_s p^2 + c_s p^4}$$

with

f in Hz and R_{dc} in μΩ/m

$$a_s = \frac{1 - 0.294A + 0.1795A^2}{147.8 - 31.55A + 11.57A^2}$$

$$b_s = \frac{1 - 0.933A + 0.91A^2}{31.81 - 6.77A + 2.46A^2}$$

$$c_s = \frac{1 - 0.41A + 0.11A^2}{226.46 - 5.3A + 5.35A^2}$$

with $A = b/a$

2A.1.4 Parallel Bars

2A.1.4.1 Proximity Factor – Anti-parallel Currents

The currents in adjacent bars induce eddy currents in neighbours. For thin wide strips placed with their long sides facing each other, there is usually a reduction in losses as the current becomes distributed more uniformly across the width of the strip. For lower values of b/a the losses increase. This is illustrated in the next graphs.

If the strips are too close together, the flow of coolant between them may be impaired, the temperature may rise, the resistance increase and so the ohmic losses become larger.

Figure 34 (a-e) shows the shape factor, R_{ac}/R_{dc}, as a function of the spacing expressed as s/a for various values of $\sqrt{f/R_{dc}}$. As before, f is in Hz and R_{dc} in μΩ/m.

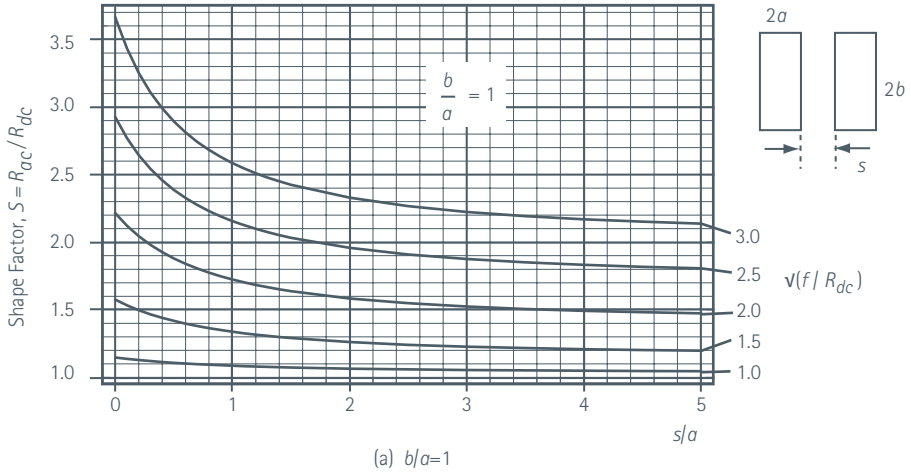

(a) b/a=1

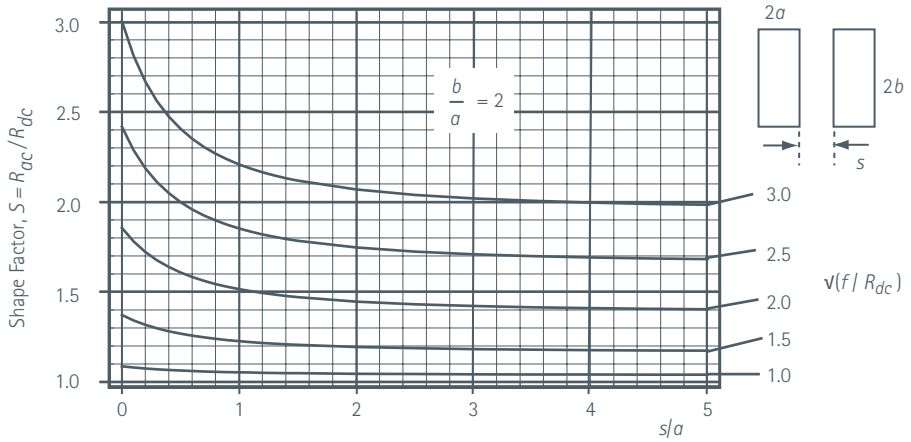

(b) b/a=2

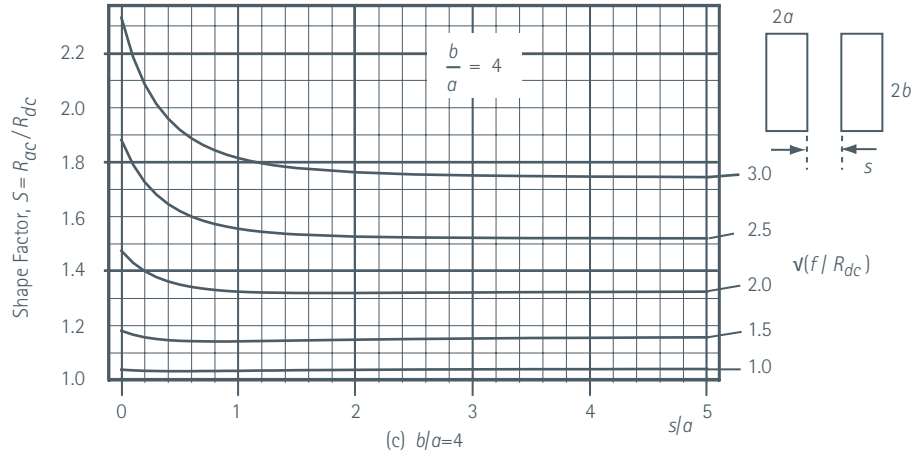

(c) b/a=4

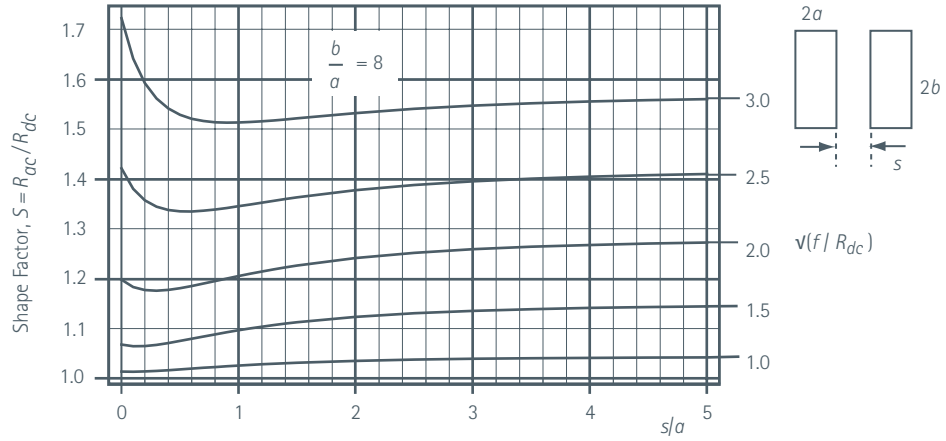

(d) b/a=8

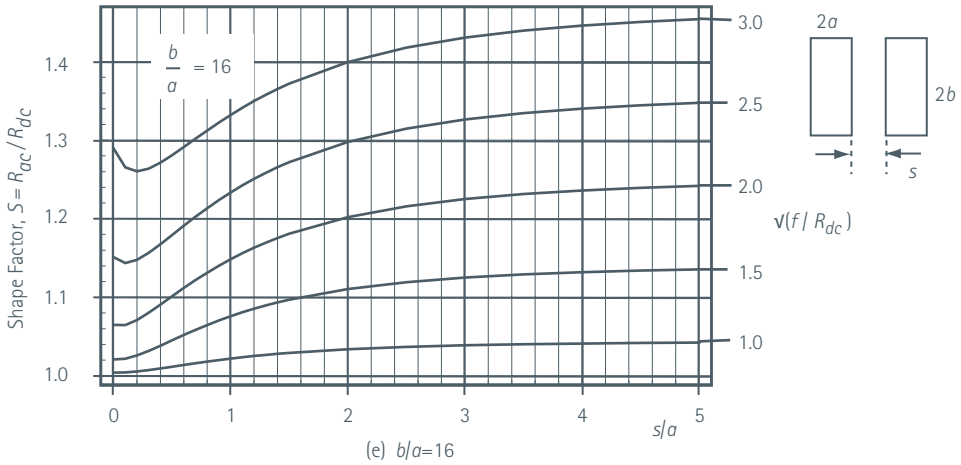

Figure 34 – Plots of the shape ratio $\frac{R_{ac}}{R_{dc}}$ versus the ratio $\frac{s}{a}$ for various values of $\sqrt{\frac{f}{R_{dc}}}$ for anti-parallel currents

2A.1.4.2 Proximity Factor – Parallel Currents

If a single busbar is replaced by two busbars of the same total cross-section, the losses may be reduced for one or more of three reasons:

1. The exposed surface area will be larger, the cooling more effective, the temperature lower, the resistivity lower and so losses lower.
2. The shape factor R_{ac}/R_{dc} will be reduced since the ratio for each bar will be lower. The reason for this is that the factor $\sqrt{f/R_{dc}}$ will be less for each bar than for the single bar, since R_{dc} of each bar will be twice that of a single bar. A lower value of $\sqrt{f/R_{dc}}$ means a lower shape factor.
3. The two new bars may be of improved shape so as to give rise to an even lower shape factor than the original design of single bar.

In considering how to design a divided bar, one may perhaps think of an original single bar and split it into two equal halves – for this reason, the width of the bars in this section is *a* rather than 2*a*, as used elsewhere. This is the idea behind the next plots.

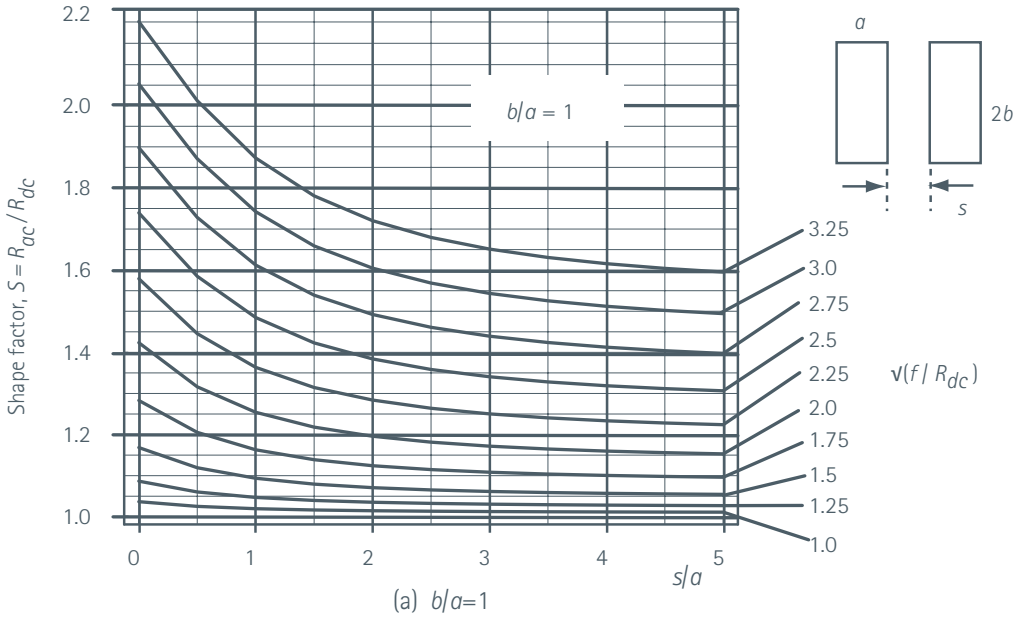

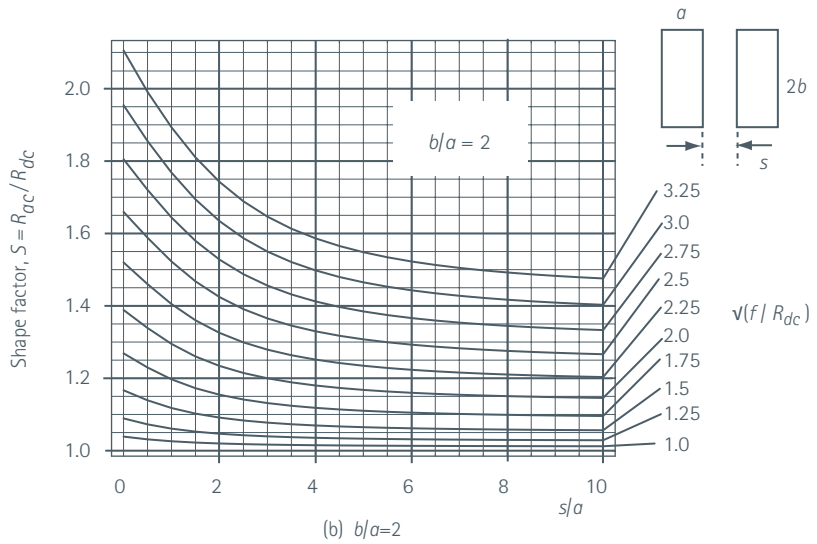

(b) b/a=2

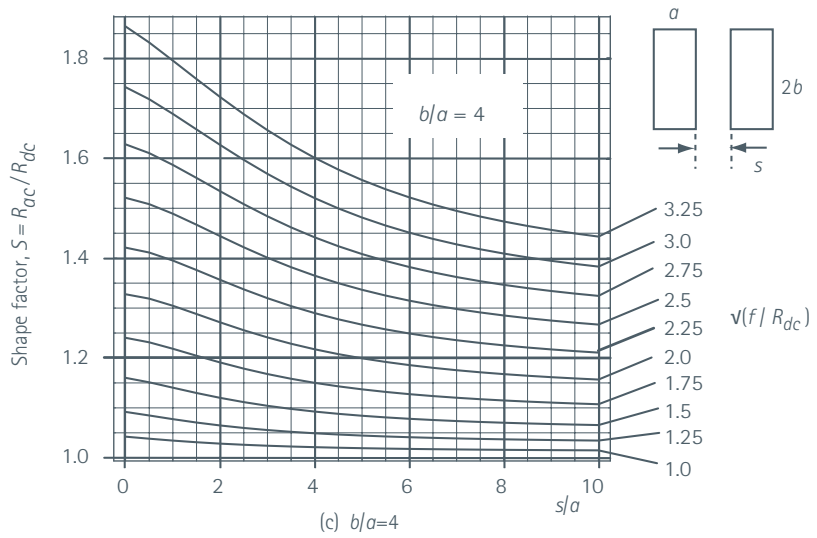

(c) b/a=4

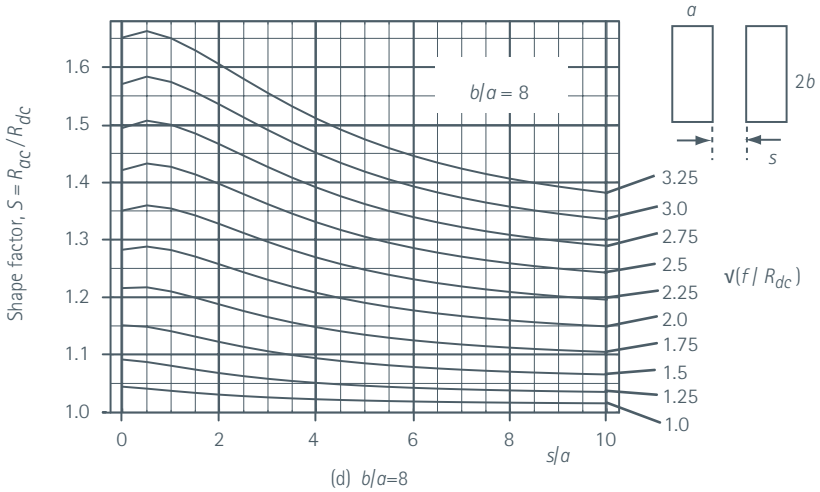

(d) b/a=8

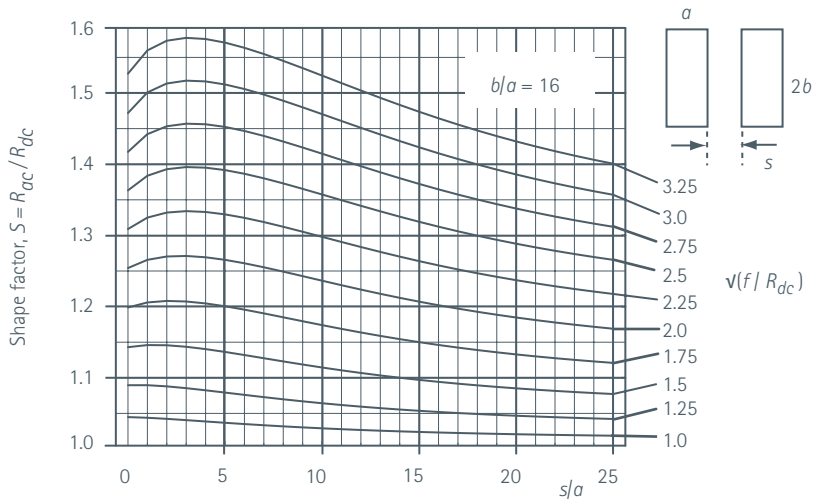

(e) b/a=16

Figure 35 – Shape factor $S = \frac{R_{ac}}{R_{dc}}$ as a function of the separation s for various values of $\sqrt{\frac{f}{R_{dc}}}$ with R_{dc} in μΩ/m and f in Hz

2A.1.5 Three-phase Configurations

In the following plots, the resistance to balanced three-phase positive sequence currents is shown. There will also be zero sequence and negative sequence voltages but these produce no losses and are anyway smaller than the positive phase sequence voltages.

2A.1.5.1 Linear Plots

The shape factor R_{ac}/R_{dc} is shown in Figure 36 as a function of the parameter p for various aspect ratios of the bar layout.

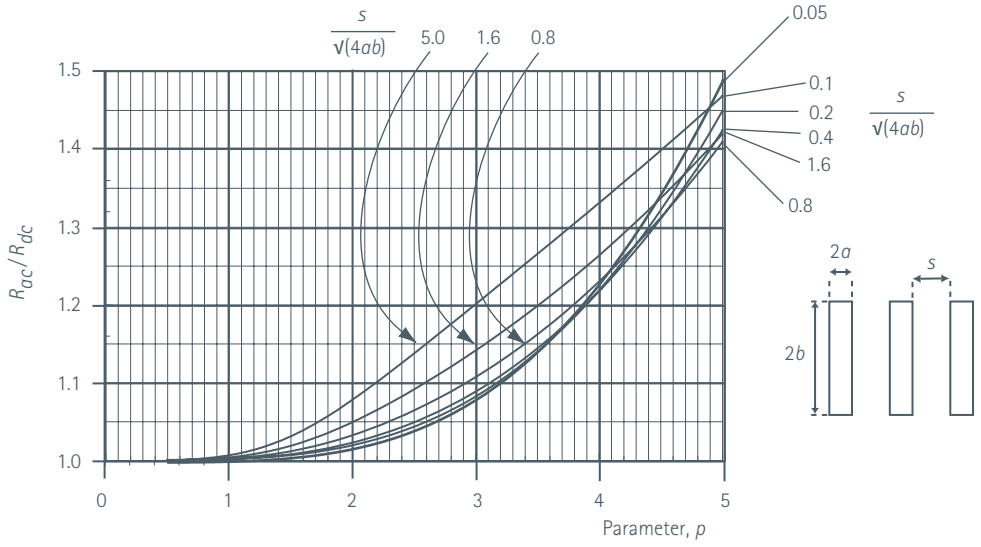

(a) b/a=16

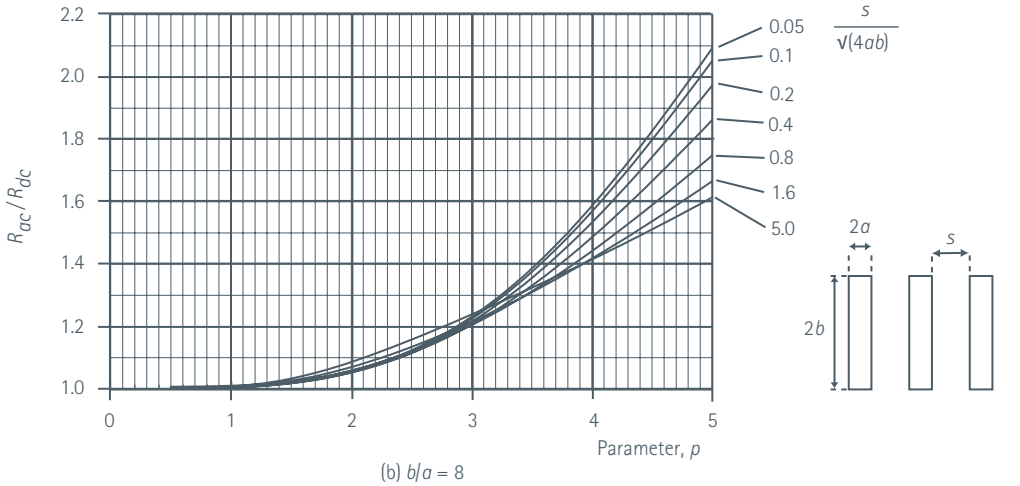

(b) $b/a = 8$

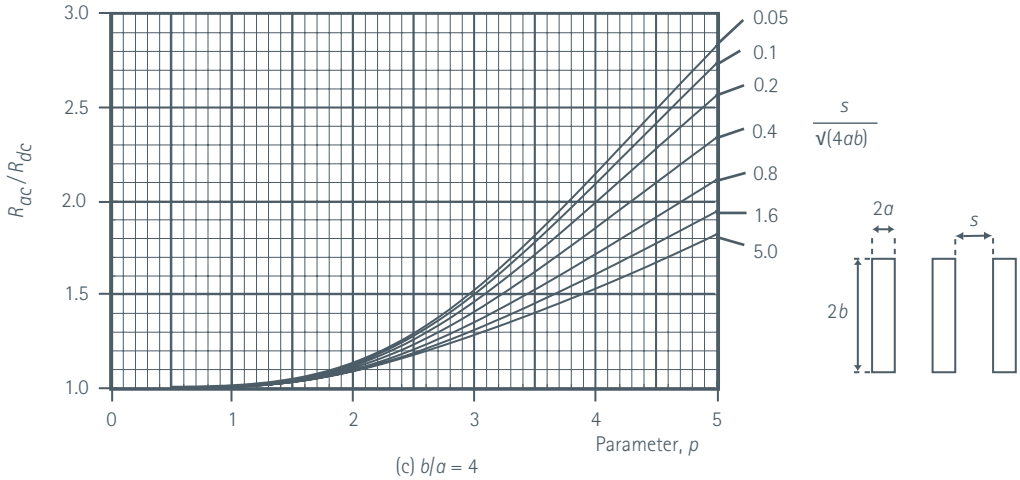

(c) $b/a = 4$

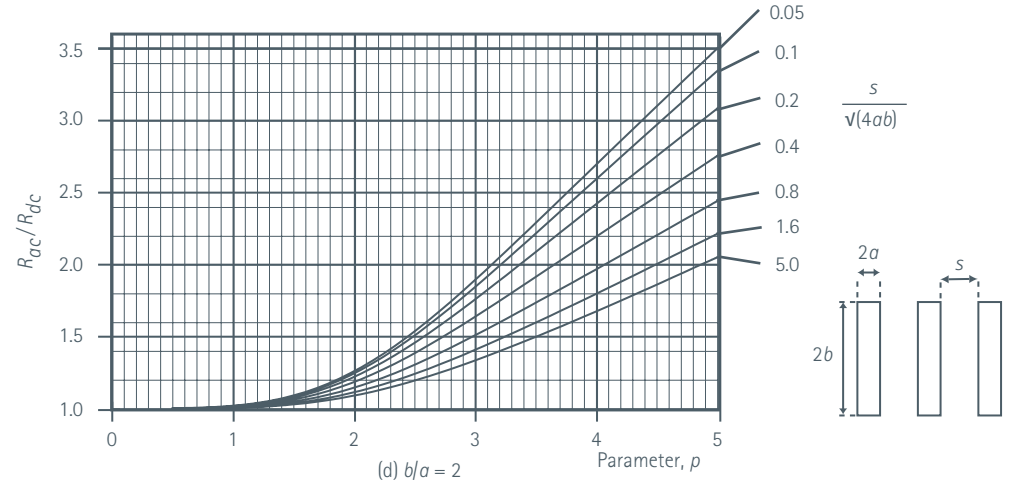

(d) $b/a = 2$

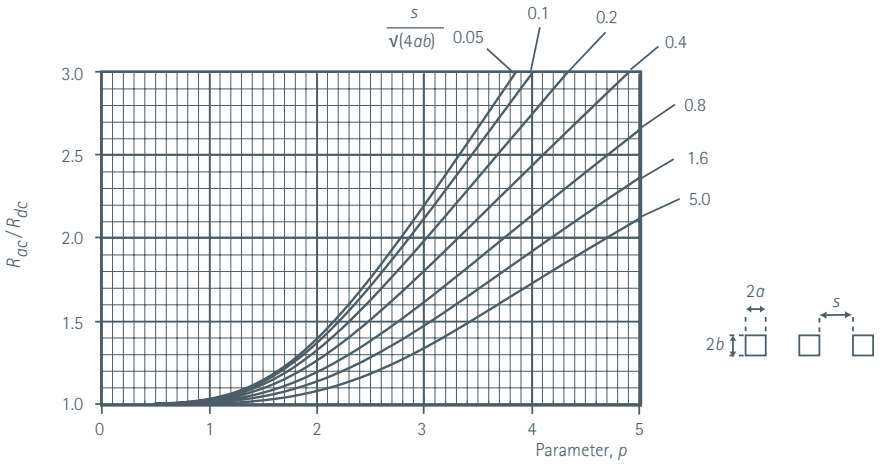

(e) $b/a = 1$

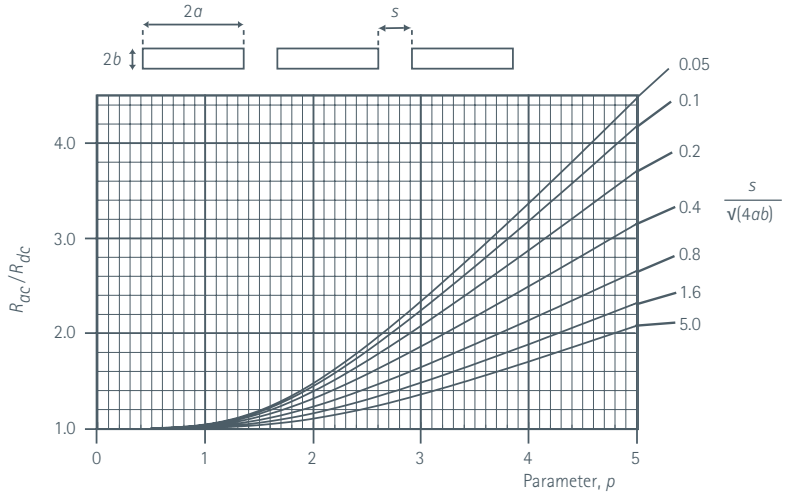

(f) $a/b = 2$

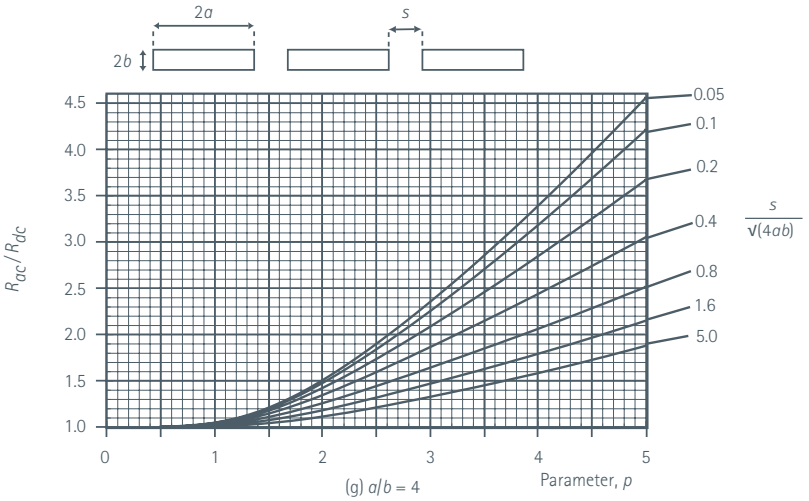

(g) $a/b = 4$

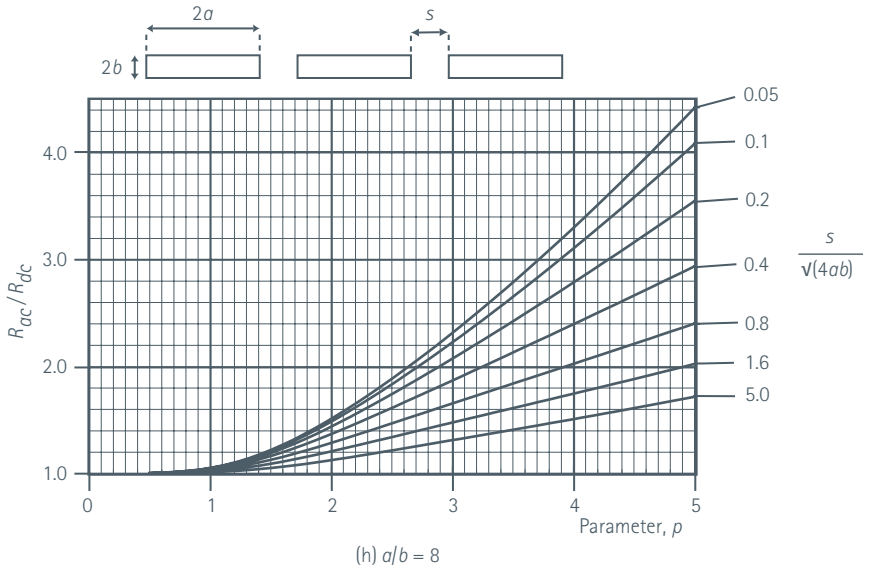

(h) $a/b = 8$

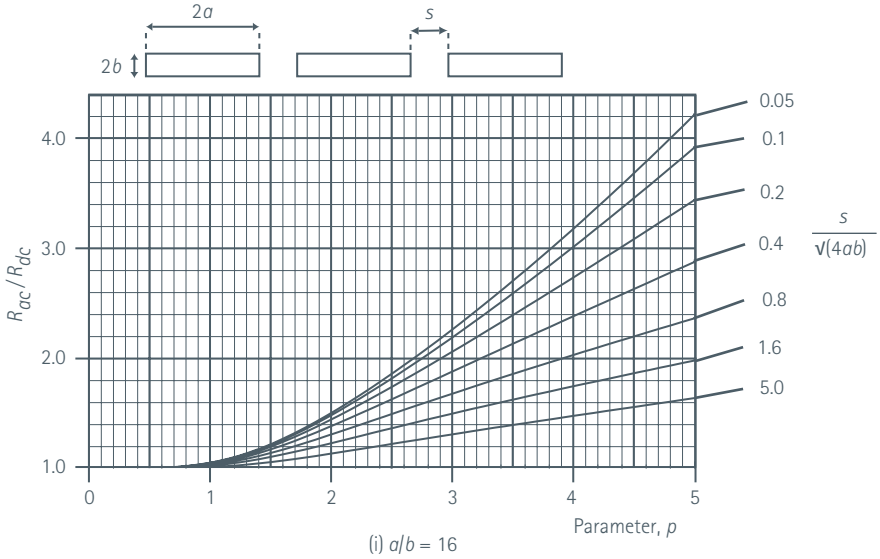

(i) $a/b = 16$

Figure 36 – Linear plots of R_{ac}/R_{dc} versus p where $p \approx 1{\cdot}5853\sqrt{\frac{f}{R_{dc}}}$ with R_{dc} in μΩ/m and f in Hz

2A.1.5.2 Logarithmic Plots

For lower losses, using a pseudo-logarithmic scale for R_{ac}/R_{dc} gives clearer plots, as shown in Figure 37.

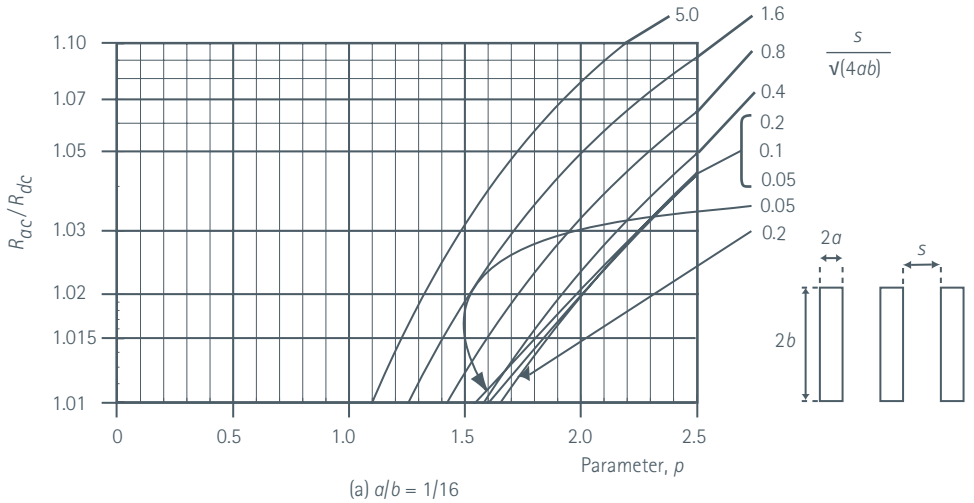

(a) $a/b = 1/16$

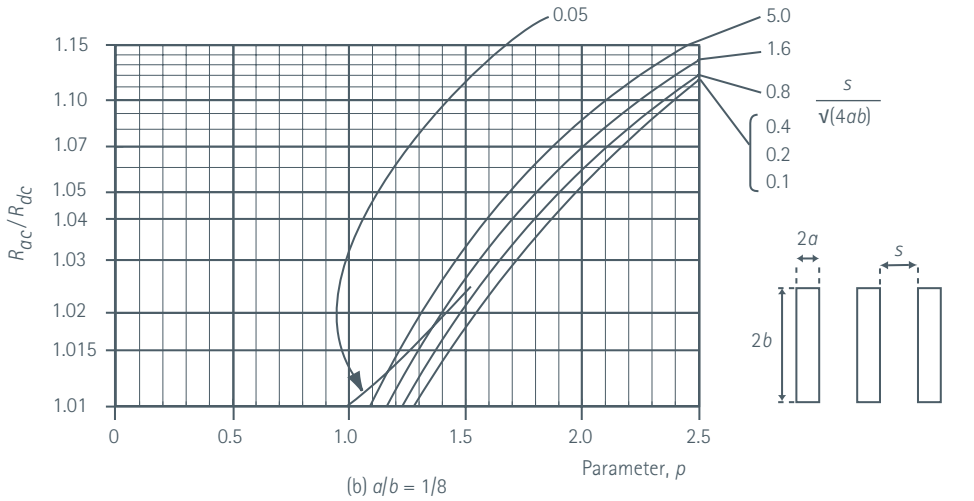

(b) $a/b = 1/8$

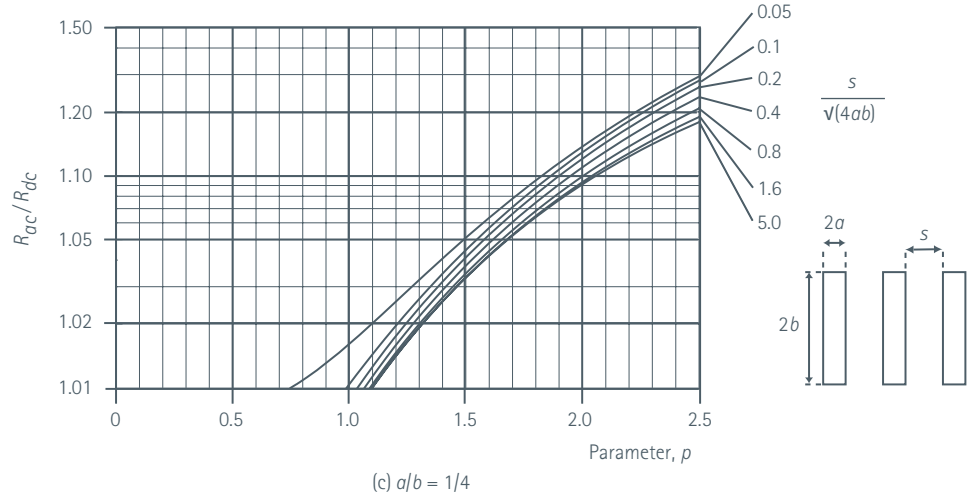

(c) $a/b = 1/4$

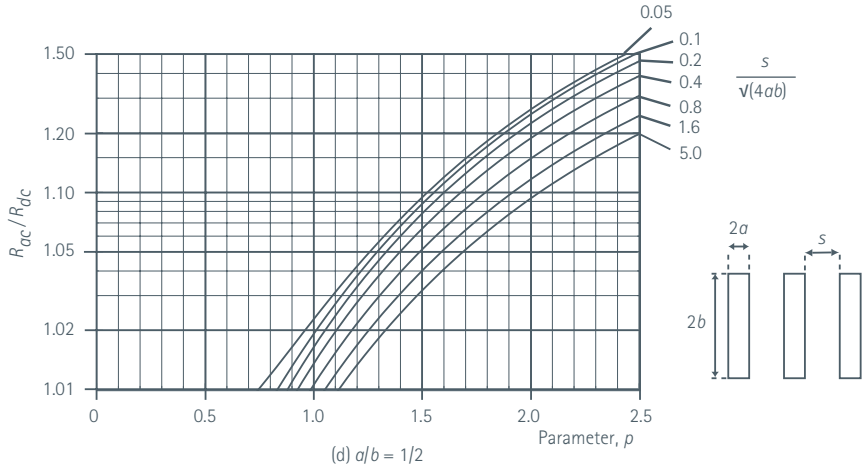

(d) $a/b = 1/2$

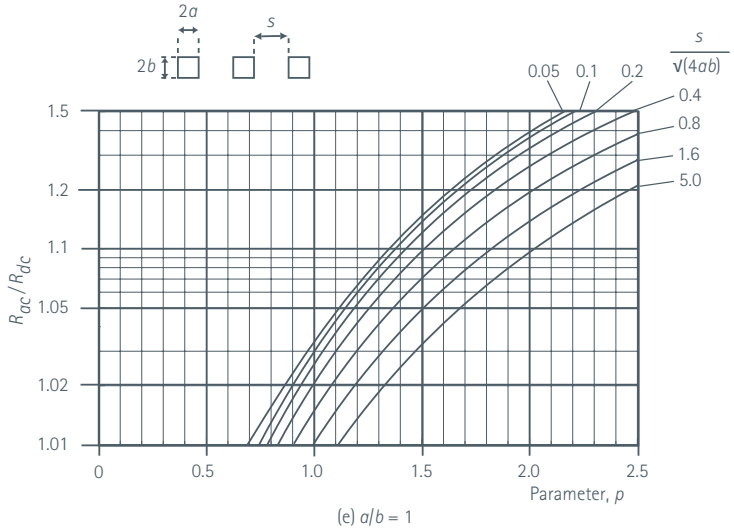

(e) $a/b = 1$

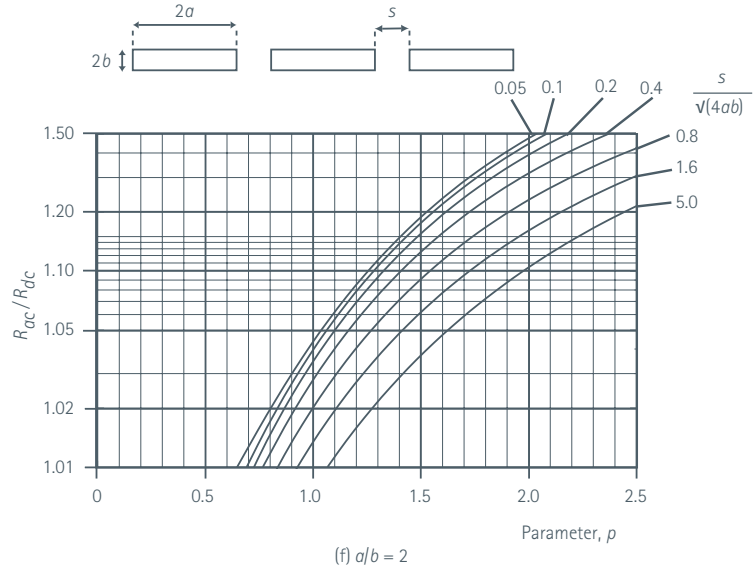

(f) $a/b = 2$

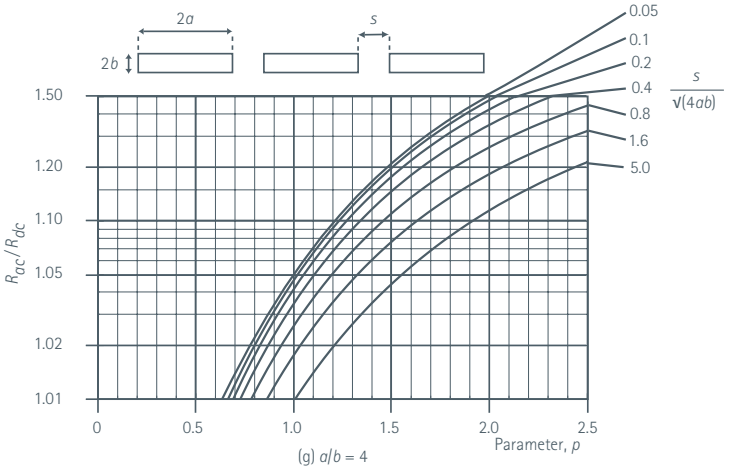

(g) $a/b = 4$

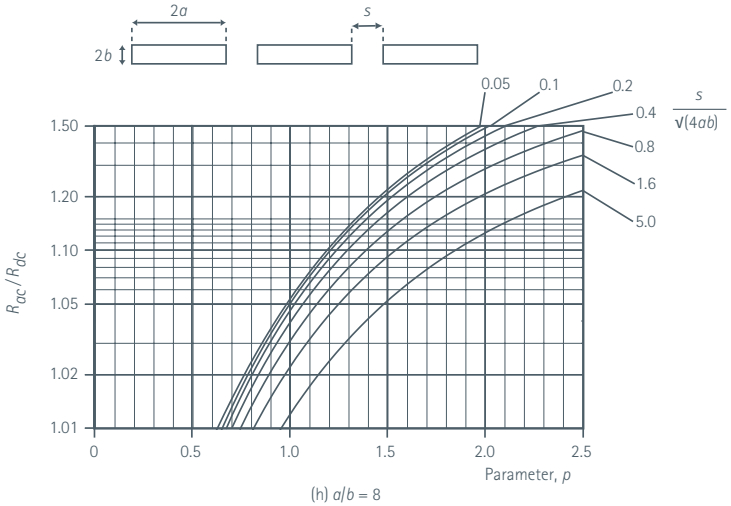

(h) $a/b = 8$

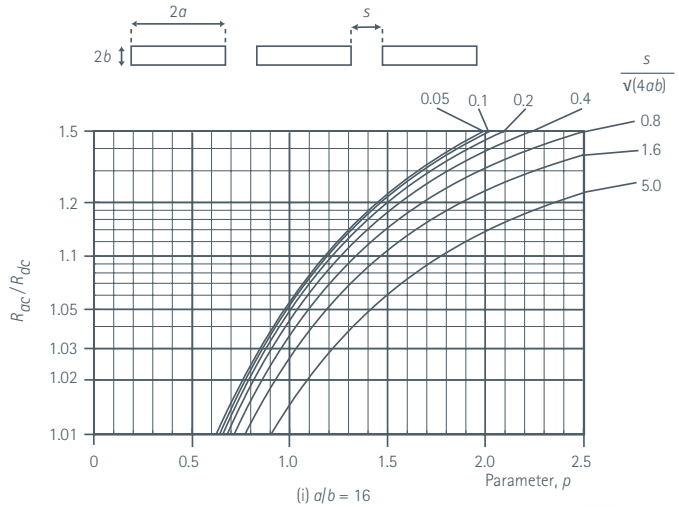

(i) $a/b = 16$

Figure 37 – Quasi logarithmic plots of R_{ac}/R_{dc} versus p where $p \approx 1{\cdot}5853\sqrt{\frac{f}{R_{dc}}}$ with R_{dc} in μΩ/m and f in Hz

3.0 Life Cycle Costing

David Chapman

3.1 Introduction

Life Cycle Costing (LCC) is a technique used to estimate the total costs of a project, installation or facility during the whole of its economic life, taking into account all costs and benefits. The use of LCC enables organisations to maximise the output value they generate for the available input resources. In the case of private enterprise, this means increasing profit – maximising the bottom line. In the case of public services, increased value means improving the quality and quantity of the services provided commensurate with the level of funding available.

In the context of electrical installation design, LCC is used to inform design choices. Usually, this means that all the costs, including investment cost, running costs and end-of-life costs, are compared for design options. Since the objective is to minimise the lifetime cost rather than to determine it, everything that remains the same for each design option can be ignored, simplifying the analysis and allowing greater focus on the differences.

This is a departure from the normal approach, in which the installation is designed to minimise initial cost with little regard to the future; an example might be the selection of a damper controlled ventilation system (which would be cheap to buy but very expensive to run) rather than, say, a variable speed fan, which would be more expensive to buy, but much cheaper to run.

In established facilities, the existing structures, operating procedures and technology already in use will determine the life cycle costs of many processes but, when new production lines or services are introduced or updated, or when additional facilities are constructed, there is an opportunity to specifically design the infrastructure using life cycle costing to achieve the lowest lifetime cost.

Often the focus on lifetime cost reveals that, because of the high cost of energy, the running costs are by far the greatest part of the total cost, meaning that the lowest life cycle cost design is one in which energy consumption has been carefully considered.

The advantage of LCC is obvious, so why is it so often ignored?

The first reason is that the benefit of LCC – primarily lower annual running costs – are an advantage to the operator of the facility, while the quick profit gained by installing the lowest price equipment is a benefit to the M&E contractor. Solving this issue requires the client – the building operator – to specify requirements to be met by the M&E contractor concerning operating costs.

Another reason is the perceived difficulty of assessing financial parameters, such as the cost of energy, discount rates, etc. for some time into the future. However, when LCC is used as a comparative tool to assess the relative costs of different design approaches, different equipment choices or different standards for installation practice, precise information is not needed – the objective is to determine, with a good degree of certainty, the lowest cost, rather than the exact cost. Performing a sensitivity analysis, by estimating the LCC for each option using a few values representing the predicted maxima and minima, improves confidence in the result.

A third perceived problem is that of dealing with risk in the project. Business decisions are always subject to change, perhaps due to changes in market conditions or technological advances leading to the installation becoming obsolete, so that it is sometimes difficult to define 'lifetime'. This concern, coupled with occasionally volatile economic conditions, led to the adoption of a rather conservative view of investment which required short payback times. This encouraged a 'lowest investment cost' approach, arguing that the smaller the sum invested, the easier it should be to recover and the lower the risk. Expressing all the costs in terms of their net present value (NPV) discounts future financial sums and reflects the possibility that the project may not be viable for as long as expected.

3.1.1 The Future Value of Money – Net Present Value

A sum of money which is to be paid or received some time in the future does not have the same value as the same sum of money today. This is because money available today could be invested to generate a profit or used to pay an outstanding debt but, since money is not available, it would need to be borrowed. A sum promised in the future cannot be committed and so has less value today. This is very relevant to the assessment of life cycle cost since costs and benefits that accrue in the later years would be given undue weight if they were included at full value.

The problem in assessing the lifetime cost is that the setting up costs occur at the beginning of the project while the costs of energy losses occur over a long period of time, so it is necessary to add together costs which arise, and have to be paid for, at different times. This is where the time value of money must be included in the calculation.

The simple addition of all future energy costs to the initial costs would be to imagine that sufficient money is to be put aside at the start of the project to pay all future bills or, put another way, that all future bills for energy costs would be paid in full at the start of the project.

This would not be an economical way to make provision for future payments and would unnecessarily inflate the total cost of the project. A more practical way would be to consider what the energy costs would be worth if the money were to be set aside to earn interest until the time came to pay each bill. It is evident that this procedure would require smaller amounts to be set aside.

It is common practice to express all costs and benefits in terms of 'Net Present Value' (NPV) at the start of the project using an appropriate 'discount rate'. The discount rate depends to a large extent on the cost of financing the business which will be determined by, for example, commercial interest rates and the cost of raising money from the markets, but it will also include an allowance for risk.

Allowing for risk can be complex. In a commercial building the risk may be low because the organisation is likely to continue to require the facility even though the business focus may change. In other areas, such as advanced technology, the risk may be very high; the development of practical electric vehicles requires many technological advances coupled with extensive infrastructure and behavioural changes which are not within the control of the vehicle developer and may not happen without timely policy initiatives. Higher perceived risk implies a higher discount rate.

The discount factor, *r*, to be applied to sums for a particular year, is given by:

$$r = \frac{1}{\left(1 + \frac{i}{100}\right)^n}$$

where:

n is the number of years since the start
i is the discount rate (%).

Table 8 below shows the annual discount factors for various discount rates over a period of 20 years.

Table 8 – Discount Factors for Various Discount Rates

	Discount Rate (%)									
Year	**1**	**2**	**3**	**4**	**5**	**6**	**7**	**8**	**9**	**10**
0	1	1	1	1	1	1	1	1	1	1
1	0.990	0.980	0.971	0.962	0.952	0.943	0.935	0.926	0.917	0.909
2	0.980	0.961	0.943	0.925	0.907	0.890	0.873	0.857	0.842	0.826
3	0.971	0.942	0.915	0.889	0.864	0.840	0.816	0.794	0.772	0.751
4	0.961	0.924	0.888	0.855	0.823	0.792	0.763	0.735	0.708	0.683
5	0.951	0.906	0.863	0.822	0.784	0.747	0.713	0.681	0.650	0.621
6	0.942	0.888	0.837	0.790	0.746	0.705	0.666	0.630	0.596	0.564
7	0.933	0.871	0.813	0.760	0.711	0.665	0.623	0.583	0.547	0.513
8	0.923	0.853	0.789	0.731	0.677	0.627	0.582	0.540	0.502	0.467
9	0.914	0.837	0.766	0.703	0.645	0.592	0.544	0.500	0.460	0.424
10	0.905	0.820	0.744	0.676	0.614	0.558	0.508	0.463	0.422	0.386
11	0.896	0.804	0.722	0.650	0.585	0.527	0.475	0.429	0.388	0.350
12	0.887	0.788	0.701	0.625	0.557	0.497	0.444	0.397	0.356	0.319
13	0.879	0.773	0.681	0.601	0.530	0.469	0.415	0.368	0.326	0.290
14	0.870	0.758	0.661	0.577	0.505	0.442	0.388	0.340	0.299	0.263
15	0.861	0.743	0.642	0.555	0.481	0.417	0.362	0.315	0.275	0.239
16	0.853	0.728	0.623	0.534	0.458	0.394	0.339	0.292	0.252	0.218
17	0.844	0.714	0.605	0.513	0.436	0.371	0.317	0.270	0.231	0.198
18	0.836	0.700	0.587	0.494	0.416	0.350	0.296	0.250	0.212	0.180
19	0.828	0.686	0.570	0.475	0.396	0.331	0.277	0.232	0.194	0.164

Energy prices are likely to increase over the lifetime of the project so the cost will increase each year by the factor:

$$1 + \frac{b}{100}$$

where *b* is the expected average percentage rate of increase of energy prices or, in the absence of information, the rate of general inflation, over the project lifetime.

It is also likely that the load carried by the busbar system will grow over the life of the installation and this must to be taken into account in two ways.

Firstly, the cost of energy in later years must be modified accordingly. Although load changes will occur at discrete (and unknown) points in the system lifetime, it is easier to assume that they occur at a uniform rate. The correction factor for each year is:

$$\left(1 + \frac{a}{100}\right)^2$$

where *a* is the average percentage increase in load current over the project lifetime.

Secondly, the system must be designed, from a safety point of view, to cope with the final load current which is given by

$$I_f = I_i \times \left(1 + \frac{a}{100}\right)^N$$

where:

I_f is the load current at end of life
I_i is the initial load current
N is the circuit lifetime in years.

The overall correction factor, including discount rate, becomes:

$$r = \frac{\left(1 + \frac{a}{100}\right)^2 \times \left(1 + \frac{b}{100}\right)}{1 + \frac{i}{100}}$$

The NPV of the lifetime energy cost is therefore

$$NPV = C(r + r^2 + r^3 + \cdots + r^{N-1} + r^N)$$

where:

N is the project lifetime in years
C is the first year cost

or

$$NPV = Cr(1 + r + r^2 + \cdots + r^{N-2} + r^{N-1})$$

The term in parentheses in the equation above is a standard series so that

$$NPV = Cr\frac{(1 - r^N)}{(1 - r)}$$

and

$$NPV = CQ$$

where Q, the discount ratio, is given by

$$Q = r\frac{(1-r^N)}{(1-r)}$$

Note that if $r = 1$, the equation for Q cannot be evaluated, but from the original series it can be seen that in that case $Q = N$.

3.1.1.1 Monthly Payments

Electricity accounts are usually settled each month, even though agreements with regard to prices and financial matters may be made annually. In this case the following modifications to the derivation of the discounting factor Q may be appropriate. The difference in the value of NPV from that based on annual payments is small.

Define the monthly value of r as r_m where

$$r_m = \sqrt[12]{r}$$

Now, if the life of the project is N years, there will be $12N$ payments so the NPV is given by

$$NPV = C_m r_m (1 + r_m + r_m^2 + \cdots + r_m^{12N-2} + r_m^{12N-1})$$

$$NPV = C_m r_m \frac{(1-r_m^{12N})}{(1-r_m)}$$

But since

$$r_m = \sqrt[12]{r}$$

then

$$NPV = C_m r_m \frac{(1-r^N)}{(1-r_m)}$$

and

$$Q_m = r_m \frac{(1-r^N)}{(1-r_m)}$$

Examples

For an installation with a projected life of 10 years and a discount rate of 5%, assuming 0% energy cost inflation and no load growth, paid annually,

$$r = \frac{1}{1.05} = 0.95238$$

$$Q = 0.95238 \times \frac{(0.38609)}{(0.04762)} = 7.7216$$

$$NPV = First\ year\ energy\ cost \times 7.7216$$

If paid monthly,

$$r_m = \sqrt[12]{0.95238} = 0.995942$$

$$Q_m = 0.995942 \times \frac{(1-0.95238^{10})}{1-0.995942} = 0.995942 \times \frac{0.38609}{0.004058} = 94.76$$

$$NPV = First\ month\ energy\ cost \times 94.76$$

For the same installation with a discount rate of 5%, energy price inflation of 3% and an average load current growth of 2%,

$$r = \frac{\left(1 + \frac{2}{100}\right)^2 \times \left(1 + \frac{3}{100}\right)}{1 + \frac{5}{100}}$$

$$r = \frac{(1.02)^2 \times 1.03}{1.05} = 1.020583$$

Note that r is > 1.

$$Q = 1.020583 \times \frac{-0.29049}{-0.020583} = 14.4$$

$$NPV = First\ year\ energy\ cost \times 14.4$$

3.1.2 Loading

Few installations run at full load continuously. The maximum current must be used to select the initial conductor size and protective device rating but, for financial purposes, the rms average load must be used. This requires some knowledge about the load profile. To find the rms load, the profile is divided into a number of equal timeslots and the square of each current value calculated. The squares for all the time slots are summed, averaged and the root value calculated. The result is that current which, if it flowed continuously, would be equivalent to the actual load.

However, there is a problem with this method because the temperature of the busbar, and therefore the resistance, changes with current, meaning that energy losses for periods of low currents are overestimated, while those for periods of high current are underestimated. In practical terms the effect is small; firstly, the error is unlikely to shift the choice of bar size from one standard size to another and, secondly, for an optimised bar the current density is lower so the temperature rise, and therefore the variation, is much smaller.

Where the load profile is more complex, or there is a need for great accuracy, the suggested approach is to construct a straight line approximation of the load profile, calculate the energy loss at each current level and then determine the time average of the energy loss.

3.1.3 Lifetime

Lifetime can have several meanings. At the design stage, lifetime is the period for which the installation is expected to be needed to fulfil its original purpose. For a product line this may be quite short, while for a commercial building it will be rather longer. In practice, installations are often used for far longer because, for example, new products can be manufactured using the same installation, perhaps with small modifications. The useful lifetime is therefore longer than the initial 'economic' lifetime. The result is that the initial assessment – for the economic lifetime - gives a lower weight to running costs than would have been the case for the actual lifetime. It also delays the end-of-life so any benefit from recovering scrap conductor material is very heavily discounted so that it does not influence the financial decision.

3.1.4 Sensitivity Analysis

In most cases it will not be possible to accurately know all the data, for example, the design of the plant may not be finalised and future electricity costs cannot be determined accurately, so it is necessary to test the result to check how dependent the appraisal is on each variable and make an appropriate judgement.

3.2 Application to an Electrical Installation

Engineering design is always concerned with compromise within the boundaries of the design requirement. The functional requirements must be met, of course, but there are many ways of doing so; using more final circuits will provide more flexibility and better isolation for sensitive loads, while using larger conductor cross-sections will reduce energy losses and voltage drop resulting in lower energy losses and better dip resilience. Specifying energy efficient load equipment will reduce energy consumption. Each of these decisions has an impact on the future running costs of the installation in both energy and maintenance costs and an impact on the cost of the installation and its commissioning.

3.2.1 Installation Design

Many design decisions will be made based on the designer's experience of having done similar designs in the past and, for many parts of an installation, the 'business-as-usual' installation may also be the one with the lowest LCC because the base level is set by installation standards. For other areas there is an opportunity to reduce the LCC by optimising the design. For example:

1. Selecting energy efficient equipment will reduce energy costs. This includes, for example, transformers, motors, pumps and fans.
2. Considering energy efficiency when determining the conductor size for cables and busbars will reduce energy losses considerably in circuits feeding heavy loads. The 5% voltage drop at the load terminals, permitted by standards, represents an efficiency of only 95% - for a length of conductor! Unless the duty factor of the load is low, designing for a much lower voltage drop makes sense and reduces the LCC.
3. Designing for reliability by using separate dedicated circuits for sensitive equipment and heavy fluctuating loads and designing for reduced voltage drop in the installation to improve resilience against voltage disturbances will reduce downtime and maintenance costs, reducing the LCC.

The decisions made at the design stage determine the scale of the LCC, so this stage is extremely important – it is worth investing time in this process to reduce future costs.

3.2.2 Installation Costs

The installation costs include all the electrical design and installation costs for the project and, since they all occur at the start of the project, are therefore taken into account at full cost. When comparing the LCCs of different design options, only those elements that vary would need to be taken into account.

3.2.3 Recurring Costs

Recurring annual costs generally fall into two categories:

3.2.3.1 Maintenance Costs

All facilities require a certain amount of expenditure on maintenance. Reducing this requirement by, for example, designing for a lower working temperature to give a longer, more reliable life, or choosing lighting equipment with a long service life to reduce replacement frequencies, can significantly reduce costs.

3.2.3.2 Energy

Energy is expensive and the present upward trend is likely to continue making energy costs extremely important. In many industrial processes, energy cost accounts for the majority of the total lifetime cost, so measures taken to increase energy efficiency at the design stage are often extremely cost-effective. LCC provides a methodology to determine the economic optimum conductor size for a given loading and duty cycle.

However, designers must also consider voltage drop. Standard installation practice allows a maximum 5% voltage drop between the origin of the installation and the load terminals. In many cases, this condition will be met or exceeded by the conductor size corresponding to the economic optimum, but this cannot be assumed. For example, the economic optimum conductor size for a load with a low duty factor may be relatively small, but the conductor length may introduce an excessive voltage drop. The installation designer must take care to allocate the voltage drop 'budget' to the various parts of the installation and, because busbars tend to be used in the higher current parts of the system, they deserve greater attention. The voltage drop should always be checked once the economic optimum has been determined.

The questions that have to be answered are: what is the conductor size with the lowest LCC for a given circuit load, duty factor and lifetime, and is the voltage drop sufficiently low?

The following simple example calculates the total cost – conductor cost plus energy loss - for a simple single phase circuit using a range of cross-sections and a range of operating times. The circuit feeds a load of 500 A.

Table 9 lists the maximum working current for a range of vertically mounted busbars, assuming an ambient temperature of 35ºC and a working temperature of 90ºC, operating in free air. The material costs listed are based on a copper price of $7500 per tonne.

Note that the current-carrying capacity of a bar is not proportional to the cross-sectional area (assuming the same ambient and working temperatures etc). This is because convection becomes less efficient for larger bars since the air cooling flowing up the face at the top of the bar has already been warmed as it flows up the bottom of the face. Consequently, the maximum busbar rating cannot be directly scaled although, since the difference is not very large, scaling can be used to estimate the starting point for calculation.

Table 9 – Maximum Working Current for a Range of Busbar Sizes

Width (mm)	Thickness (mm)	Area (mm^2)	Weight (kg)	Max Current (A)	Material Cost (€)
25	6.3	158	1.403	530	7.518
31.5	6.3	198	1.768	639	9.472
40	6.3	252	2.245	776	12.029
50	6.3	315	2.807	932	15.036
63	6.3	397	3.536	1127	18.945
80	6.3	504	4.491	1390	24.057
100	6.3	630	5.613	1662	30.071
125	6.3	788	7.017	1987	37.589
160	6.3	1008	8.981	2433	48.114

In Table 10 the power loss for each metre length of busbar at a current of 500 A is shown, calculated at the estimated working temperature (which is different for each size - see '2.0 Current-Carrying Capacity').

Table 10 – Resistance and Power Loss at 500 Amps

Width (mm)	Thickness (mm)	Area (mm^2)	Max Current (A)	Resistance at 20ºC (µohm/m)	Resistance at working temperature (µohm/m)	Loss at 500 Amp (W/m)
25	6.3	158	530	109.460	138.100	34.53
31.5	6.3	198	639	86.873	104.647	26.16
40	6.3	252	776	68.412	79.637	19.91
50	6.3	315	932	54.730	62.164	15.54
63	6.3	397	1127	43.436	48.462	12.12
80	6.3	504	1390	34.206	37.889	9.47
100	6.3	630	1662	27.365	29.982	7.50
125	6.3	788	1987	21.892	23.635	5.91
160	6.3	1008	2433	17.103	18.465	4.62

This data is plotted in Figure 38.

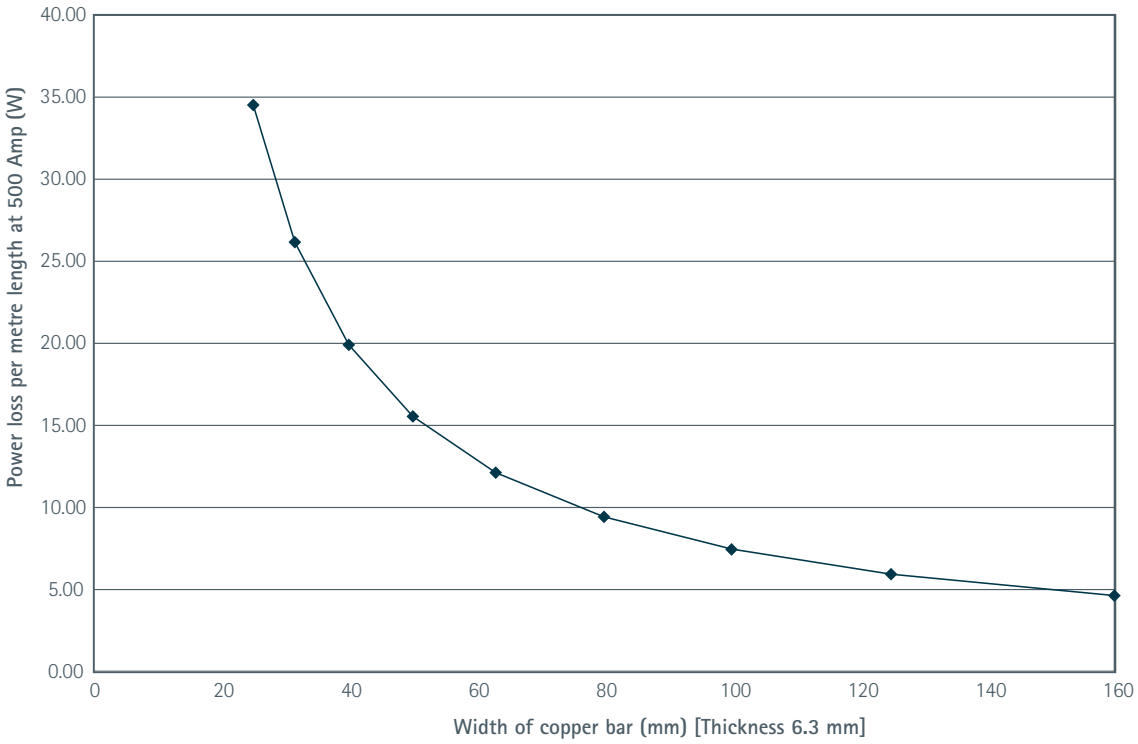

Figure 38 – Power loss versus width for 6.3 mm thick copper bars

The power loss needs to be expressed in terms of money by converting to energy loss (by multiplying by the operation time) and multiplying by the cost of energy. For the purposes of this exercise, the cost of energy is assumed to be 0.15 Euro per kWh. Table 11 and Figure 39 show the energy cost per metre for a range of operation times.

Table 11 – Energy Cost per Metre for Various Widths of Copper Bars at 500 A Load

	Cost of Energy (€ per metre)				
Width (mm)	**2000 hrs**	**5000 hrs**	**10 000 hrs**	**20 000 hrs**	**50 000 hrs**
25	10.36	25.89	51.79	103.58	258.94
31.5	7.85	19.62	39.24	78.49	196.21
40	5.97	14.93	29.86	59.73	149.32
50	4.66	11.66	23.31	46.62	116.56
63	3.63	9.09	18.17	36.35	90.87
80	2.84	7.10	14.21	28.42	71.04
100	2.25	5.62	11.24	22.49	56.22
125	1.77	4.43	8.86	17.73	44.32
160	1.38	3.46	6.92	13.85	34.62

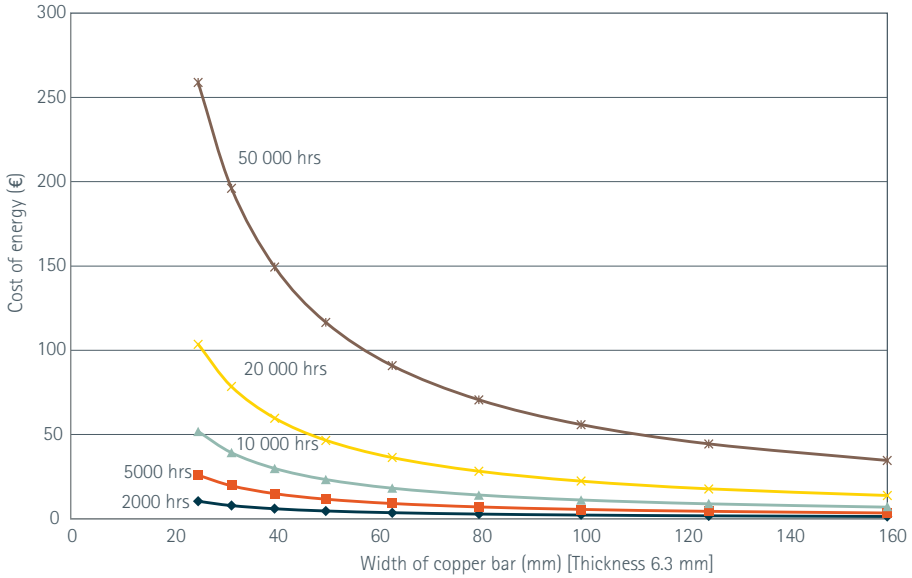

Figure 39 – Cost of energy loss per metre versus width for 6.3 mm thick copper bars for a range of operating times

By comparison with the material costs in Table 9 it is immediately apparent that, for any significant operational life, the cost of energy is by far the dominant element in the total cost of the system. Consider, for example, the 5000 hour operation case.

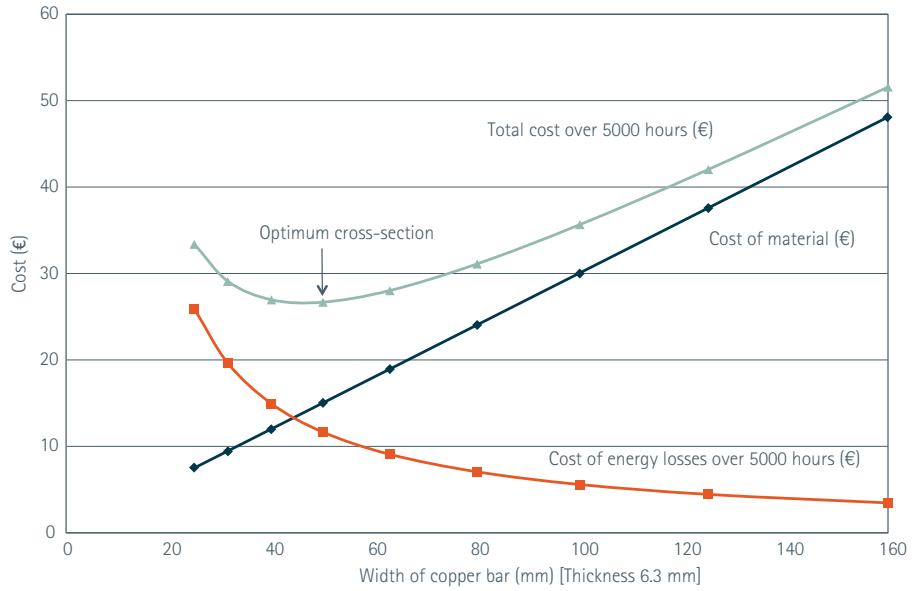

Figure 40 – Total cost per metre versus bar width for 5000 hours operation at 500 A load

Figure 40 shows the total cost, material cost (from Table 9) and energy cost (from Table 11) per metre of bar. As the width of the bar increases, the cost of material increases linearly, while the cost of energy decreases super inversely as the resistance and temperature decrease. The total cost curve shows a clear minimum where the total cost is optimised between investment cost (material) and operating costs (energy).

Because the cost of energy is proportional to operation time, the optimum bar width also increases with operation time, as shown in Figure 41, which plots the total cost per metre of bar for a range of operation times. As operation time increases, the optimum bar width increases.

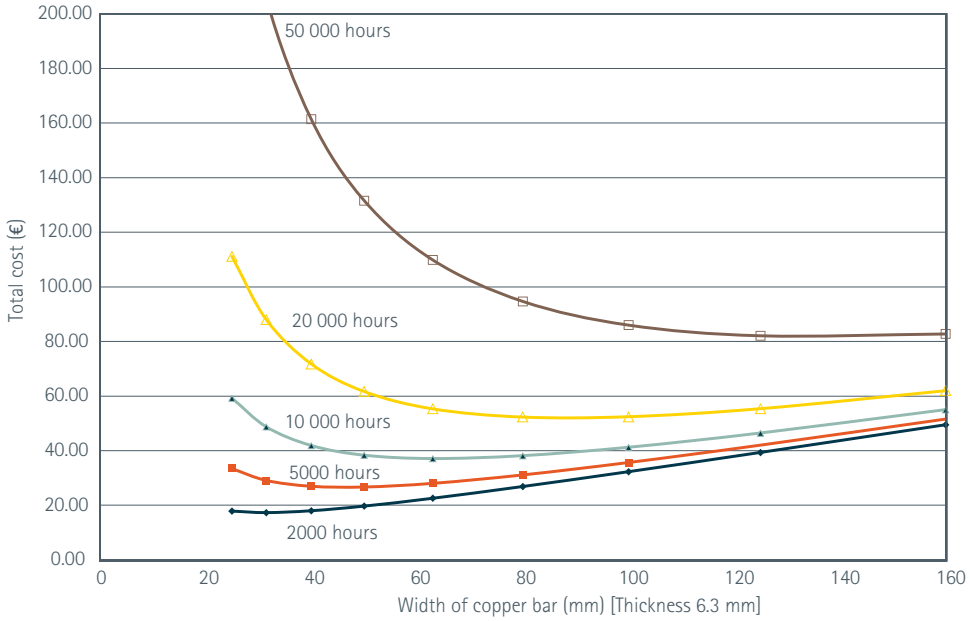

Figure 41 – Total cost per metre of bar versus bar width for a range of operating times

Figures 40 and 41 illustrate two important points:

At the minimum bar size – i.e. the size that would be selected by conventional methods – the cost of lifetime energy is many times the cost of the conductor; a factor of approximately 3.4 at 5000 hours. In fact, such a bar wastes its own cost in energy in less than 1500 operational hours, at the material and energy costs used in this example.

The minimum of the total cost curve is shallow, meaning that there is some latitude for judgement in the selection of the final size with a high degree of confidence in the outcome. For example, if the operational hours were not well known, but could be expected to be between 20 000 and 50 000 hours, a 100 mm bar could be confidently selected, being a little over optimum size for 20 000 hours and a little under optimum size for 50 000 hours.

Figure 42 is an alternative plot of the data in Figure 41 showing the optimum current density for a range of operating hours. As would be expected, the optimum current density reduces as operating hours increase.

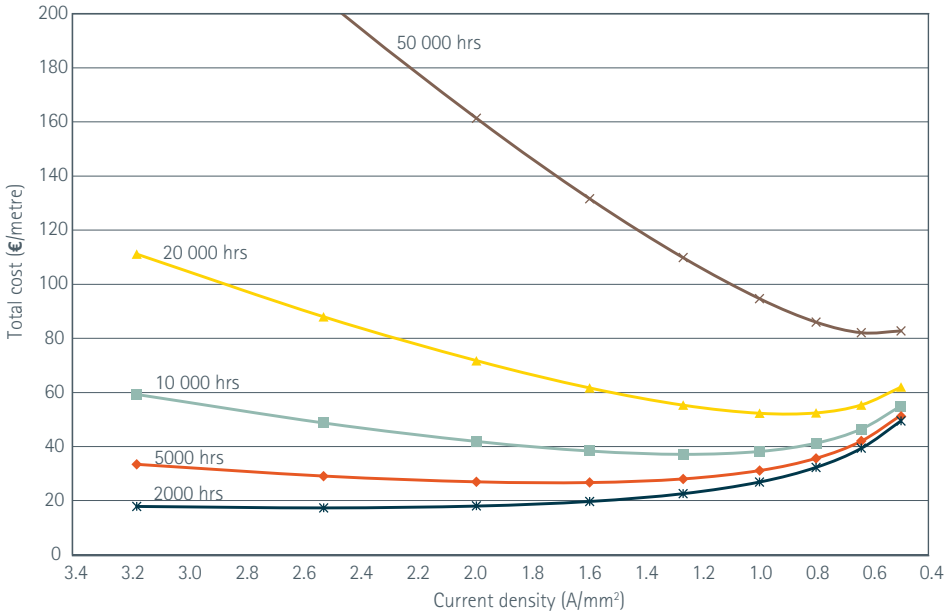

Figure 42 – Total cost per metre against current density for a range of operation times

Figure 43 shows the estimated working temperature plotted against bar width at 500 A load assuming an ambient of 35°C. As would be expected, lower current density results in reduced temperature rise, bringing the benefit of increased reliability due to reduced thermal stresses on joints and mountings, as well as optimised lifetime costs.

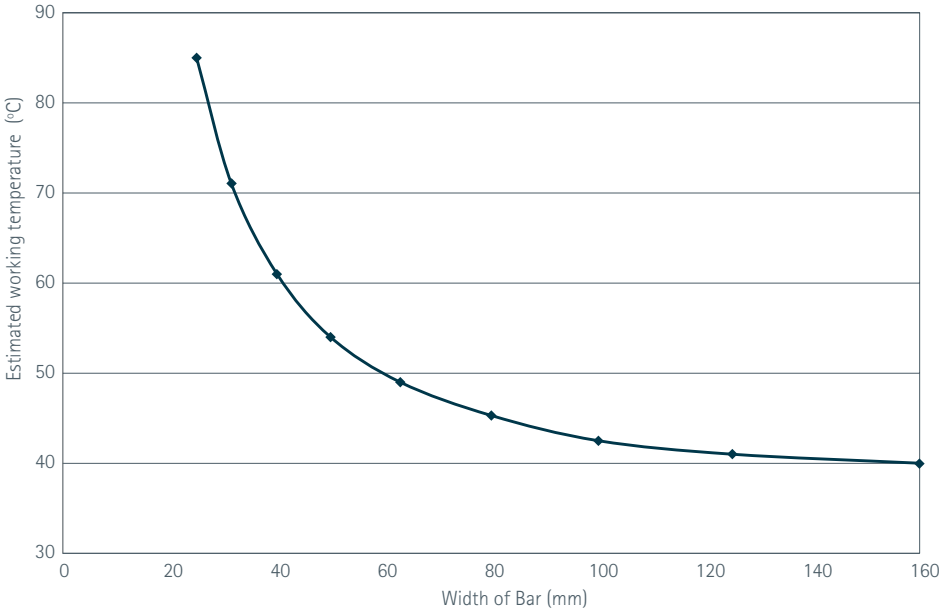

Figure 43 – Estimated working temperature versus width of bar (mm) for 500 A load

So far, this simple analysis has ignored the time value of money; to make the argument credible to financial managers, that must be corrected. In Table 12 the discount factors from Table 8, the material cost figures from Table 9 and the cost of energy loss figures from Table 11 are used to calculate the net present value – i.e. the discounted cost – of operating each metre of bar for 5 years at 2000 hours load per year. The assumed discount rate is 5% but for the sake of clarity, no account is taken of inflation or load growth.

In this case, because the energy is paid for throughout the operating time, no discount is applied to Year 0. Local accounting practice may require discounting to be applied to Year 0 in some cases.

Table 12 – Present Value (€) per Metre of Bar

Discount Factor			Cost of Energy (2000 hours per year)						
			Year 0	Year 1	Year 2	Year 3	Year 4	Total	
			1	0.952	0.907	0.864	0.823		
Bar Width (mm)	Power Loss per Metre (watt)	Cost of Bar (euro)							Total
25	34.53	7.518	10.36	9.8627	9.3965	8.9510	8.5263	47.10	54.61
31.5	26.16	9.472	7.85	7.4732	7.1200	6.7824	6.4606	35.69	45.16
40	19.91	12.029	5.97	5.6834	5.4148	5.1581	4.9133	27.14	39.17
50	15.54	15.036	4.66	4.4363	4.2266	4.0262	3.8352	21.18	36.22
63	12.12	18.945	3.63	3.4558	3.2924	3.1363	2.9875	16.50	35.45
80	9.41	24.057	2.82	2.6846	2.5577	2.4365	2.3209	12.82	36.88
100	7.45	30.071	2.24	2.1325	2.0317	1.9354	1.8435	10.18	40.25
125	5.93	37.589	1.78	1.6946	1.6145	1.5379	1.4649	8.09	45.68
160	4.62	48.114	1.38	1.3138	1.2517	1.1923	1.1357	6.27	54.39

Figure 44 shows the comparison between the discounted and non-discounted cost, this time for a 10 year life.

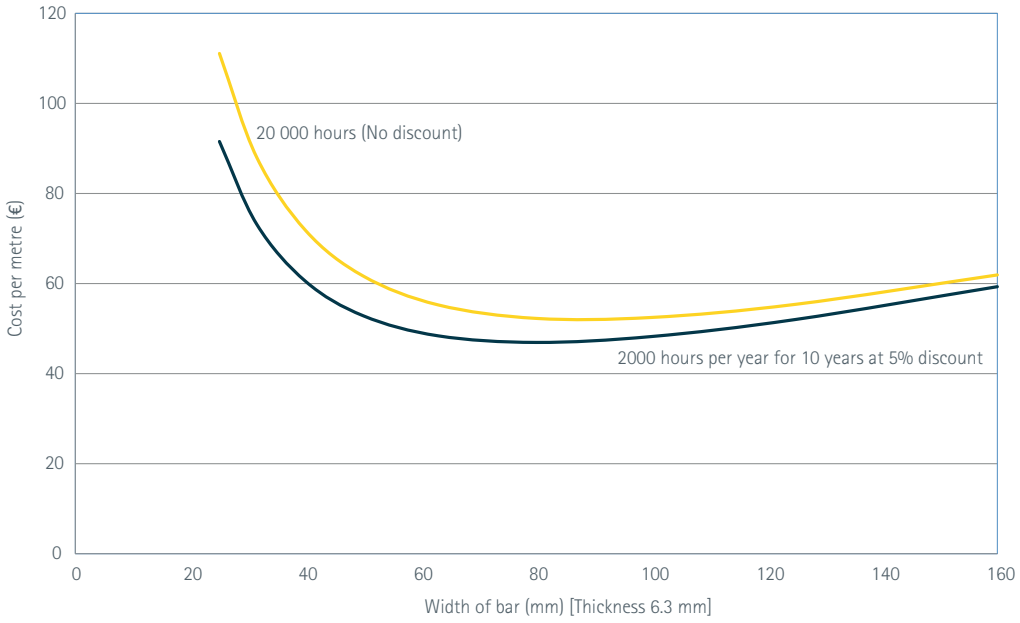

Figure 44 – Cost per metre (€) against bar width for a) 20 000 hours operation without discount and b) 2000 hours per year for 10 years at 5% discount

The effect of discounting is, of course, to progressively reduce the value of the later years and therefore the total cost. But, as Figure 44 clearly shows, it also shifts the minimum cost bar width towards a lower value. This is an obvious conclusion if discounting is viewed as reducing the operating time in later years instead of the cost of each operating hour in later years.

A warning is appropriate at this point; using exaggerated discount rates will reduce the viability of any investment in the same way as imposing too-short a payback period would, so it is important that discount rates are chosen with care and without prejudice.

3.2.4 End of Life Costs

At the end of life the installation must be removed and the materials recycled. In electrical systems the copper conductor has significant value, making recovery worthwhile; however, it is so far into the future, it is often assumed that the discounted value will be low. However, commodity prices are very volatile with an underlying upward trend so, if material price inflation is included in the calculation, the NPV of the residual material may be significant.

An additional problem is that the task of removing the installation is usually carried out by a third party under contract, so the operator sees a contract cost, while the third party receives the revenue from recycled materials.

3.3 Conclusion

Life cycle costing provides a more realistic view of the cost of a project and is particularly useful in comparing two or more design options. The curve of LCC versus conductor size is quite flat near the minimum; selecting the largest conductor size in range provides both a short term optimum and reduced exposure to future energy price increases.

4.0 Short-Circuit Effects

David Chapman & Professor Toby Norris

4.1 Introduction

Like all electrical circuits, busbars need to be protected against the effects of short-circuit currents. The open construction of busbars increases the risk of faults, e.g. by the ingress of foreign bodies into air gaps, and the risk of consequent damage is high due to their high normal operating currents and the amount of energy available.

Very high currents lead to rapid and extreme overheating of the bars with consequent softening of the material and damage to the support structure. At the same time, the electromagnetic forces generated will distort the softened conductors which may break free from their supports. Resonance effects may make the situation worse.

4.2 Short-Circuit Heating of Bars

The maximum potential short-circuit current depends on the source impedance of the supply and reduces along the length of the bar as the impedance increases. For the purpose of ensuring the safety and integrity of the bar, the short circuit current should be initially calculated close to the feed end of the bar, making no allowance for bar impedance, to establish the worst case.

When a fault occurs, the short-circuit current will be many times the normal operating current and will flow until the protective device operates. Because the time duration is small – a few seconds at most – it is usual to assume adiabatic heating, in other words, that, over the time scale of interest, there is no significant cooling effect and that all the heat generated by the current flow is retained in the bar. Therefore it is assumed that the temperature rise of the bar is simply linear - this simplifies the calculation significantly and yields a conservative result.[1]

The amount of heat energy required to raise the temperature of a unit mass of material by one degree Centigrade is called the specific heat. For copper, at room temperature, the value is 385 Joule/kg/K. Knowing the mass of the bar and the energy produced by the short circuit current, the temperature rise can be calculated:

$$Q = S\,m\,t_r \text{ or}$$

$$t_r = \frac{Q}{S\,m}$$

where:

- Q is the amount of heat added to the bar (Joule)
- S is the specific heat of the bar material (J/kg/K)
- m is the mass of the bar (kg)
- t_r is the temperature rise.

The amount of energy dissipated in the bar is:

$$Q = PT$$

where:

- P is the power dissipated in the bar (W)
- T is the time for which the power is dissipated (seconds).

Therefore, $t_r = \frac{PT}{Sm}$ or $\Delta t_r = \frac{P}{Sm}$

where Δt_r is the rate of temperature rise in degrees C per second.

The power dissipated in the bar is given by

$$P = I^2 R \text{ or}$$

$$P = I^2 \frac{\rho l}{A}$$

[1] A similar simplification is made in determining cable behaviour under fault conditions.

where:

R is the resistance of the bar (Ω)
ρ is the resistivity of the bar material (Ωm)
l is the length of the bar (m)
A is the cross-sectional area of the bar (m^2).

Substituting for *W* and *M* gives:

$$\Delta t_r = \frac{I^2 \rho l}{A S D l A} = \frac{I^2 \rho}{A^2 S D} = \frac{\rho}{SD}\left(\frac{I}{A}\right)^2$$

where:

D is density (kg/m^3).

Two of the physical constants, specific heat and resistivity, vary considerably with temperature so it is not obvious which values should be used. Resistivity increases with temperature (by a factor of 1.6 from 20ºC to 300ºC) so increasing the energy dissipated as the temperature increases, while specific heat falls by around 8% over the same range.

Using room temperature values, and adjusting to use convenient units, gives the initial rate of temperature rise as:

$$\Delta t_r \approx 5 \times 10^3 \left(\frac{I}{A}\right)^2$$

where:

I is current in kA
A is the cross-sectional area in mm^2.

At higher temperatures – in other words, as the fault current continues to flow until the protective device operates – the rate of temperature rise will increase as the resistance of the bar increases. The worst case rate of rise at the feed end of the bar is approximately:

$$\Delta t_r \approx 8 \times 10^3 \left(\frac{I}{A}\right)^2$$

However, if the short circuit is at some distance from the feed end, the fault current magnitude will be lower due to the resistance of the bar and will reduce further as the bar temperature rises.

In practice, what is important is that the final temperature of the bar remains lower than the limiting design temperature throughout the short circuit event. The limiting temperature for copper busbars is determined by the temperature resistance of the support materials but, in any case, should not exceed ~ 200ºC. The maximum circuit breaker tripping time is $200/\Delta t_r$ seconds.

Busbars that have been subject to short circuit should be allowed to cool and inspected before being returned to service to ensure that all joints remain tight and that the mountings are secure. Note that, although the heating time – the duration of the fault – is quite short, the bar will remain at high temperature for a considerable length of time. Also, because of the very high thermal conductivity of copper, parts of the bar beyond the fault will also have become hot.

4.3 Electromagnetic Stresses

Busbars are subject to mechanical forces since each is carrying a current though the magnetic fields caused by currents in other bars. When alternating currents are flowing, the forces have a steady component, but also a vibrational component at twice the frequency of the alternating current. Under normal working conditions these forces are of little consequence.

However, if the bars are mounted on supports, each section will have a resonant frequency. If this frequency is close to twice the supply current (or any significant harmonic current), then resonant vibration of these beams may occur. This rather special and uncommon circumstance can lead to high vibrational displacements and possibly to metal fatigue or loosening of joints and connections. The problem may be avoided by choosing an appropriate spacing of the supports or cured by introducing additional intermediate supports. Methods of estimating mechanical resonant frequencies are given later.

If large currents flow, such as when a short circuit occurs, the forces can be more important. The unidirectional component of the forces, exacerbated by the vibrational component, can lead to permanent bending and distortion of the bars or damage to, and even breakage of supports.

The peak, or fully asymmetrical, short-circuit current is dependent on the power factor (cos ϕ) of the busbar system and its associated connected electrical plant. The value is obtained by multiplying the rms symmetrical current by the appropriate factor given in balanced three-phase short-circuit stresses.

The peak current, *I*, attained during the short circuit, varies with the power factor of the circuit (see Table 13):

Table 13 – Power Factor and Peak Current

Power Factor	Peak Current as Multiple of Steady State rms
0	2.828
0.07	2.55
0.20	2.2
0.25	2.1
0.30	2
0.50	1.7
0.70	1.5
1.0	1.414

The theoretical maximum for this factor is 2√2 or 2.828 where cos ϕ = 0. If the power factor of the system is not known, then a factor of 2.55 will normally be close to the actual system value, especially where generation is concerned. These peak values reduce exponentially and, after approximately 10 cycles, the factor falls to 1.0, i.e. the symmetrical rms short-circuit current. As shown in Figure 45, the peak forces therefore normally occur in the first two cycles (0.04 s).

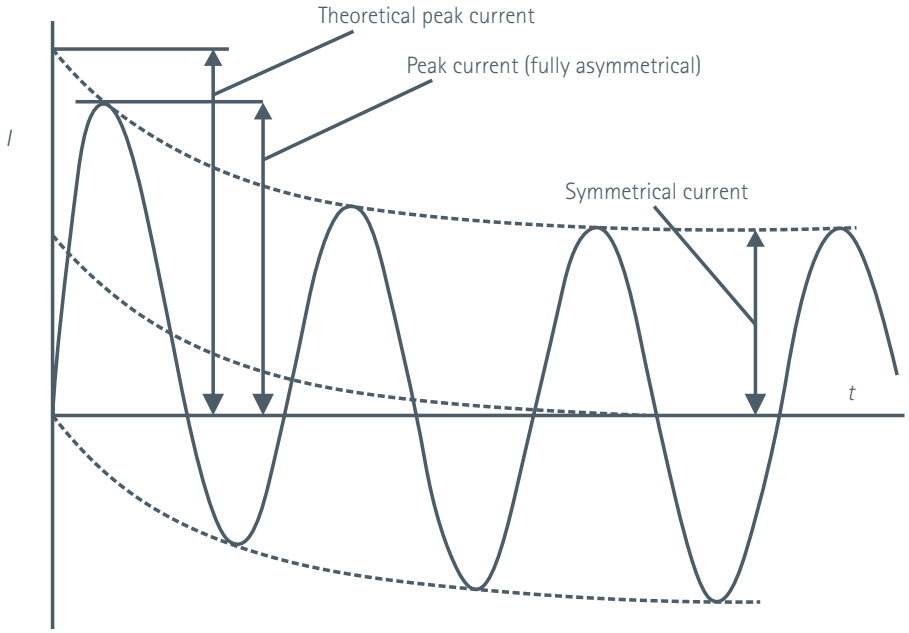

Figure 45 – Short-circuit current waveform

Bars carrying like parallel currents are attracted towards each other. Thus, if the currents in one phase are carried in separate conductors in parallel in the same phase, then the gap between them may be reduced by the mechanical forces. More usually we deal with bars carrying anti-parallel currents when the bars repel each other.

Eddy current effects in bars carrying anti-parallel currents bring the current flow in a bar closer to the sides facing the other conductor. This will lead to an increase in the repulsive force. Precise formulae for this are not available but an over-estimate of the magnitude of the force under these circumstances may be made by replacing the centre line distance in the formula for the force per unit length by the distance between the faces.

4.3.1 Estimating the Forces Between Parallel Sets of Bars

Assuming that the bars are round will give values for the forces which, used with a factor of safety in estimating strength, are normally reliable. If there are many bars in the configuration then the forces between individual pairs of bars may be simply added together, taking into account their direction. In the case of ac, one may need to take into account the phases of the currents.

Bar shape usually has a minor effect unless the bars are very close together, as will be illustrated in the example of rectangular bars.

4.3.1.1 Round Bars

For two bars with spacing *d* and carrying parallel currents I_1 and I_2, the repulsive force per unit length is

$$F = -\frac{\mu_o}{2\pi d} I_1 I_2$$

where:

d is spacing in mm
μ_o is absolute permeability = $4\pi \times 10^{-7}$ Henrys per metre
F is force per unit length in N/m.

For two bars, at spacing *d*, carrying anti-parallel direct currents (i.e. go and return currents) of magnitude *I*, the repulsive force per unit length is

$$F = -\frac{\mu_o I^2}{2\pi d}$$

$$F = 0.2 \times 10^{-3} \frac{I^2}{d}$$

For two bars at spacing, *d*, carrying anti-parallel alternating currents (i.e. go and return currents) of magnitude *I*, the repulsive force per unit length is

$$F = \frac{\mu_0 I_{rms}^2}{2\pi d}[1 - cos(2\omega t)]$$

$$F = 0.2 \times 10^{-3} \frac{I_{rms}^2}{d}[1 - cos(2\omega t)]$$

where:

d is spacing in mm
$\omega = 2\pi f$
f is frequency in Hz.

Thus we have a steady repulsive force, together with a force alternating at twice the frequency of the current of amplitude equal in magnitude to the steady component of force. The result can also be seen as a periodic force varying from zero to twice the average force.

For balanced three phase currents of rms value *I* at frequency $\omega = 2\pi f$ (ω in rad/s, f in Hz), the currents are:

$$I_A = \sqrt{2}\, I\, sin(\omega t)$$

$$I_B = \sqrt{2}\, I\, sin\left(\omega t - \frac{2\pi}{3}\right)$$

$$I_C = \sqrt{2}\, I\, sin\left(\omega t + \frac{2\pi}{3}\right)$$

The standard triangular and inline arrays are shown in Figure 46.

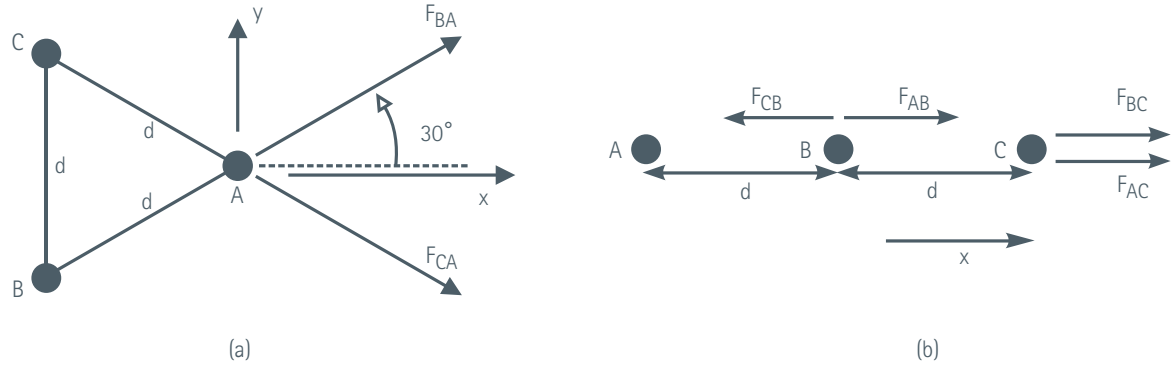

(a) (b)

Figure 46 – Three phase system with spacings d (mm). (a) triangular array, (b) inline array

4.3.1.1.1 Triangular Array

The net force per unit length in the x-direction on bar A in Figure 46(a)

$$F_x = \frac{\mu_0 I^2}{\pi d}\frac{\sqrt{3}}{2}[1 - cos(\omega t)]$$

$$F_x \approx 0.693 \times 10^{-3}\frac{I^2}{d}[1 - cos(\omega t)]$$

The net force in the y-direction on bar A in Figure 46(a)

$$F_y = \frac{\mu_0 I^2}{\pi d}\frac{\sqrt{3}}{2} sin(2\omega t)$$

$$F_y \approx 0.693 \times 10^{-3}\frac{I^2}{d} sin(2\omega t)$$

The net result is a steady force outwards along the perpendicular to the line BC of magnitude

$$F_{x\,steady} = \frac{\mu_0 I^2}{\pi d}\frac{\sqrt{3}}{2}$$

$$F_{x\,steady} \approx 0.693 \times 10^{-3}\frac{I^2}{d}$$

The alternating forces in the x and y direction are in phase quadrature and of equal magnitude and so constitute a force tending to move the conductor in a circle. The magnitude is the same as that of the steady force.

4.3.1.1.2 In-Line Array

The force per unit length in the x-direction (i.e. an outward repulsive force) on bar C in Figure 46(b) is

$$F_C = \frac{\mu_0 I^2}{\pi d}\left[\frac{3}{8} - \frac{\sqrt{3}}{4} sin\left(2\omega t - \frac{\pi}{3}\right)\right]$$

$$F_C \approx \left[0.15 - 0.1732\ sin\left(2\omega t - \frac{\pi}{3}\right)\right] 10^{-3}\frac{I^2}{d}$$

This is a steady outward force with a superposed 2nd harmonic vibration. The amplitude of the harmonic force is slightly greater than the steady force.

The force per unit length on the centre bar, B, is purely vibrational. In the x-direction it has magnitude

$$F_B = \frac{\mu_0 I^2}{\pi d}\frac{\sqrt{3}}{2} sin\left(2\omega t - \frac{\pi}{3}\right)$$

$$F_B \approx 0.346 \times 10^{-3}\ sin\left(2\omega t - \frac{\pi}{3}\right)\frac{I^2}{d}$$

The force per unit length in the x-direction on bar A is

$$F_A = -F_B - F_C = \frac{\mu_0 I^2}{\pi d}\left[-\frac{3}{8} - \frac{\sqrt{3}}{4} sin\left(2\omega t - \frac{\pi}{3}\right)\right]$$

$$F_A \approx \left[-0.15 - 0.1732\ sin\left(2\omega t - \frac{\pi}{3}\right)\right] 10^{-3}\frac{I^2}{d}$$

This too is on average a repulsive force outwards in the negative x-direction.

4.3.1.2 Bars of Rectangular Section

For bars of rectangular section set out orderly, the force between the two may be expressed as the force computed as if they were round bars multiplied by a correction factor. Thus the force, in N/m, between two rectangular bars with centre line spacing *d*, is

$$F = K\frac{\mu_0 I^2}{2\pi d}$$

$$F = 0.2 \times 10^{-3} K\frac{I^2}{d}$$

The factor *K* depends on the length of the sides, a and b, of the rectangular cross-section and the spacing, *d*, of the centre lines.

K is shown in Figure 47 as a function of $\frac{d-a}{a+b}$

Note that the curves labelled a/b = 0 and b/a = 0 represent limiting values.

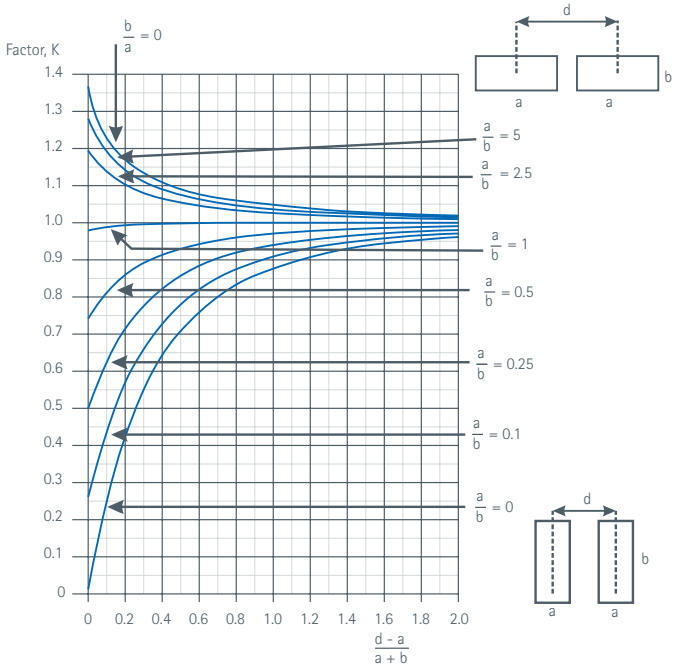

Figure 47 – Factor K for calculating the force between two bars of rectangular section

For a pair of rectangles whose long sides face each other, it will prove helpful to use the equations below in which d is replaced by b and factor K replaced by K_b which is plotted in Figure 48.

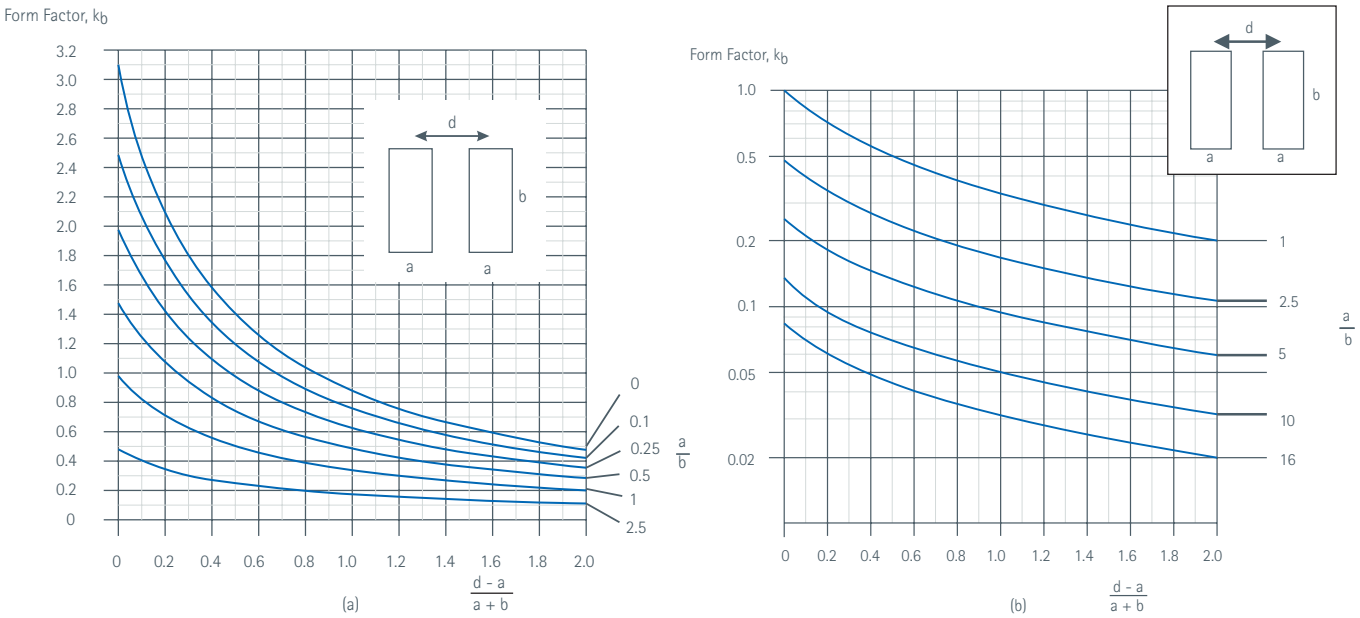

Figure 48 – Form factor K_b. (a) low values of a/b (long sides facing each other) (b) high values of a/b.

An approximate formula for K_b accurate to within 4% for $0 < \frac{d-a}{a+b} < 2$ and $\frac{1}{16} < \frac{a}{b} < 16$ is:

$$K_b \approx \frac{2.98}{\left[1 + 2.228\left(\frac{a}{b}\right)\right][1 + AF + BF^2]}$$

where:

$$F = \frac{d-a}{a+b}$$

$$A = \frac{2.46 + 45.75\left(\frac{a}{b}\right) + 9.25\left(\frac{a}{b}\right)^2}{1 + 24.4\left(\frac{a}{b}\right) + 4.68\left(\frac{a}{b}\right)^2}$$

$$B = \frac{0.27 - 0.23(ab)}{1 + 2.23\left(\frac{a}{b}\right)}$$

4.4 Mounting Arrangements

The mountings are required to restrain the busbars under all conditions to ensure that:

- the material is not over stressed
- a safe distance is maintained between bars in normal service and under short-circuit conditions by limiting maximum deflection
- the bars do not vibrate excessively (which would impair the long term efficacy of joints).

4.4.1 Maximum Permissible Stress

The maximum permissible stress in a conductor is the resultant of:

- its own natural weight (F_m) and
- in the case of busbars installed out of doors, the additional forces of wind (F_W) and ice (F_i) loadings and
- the magnetic forces resulting from a short circuit, noting that the direction of a short-circuit force (F_S) depends on the position of adjacent phases and the direction of the currents in them.

In a general case, the resultant can be calculated by the following method:

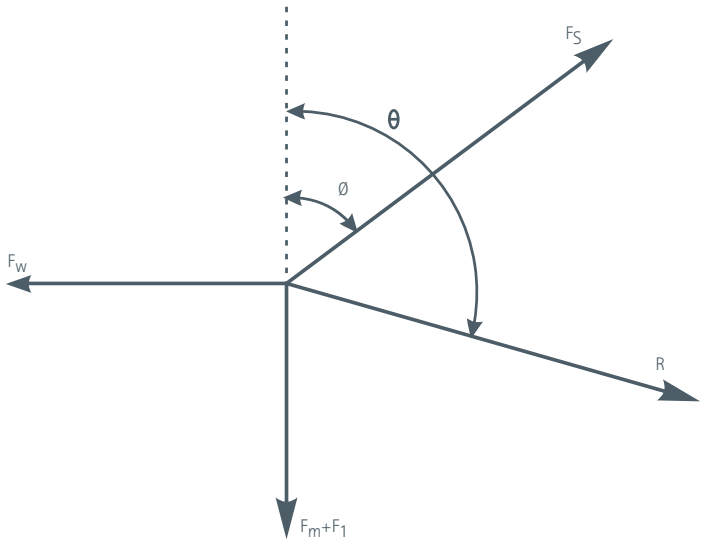

$$R = \sqrt{\left[\left(F_s cos\varphi - (F_m + F_i)\right)^2 + (F_s sin\varphi - F_w)^2\right]}$$

and

$$\theta = tan^{-1}\left(\frac{F_m\, sin\varphi - F_w}{F_m\, cos\varphi - (F_m + F_s)}\right)$$

The maximum skin stress in the conductor can then be calculated using the following formula:

$$f = \frac{RDL^2}{16\, I}$$

where:

f is maximum skin stress, N/mm^2
L is span, mm
I is moment of inertia, mm
D is diameter or depth of rectangular section, mm.

This equation is valid for a uniformly loaded single beam which is freely supported at both ends or freely supported at one end and fixed at the other. For a beam which is horizontally fixed at both ends, maximum skin stress is reduced to one third at the centre and to two-thirds at its ends.

The maximum permissible stress is dependent on the conductor material, temper, etc. but must not exceed the material proof stress otherwise permanent deformation will occur. For a conductor manufactured from hard drawn copper, the value is approximately 245 N/mm^2.

4.4.1.1 Moment of Inertia

In the above formula the moment of inertia, *I*, for the section of the beam has to be calculated about the neutral axis which runs parallel to the beam where the beam has zero tensile forces. In most cases this is the same axis of the centre of cross-section.

Shaped profiles have much higher values of moment of inertia than simple bars and rods (see Section 5.0 Busbar Profiles).

For a rectangular section of depth *D* mm and breadth *B* mm

$$I = \frac{1}{12} BD^3$$

For a circular section of diameter D mm

$$I = \frac{\pi}{64} D^4$$

or

$$I = 0.491 D^4$$

For a tubular section of internal diameter *d* mm and external diameter *D* mm

$$I = \frac{\pi}{64}(D^4 - d^4)$$

or

$$I = 0.491\ (D^4 - d^4)$$

It should be noted that the value of *I* for a given cross-section is dependent on the direction in which each individual force is applied.

4.4.2 Deflection

It is important to know how far a bar will deflect so that the necessary clearances between bars and other structures can be maintained.

The maximum deflection of a beam carrying a uniformly distributed load, and freely supported at each end, is given by the formula:

$$\Delta = \frac{5F_m L^4}{384\,EI}$$

where:

Δ is maximum deflection, mm
F_m is weight per unit length of loaded beam, N/mm
L is beam length between supports, mm
E is modulus of elasticity (124 x 10^3N/mm^2)
I is moment of inertia of beam section, mm^4.

If one end of a beam is rigidly fixed in a horizontal position, the deflection is 0.415 times that given by the above formula. If both ends of a beam are rigidly fixed in a horizontal position, the deflection is 0.2 times that given by the above formula.

Thus, with a continuous beam freely supported at several points, the maximum deflection in the centre spans may be assumed to be 0.2 times that given by the formula, while the deflection in the end spans is 0.415 times. Therefore, the deflection in the end spans may be assumed to be twice that in the centre spans, assuming equal span distances.

4.4.3 Natural Frequency

The natural frequency of a beam simply supported at its end is:

$$f_n = \frac{17.74}{\sqrt{\Delta}}$$

and for a beam with both ends fixed horizontally it is:

$$f_n = \frac{18.04}{\sqrt{\Delta}}$$

where:

f_n is natural frequency, Hz
Δ is deflection, mm.

As the deflection with fixed ends is 0.2 times the value with freely supported ends, it follows that the natural frequency is increased by 2.275 times by end-fixing; fixing one end only increases the natural frequency by about 50%.

Busbar systems should be designed to have a natural frequency which is not within 30% of the vibrations induced by the magnetic fields resulting from the currents, including any significant harmonic currents, flowing in adjacent conductors.

Where equipment is to be mounted outside, natural frequencies of less than 2.75 Hz should be avoided to prevent vibration due to wind eddies.

5.0 Busbar Profiles

David Chapman

5.1 Introduction

Busbar profiles are very often used in distribution panels and switchboards where they have some distinct advantages. The design considerations for this application are significantly different from the relatively long vertical and horizontal busbars discussed previously. For example, the bars are semi-enclosed in cabinets, so it is the air flow through the cabinet which determines the cooling available. Moreover, these cabinets contain a substantial number of devices such as circuit breakers, which also generate heat and rely on the busbar system to remove it. Space constraints, mounting considerations and ease of assembly also favour the use of profiles.

Profiles are more difficult and costly to manufacture than flat bars due to technical contraints, including:

- Complex design
- More elaborate machine set-up
- More delicate production process
- More complicated packaging.

These constraints are now mostly under control and currently several fabricators produce hundreds, or even thousands, of different shapes for electrical applications.

Many electrical parts, which are often cut from sheet, can be economically produced by slicing a profiled bar.

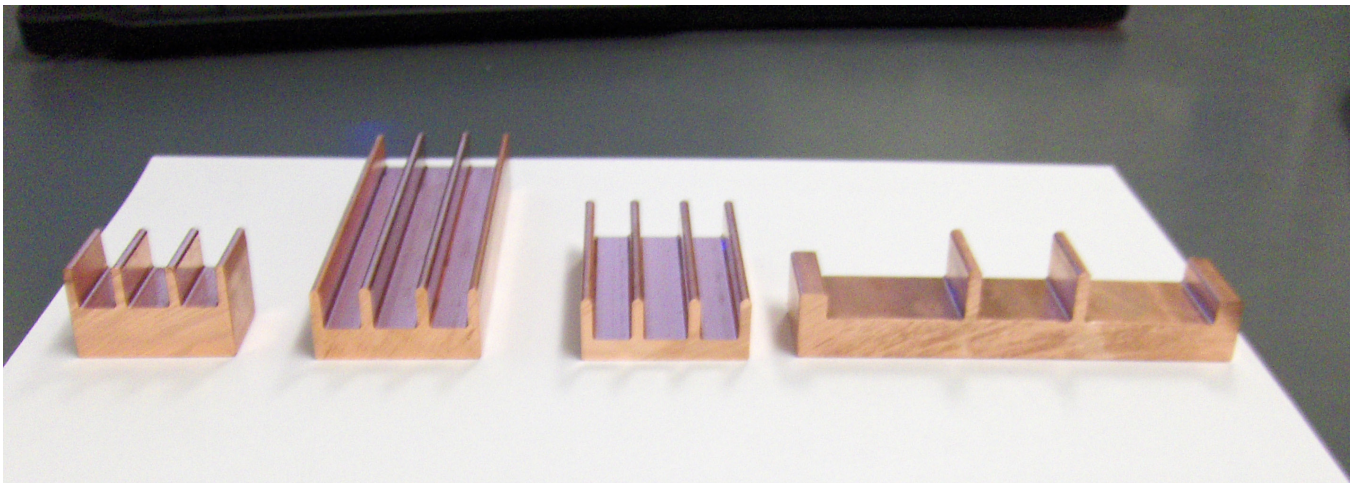

Figure 49 – Typical copper profiles

5.2 Reasons for Using Profiles

Profiles can be used to reduce the weight of copper conductors in an existing product. For an existing oversized conductor, the design flexibility available to define the shape of drawn copper profiles allows the engineer to design a profile smaller without affecting those surfaces which are constrained by the presence of existing support points, or contact interfaces.

5.2.1 Skin Effect Reduction

Skin effect losses are perhaps less important in switchgear, where the lengths are relatively short, than it is in long distribution busbars. However, taking proper account of skin effect often allows the amount of material to be significantly reduced.

5.2.2 Weight and Cost Saving

As discussed elsewhere, the apparent impedance of thick section conductors is increased due to skin effect, meaning that the current density in the centre is much lower than that at the surface. In a simple rectangular bar, there are areas of the cross-section in which the current density is comparatively low; using a correctly designed profile allows for a near homogeneous current density across the section that allows material to be removed from these areas, saving material, cost and weight.

5.2.3 Integrated Fixings and Mountings

Profiles can be designed to allow fast, hole-free assembly and jointing, which can significantly reduce the time required to assemble bars in a cabinet, improving consistency and quality.

5.2.4 Retention of Intellectual Integrity

Using bespoke profiles allows OEMs to ensure that cabinets assembled by sub-contractors conform to their specifications, avoiding the risk of substitution of inferior materials and assembly processes.

5.3 Economics of Profiles

The material savings generated by replacing a standard conductor by a profile of even a slightly smaller cross-section can easily offset the higher processing costs. At current refined copper prices, by far the largest contributor to the cost of a drawn copper profile is the cost of the copper material itself.

Using profiles also gives the opportunity to capture other savings:

- Hole-free joints and mountings yielding to lower assembly time and reduced complexity
- Lower scrap generated at the point of use (drilling and cutting not required)
- Flexible sourcing (optimum profiled conductor or standard product with identical supports and mounting points)
- Optimum material usage for the specific application
- Easier re-engineering and conductor optimisation on an existing product.

5.4 Practical Profiles

5.4.1 Manufacturing Process

Profiles are manufactured by extrusion, followed by one or more stages of drawing. The copper is extruded, either continuously or discontinuously through a die along a horizontal bench which supports the material. It is either cut into lengths or coiled for further processing.

The profile is then drawn through one or more dies, the last of which defines the final size and shape. Drawing is a cold working process so the drawn material is significantly hardened. The choice of extruded size and the number of drawing stages and their reductions determines the final hardness of the material; usually, the aim is to achieve the final size and shape without excessive hardening.

For profiles it is important that the size reduction during drawing is uniform – in other words that, while the size is reduced, the shape remains similar – to prevent differential hardening of the bar. For example, inappropriate tool and process design can, among other things, lead to problems with twisting, more so for asymmetric profiles.

5.4.1.1 EN 13605

EN 13605 is the standard that specifies the composition, properties and dimensional tolerances for copper profiles and profiled wire for electrical purposes which would fit within a circumscribing circle with a maximum diameter of 180 mm. The standard also specifies how ordering information should be structured between supplier and customer.

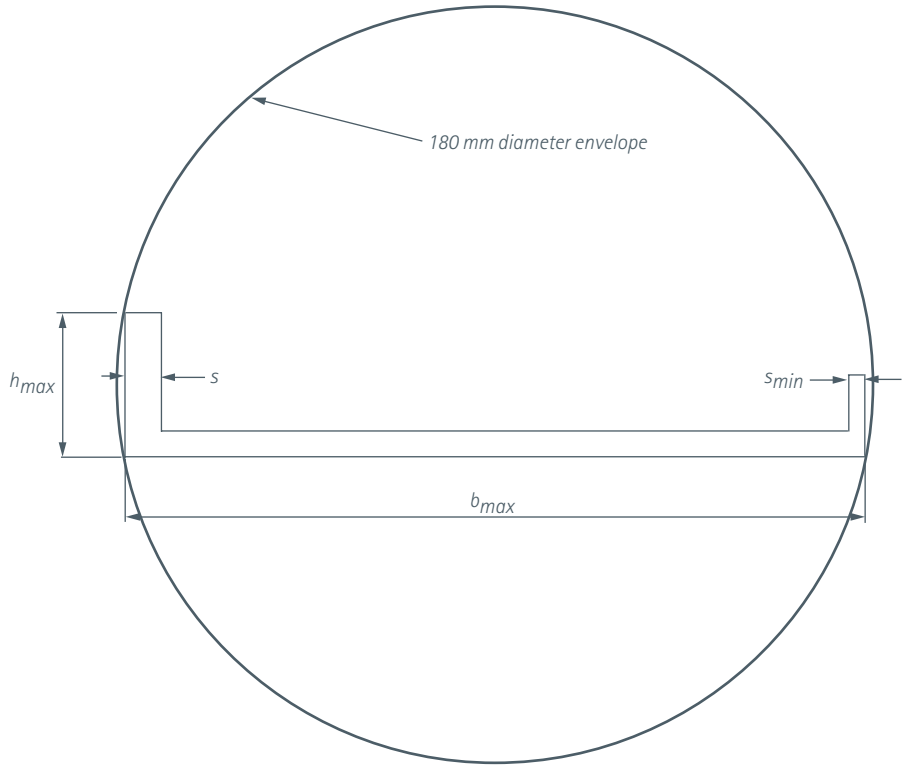

Figure 50 – A non-typical profile indicating the dimensions used in the standard

It is not intended here to describe the requirements of the standard in great detail but some aspects which are particularly relevant to profiles deserve mention.

Figure 50 shows a non-typical profile and the dimensions used to specify tolerances. Note that the standard is limited to those profiles that have a cross-section that can be contained within a circle of 180 mm diameter. A large majority of profiles are smaller than this, typically limited to 165 mm x 30 mm or 65 mm square with a weight of 30 kg/m. Some manufacturers are capable of manufacturing much larger profiles with maximum dimensions and the appropriate tolerances must be agreed between customer and supplier. Maximum dimensions for two processes are given in Table 17.

The tolerances on the major dimensions, *b* and *h* in Figure 50, are categorised by value and defined in six groups according to:

- The diameter of the circumscribing circle diameter in three groups, up to 50 mm, between 50 mm and 120 mm and between 120 mm and 180 mm
- The ratio of the maximum dimension (*b* or *h*) to the minimum thickness (s) into two sets:
  - $b_{max} < 20\ s_{min}$ or $h_{max} < 20\ s_{min}$
  - $b_{max} \geq 20\ s_{min}$ or $h_{max} \geq 20\ s_{min}$.

Tables 14, 15 and 16 list the tolerances.

Table 14 – Tolerances for Dimensions *b* and *h* for b_{max} or h_{max} <20:1

Nominal Dimensions *b* and *h* (mm)		Tolerances for Dimensions *b* and *h* within a Circumscribing Circle		
Over	Up to and including	<= 50	>50, <=120	>120, <=180
-	10	±0.11	±0.18	±0.29
10	18	±0.14	±0.22	±0.35
18	30	±0.17	±0.26	±0.42
30	50	±0.20	±0.31	±0.50
50	80		±0.37	±0.60
80	120		±0.44	±0.70
120	180			±0.80

Table 15 – Tolerances for Dimensions *b* and *h* for b_{max} or h_{max} ≥ 20:1

Nominal Dimensions *b* and *h* (mm)		Tolerances for Dimensions *b* and *h* within a Circumscribing Circle		
Over	Up to and including	<= 50	>50, <=120	>120, <=180
-	10	±0.18	±0.29	±0.45
10	18	±0.22	±0.35	±0.55
18	30	±0.26	±0.42	±0.65
30	50	±0.31	±0.50	±0.80
50	80		±0.60	±0.95
80	120		±0.70	±1.10
120	180			±1.25

The tolerances on thickness *s* in Figure 50 are specified for profiles with a circumscribing circle of 50 mm and below and one of greater than 50 mm.

Table 16 – Thickness Tolerances

Nominal Thickness (mm)		Thickness Tolerance within a Circumscribing Circle	
Over	Up to and including	<=50	>50, <=180
-	3	±0.13	±0.20
3	6	±0.15	±0.24
6	10	±0.18	±0.29
10	18	±0.22	±0.35
18	30	±0.26	±0.42
30	50		±0.50

5.4.1.1.1 Straightness, Flatness and Twist

Profiled sections are often used as pre-manufactured components for switchgear assemblies where space is limited and clearance distances are important, so it is essential that the sections fit correctly. Since profiles are much stiffer than flat bars, they cannot easily be pulled into alignment during assembly, so it is essential that they are straight, flat and free from twisting. Measurement of straightness, flatness and twist is made with the test piece lying on a flat reference surface.

In Figure 51, *h* represents the deviation from straight over length *l*; h_1 must be less than 3 mm per metre length (l_1) up to 3 m while h_2 must be less than 1.2 mm for any 400 mm length. It should be noted that, for special requirements, a straightness of less than 1 mm in a 1000 mm length can be achieved.

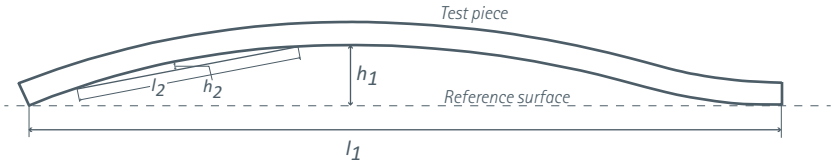

Figure 51 – Measurement of straightness

Figure 52 illustrates the measurement of flatness.

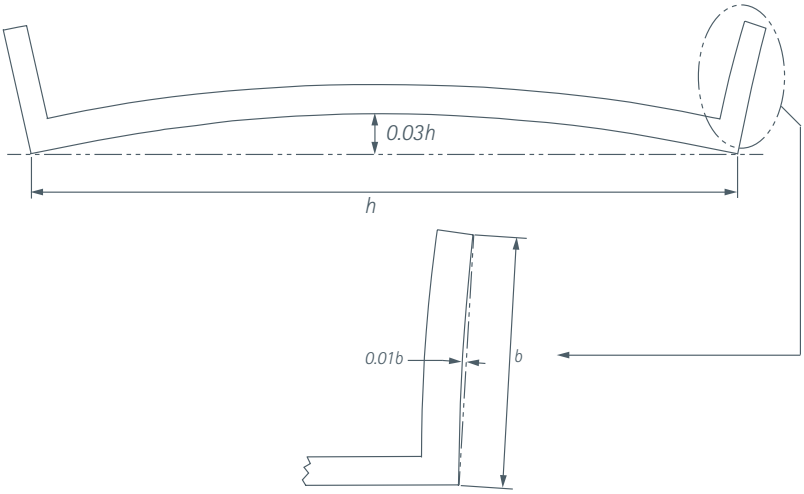

Figure 52 – Measurement of flatness

Figure 53 illustrates the method for measuring twist. The twist tolerance is defined by $f = \frac{v}{b}$

where:

- v is the displacement from the reference plane
- b is the width of the test piece
- f is a coefficient, the tolerance limit.

Again, the limiting value of f is grouped according to the diameter of the circumscribing circle (≥ 15 and ≤ 50; >50 and ≤120; >120 and ≤180) as a maximum value per metre of length and as a maximum for any length over 2 m.

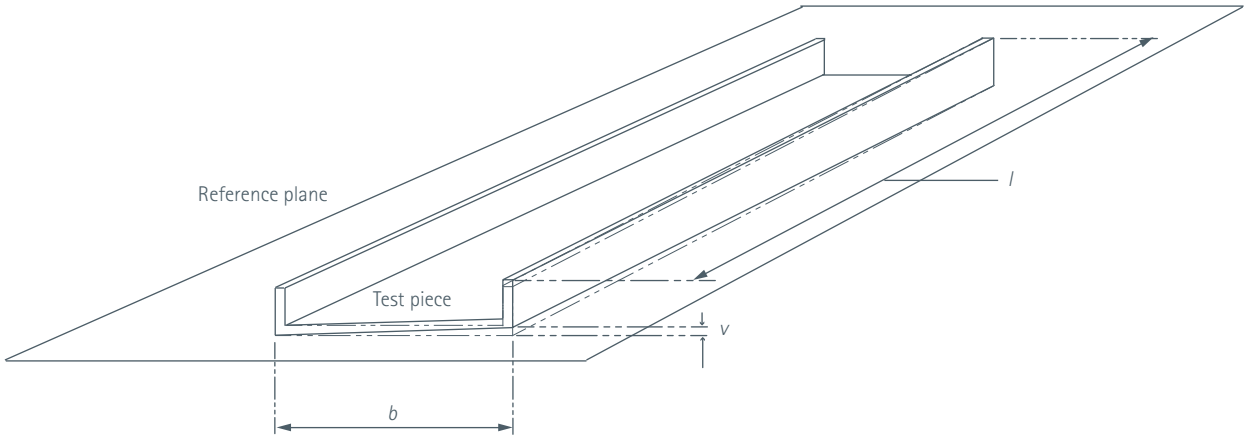

Figure 53 – Measurement of twist

Table 17 – Coefficient for Twist Tolerance

Diameter of Circumscribing Circle (mm)		Coefficient *f* for Twist Tolerance *v*	
Over	Up to and including	Per 1m length	On total length / over 2m
15[a]	50	0.08	0.15
50	120	0.05	0.10
120	180	0.04	0.08

[a] including 15

5.4.2 Design for Manufacturing

As might be expected, some profile designs are easier to manufacture than others; taking account of the capabilities of the manufacturing process during the design phase may help to reduce the cost and result in more consistent quality of the final product.

The overall size of the profile must lie within the capacity of the available plant. Manufacturers quote different limits depending on the process used, so advice should always be sought from potential manufacturers.

Table 18 – Maximum Sizes of Profile According to Two Manufacturers

	Process 1	Process 2
Maximum width	250 mm	250 mm
Maximum depth	115 mm	60 mm
Maximum cross-sectional area	8600 mm^2	3000 mm^2
Maximum weight per metre	80	30

Some specific design awareness allows the achievement of the right characteristics:

- Have a uniform wall thickness
- Have simple, soft lines and radiused corners
- Be symmetrical
- Have a small circumscribing circle
- Not have deep, narrow channels.

5.4.2.1 Wall Thickness

Small wall thicknesses require higher extrusion force (or, alternatively, a lower extrusion speed) and result in faster die wear. For simple, cost-effective, single pass drawing, wall thicknesses of less than 3 mm should be avoided.

5.4.2.2 Avoid Sharp Corners

Very sharp corners are difficult to produce consistently because the die wears very easily. Specifying a radius of 1 mm is often sufficient. In general, soft contours are to be preferred wherever the functionality of the profile allows.

5.4.2.3 Symmetry

Wherever possible, profiles should be designed to be symmetrical so that the shear centre is coincident with the centre of gravity. In an asymmetric profile, loads on the profile (including those introduced in manufacture) will result in torsional stresses and result in twisting. Unbalanced (asymmetric) profiles tend to twist during the drawing operations: tight geometric tolerances will require longer setup time and more complex tooling development.

5.4.2.4 Be Compact

Profile cross-sections with a low aspect ratio are easier to produce. The profile fits into a smaller circumscribing circle so the die will be smaller and stronger and the tolerances smaller.

5.4.2.5 Avoid Deep Narrow Channels

For profiles with channels, the depth of the channel should not exceed three times the width, otherwise the strength of the die will be compromised. A slightly higher ratio (1:4) can be achieved if the bottom is semi-circular and the corners at the opening have a large radius or are tapered.

5.4.2.6 Avoid Hollow Chambers

While hollow chambers can be formed in extruded profiles, the die is more complex and less robust. As a result, the product uniformity and die life, as well as productivity, are reduced.

5.4.3 Functional Design

Some advantages of using profiles rather than flat bars stem from the ability to integrate features into the design that will aid subsequent assembly processes such as mounting and jointing, as illustrated in Figure 54.

The lug on the end of the profile (1) can be made to match existing moulded supports. The channel (2) can be dimensioned to hold captive a hexagonal-headed bolt for attaching jointing plates. Fins (3) reduce skin effect and increase the surface area and, therefore, heat dissipation allowing the bar to run at lower temperature. The thin central section (4) also reduces skin effect.

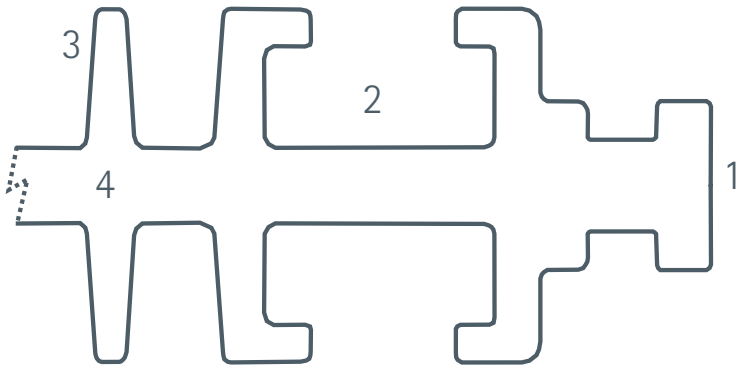

Figure 54 – Profile cross-section showing mounting lugs and slots for bolt-head

5.5 Electrical Design Considerations

5.5.1 Skin Effect

Eddy-current effects in profiles can be reduced with respect to rectangular bars because a significantly higher proportion of the copper conductor material can be located further from the centre of the magnetic field. Because skin effect is reduced, the amount of material required is reduced.

This is particularly important where two or more conductors of the same phase are placed side by side. In this configuration the current density in some areas of the bars is comparatively very low, so the bars can be shaped to remove this ineffective material.

For slim profiles – where the material thickness does not exceed 25 mm - an approximate way to assess skin effect is to calculate the average profile thickness and obtain the relevant resistance ratio from Figure 55.

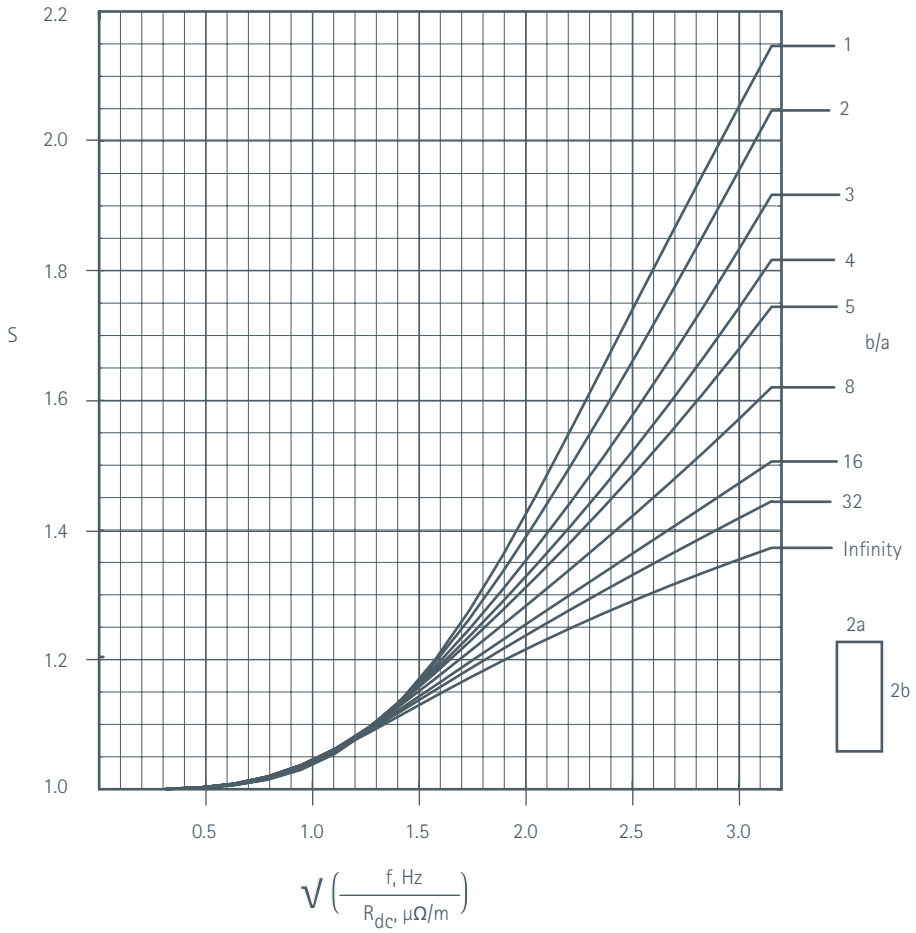

Figure 55 – R_{ac}/R_{dc} as a function of the parameter $\sqrt{f}/R_{dc}$ with f in Hz and R_{dc} in μΩ/m

5.5.2 Thermal Dissipation

Many of the components used in switchgear generate a significant amount of heat, which is dissipated by conduction via their connections to the bars. This heat, as well as that generated in the bars, must be lost by convection and, to a lesser extent, by radiation. Ultimately, the heat is removed from the cabinet by the flow of air through the cabinet by natural convection or by forced ventilation.

Since a profile has a larger surface area than an equivalent rectangular bar, the larger air-to-bar contact surface means that more heat can be lost by convection. This is particularly true for vertically orientated profiles where the fins form channels to guide the rising air. In long vertical channels, the air moves at increasing velocity as it heats up, but it also becomes less efficient at absorbing heat from the profile and it is necessary to provide baffles to spill the air so that it can be replaced by cooler air.

On the other hand, the presence of fins and channels may significantly alter the natural air flow and cause air traps where air flow is stalled. Also, the air wetting one wall of a vertical channel may interfere with the air wetting the other walls. These effects can be reduced by ensuring that:

- Horizontal fins are adequately spaced from each other
- Vertical channels are sufficiently wide
- Vertical channels are divided so that the air flow is interrupted - at fire stops, for example – and fresh air introduced.

Figure 56 shows a thermal image of two common profiles under load.

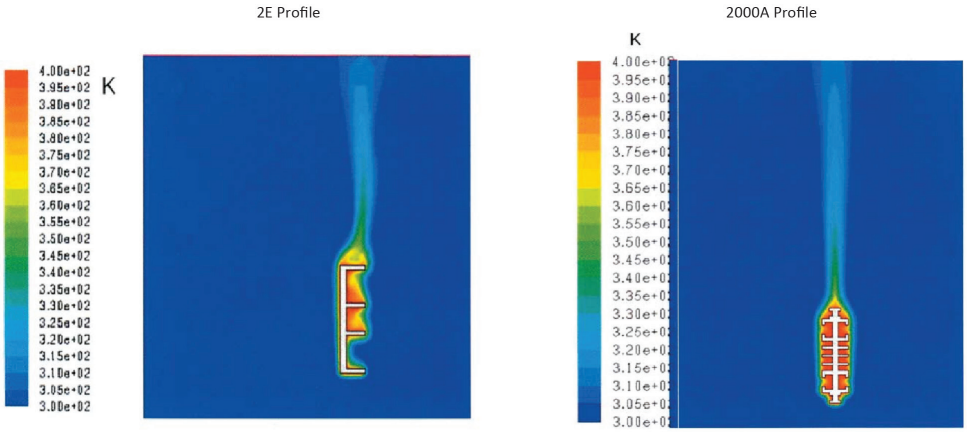

Figure 56 – Thermal image of two profiles under load

5.5.3 Jointing and Mounting

Since profiles cannot normally be overlapped, joints are usually achieved by the use of fishplates bolted to adjacent lengths of profile. Alternatively, the profiles can be designed to include channels to retain bolt heads (as shown in Figure 54) for mounting and jointing. Connecting plates are fastened to each of the outside faces of two adjacent sections of profile, as shown in Figure 57.

In the example shown, each plate is 5 mm thick and 120 mm long and is attached by four M8-bolts to each profile. The bolt torque is 19 Nm, resulting in a high contact pressure. Assembly requires the use of a torque spanner and can be accomplished by relatively unskilled operators.

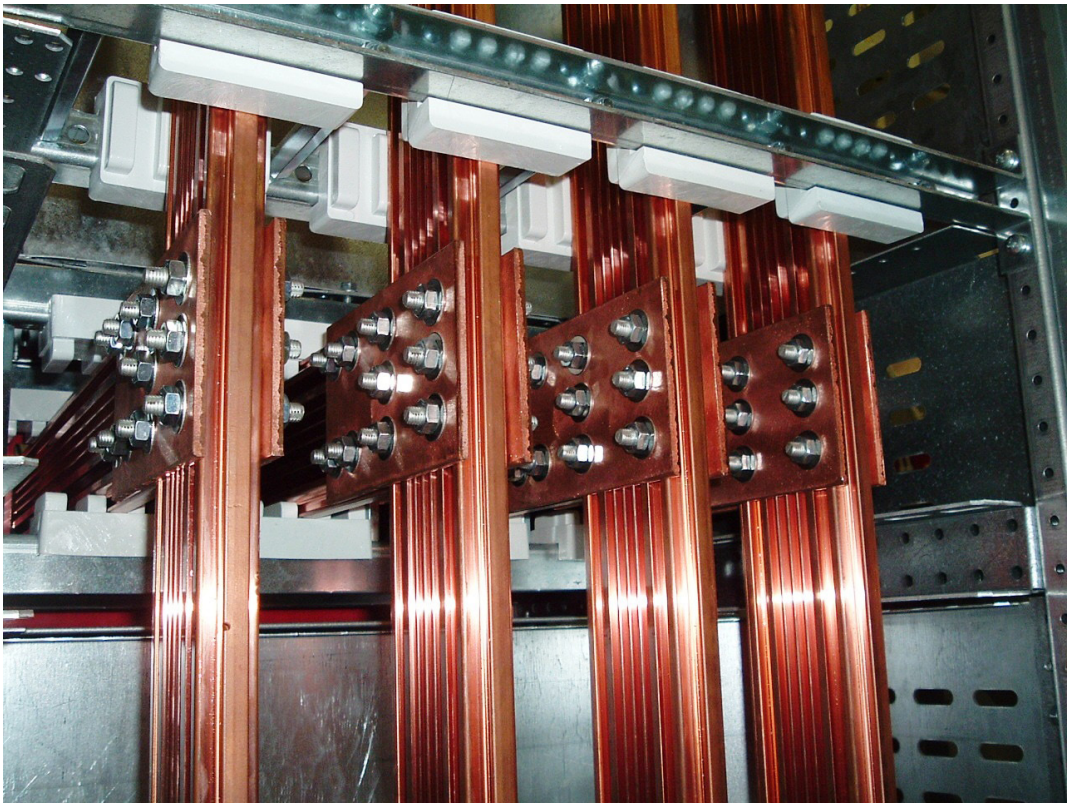

Figure 57 – Hole-free joints

Although the contact area is rather smaller than a normal flat overlap joint, the contact pressure is rather high and efficiencies (i.e. the ratio between joint conductance and conductance of an equal length of continuous profile) of higher than 100% are possible, with freedom from hot-spots and the ability to withstand the stresses due to short-circuit currents.

5.5.4 Short Circuit Performance – Moment of Inertia

Under short-circuit conditions busbars are subject to very large electromagnetic forces which deform the bars, reducing clearance distances. For the same current, the amount of deformation is determined by the moment of inertia. A higher moment of inertia results in smaller deflections, so that busbars can be placed closer together making the installation more compact.

It must be remembered that higher momentum does not increase the short-circuit capacity of the system, which is usually limited by the short-circuit temperature rise and the effect this might have on the mechanical properties of the bars and other associated components.

Because profiles are designed to have a high proportion of their mass as far as possible from the centre (to reduce skin effect), they have a relatively high moment of inertia and deform less under short-circuit conditions.

5.6 Calculation of Moment of Inertia of Complex Sections

The following section gives an outline of the procedure for calculating the moment of inertia of a complex section about the neutral axes perpendicular to the resolved components of the applied force. It is valid only for shapes that can be broken down into elements that have neutral axes which are parallel to each other, implying that the elements are either parallel or perpendicular to each other.

For a profile, the moment of inertia about the neutral axis can be calculated by the following procedure. The cross-section of the profile is divided into regular shapes, as shown in Figure 58, in which four rectangular elements are shown. First, the moment of inertia of each element about its own neutral axis is calculated (using the formula for a simple strip). Next, the composite neutral axis is determined, the individual moments of inertia referred to it and then the overall moment determined.

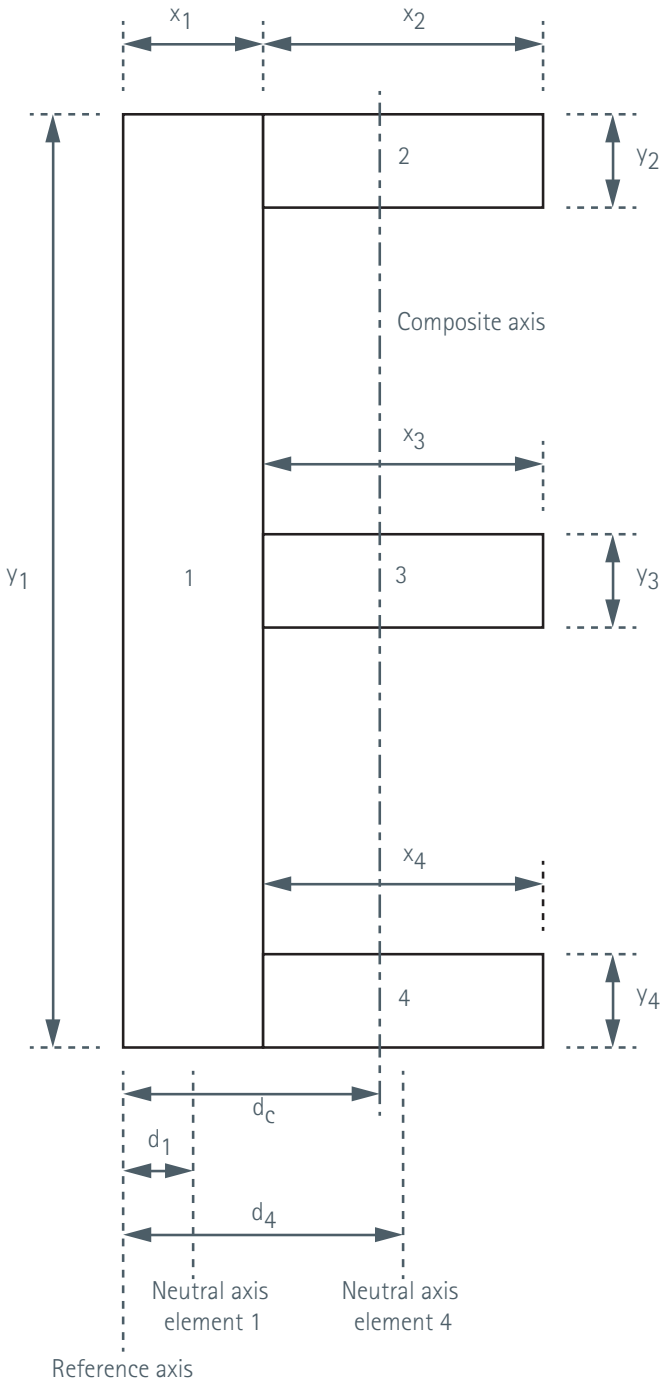

Figure 58 – Calculation of moment of inertia of a complex shape

The moment of inertia of each segment is calculated by:

$$I_i = \frac{bh^3}{12}$$

where the symbols are defined in Figure 59.

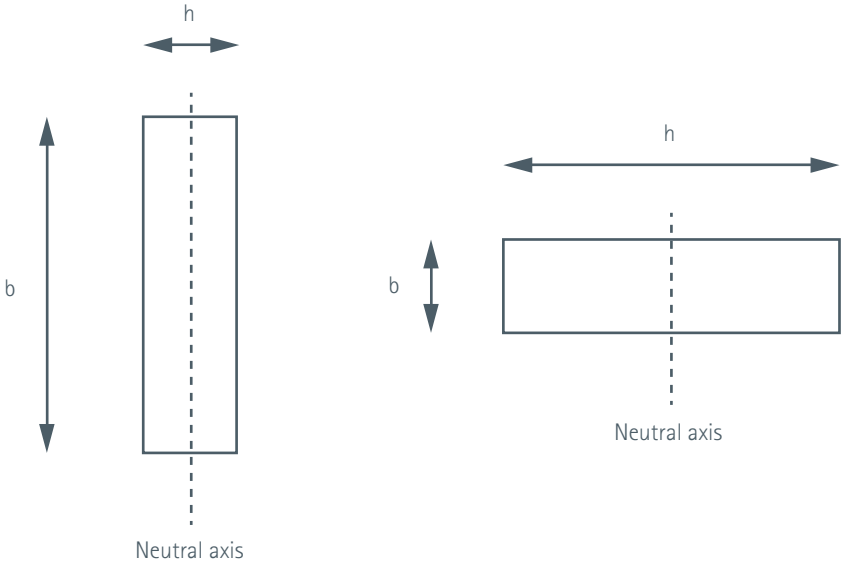

Figure 59 – Parameters used in the calculation of moment of inertia of each element

The position of the composite neutral axis is calculated as follows:

$$d_c = \frac{\sum_1^n x_i y_i d_i}{\sum_i^n x_i y_i}$$

The individual moments of inertia are referred to the composite neutral axis by:

$$I_i = I_{io} + x_i y_i k_i^2$$

and, in total

$$I = \sum_1^n I_{io} + \sum_1^n x_i y_i k_i^2$$

where, for $d_i > d_C$

$$k_i = d_i - d_c$$

else

$$k_i = d_c - d_i$$

6.0 Jointing of Copper Busbars

David Chapman

6.1 Introduction

Busbar joints are of two types; linear joints required to assemble manageable lengths into the installation and T-joints required to make tap-off connections. Joints need to be mechanically strong, resistant to environmental effects and have a low resistance that can be maintained over the load cycle and throughout the life of the joint.

6.2 Busbar Jointing Methods

Efficient joints in copper busbar conductors can be made very simply by bolting, clamping, riveting, soldering or welding. Bolting and clamping are used extensively on-site. Shaped busbars may be prefabricated by using friction stir welding.

Bolted joints are formed by overlapping the bars and bolting through the overlap area. They are compact, reliable and versatile but have the disadvantage that holes must be drilled or punched through the conductors, causing some distortion of the current flow in the bar. Bolted joints also tend to have a less uniform contact pressure than those made by clamping but, despite these issues, bolted joints are very commonly used and have proven to be reliable. They can be assembled on-site without difficulty.

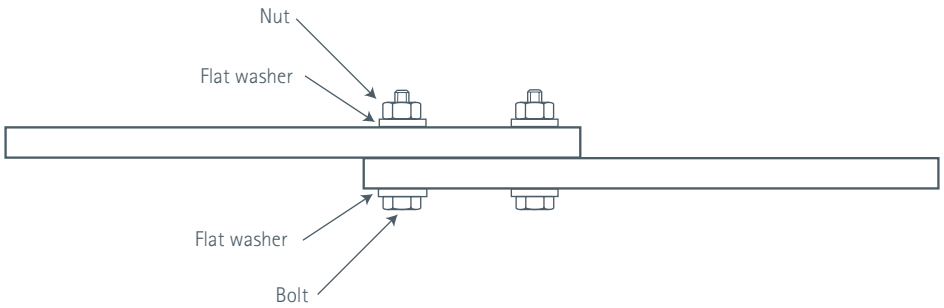

Figure 60 – A typical bolted joint

Clamped joints are formed by overlapping the bars and applying an external clamp around the overlap. Since there are no bolt holes, the current flow is not disturbed resulting in lower joint resistance. The extra mass at the joint helps to reduce temperature excursions under cyclic loads. Well-designed clamps give an even contact pressure and are easy to assemble, but take up more space than a bolted joint and are more expensive to manufacture.

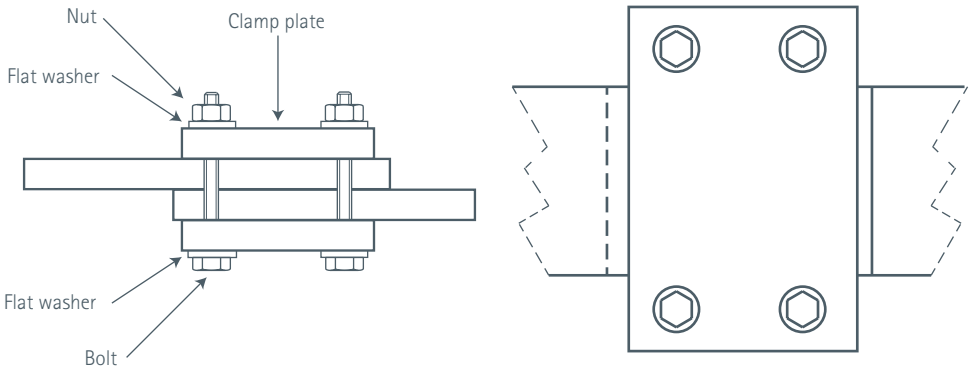

Figure 61 – A simple clamped joint

Riveted joints are similar to bolted joints. They can be efficient if well made; it is difficult to control the contact pressure. They cannot easily be dismantled or tightened in service and they are difficult to install.

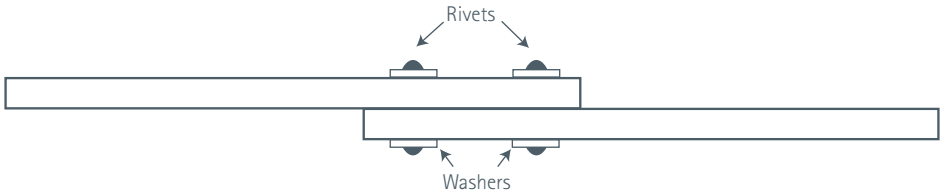

Figure 62 – A riveted joint

Soldered or brazed joints are rarely used for busbars unless they are reinforced with bolts or clamps since heating under short-circuit conditions can make them both mechanically and electrically unsound.

Figure 63 – A soldered joint

Welded joints are made by butting the ends of the bars and welding. They are compact and have the advantage that the current-carrying capacity is unimpaired, as the joint is effectively a continuous copper conductor. However, it may not be safe or desirable to make welded joints *in situ*.

Welding of copper is discussed in Copper Development Association Publication 98, Cost-Effective Manufacturing: Joining of Copper and Copper Alloys.

Figure 64 – A welded joint

The following sections apply to bolted and clamped joints.

6.3 Joint Resistance

In principle, a clamped or bolted joint is made by bringing together two flat surfaces under controlled (and maintained) pressure, as shown in Figure 65.

Figure 65 – An overlapped joint

The resistance of a joint is mainly dependent on two factors:

1. The streamline effect or spreading resistance, R_S, due to the diversion of the current flow through the joint
2. The contact resistance or interface resistance of the joint, R_i.

The total joint resistance, R_j, is given by:

$$R_j = R_S + R_i$$

This applies specifically to direct current applications. Where alternating currents are flowing, the changes in resistance due to skin and proximity effects in the joint zone must also be taken into account.

6.3.1 Streamline Effect

When current flows through a joint formed by two overlapping conductors, the lines of current flow are distorted and the effective resistance of the joint is increased since current flows only through a portion of the material.

Provided that the width of both bars is the same, the streamline effect is dependent only on the ratio of the length of the overlap to the thickness of the bars and not on the width. This is shown in Figure 66.

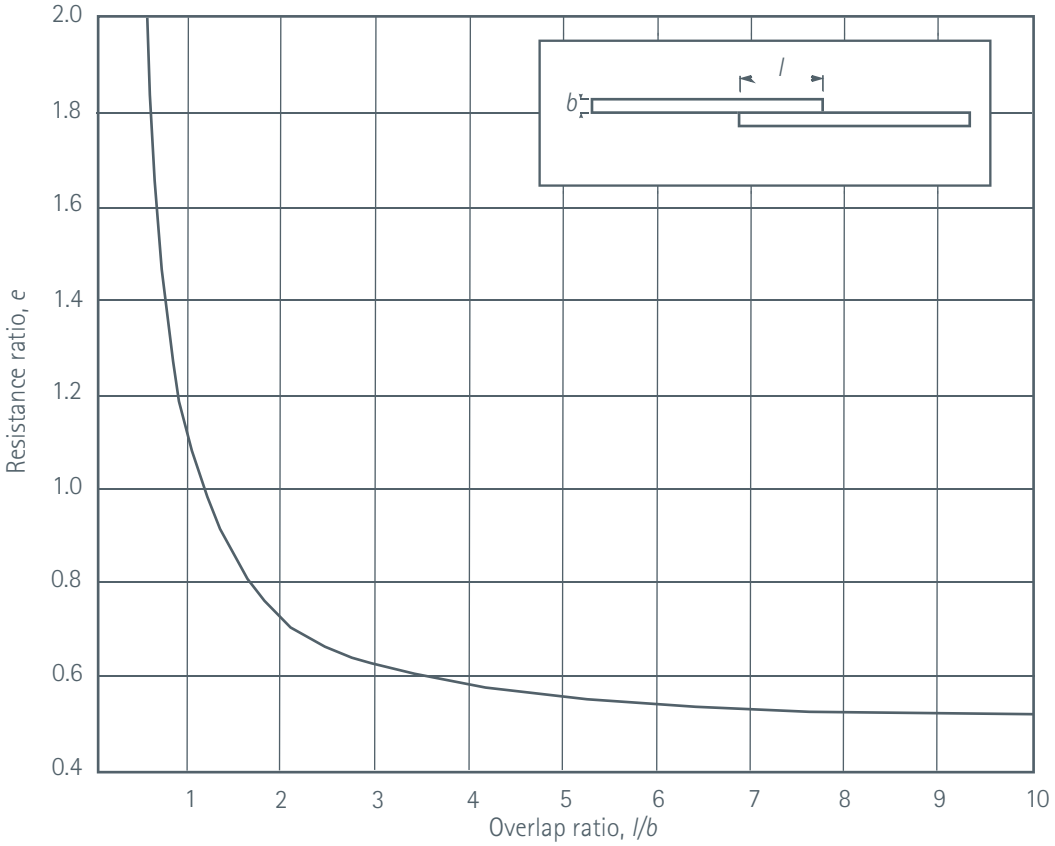

Figure 66 – Streamline effect in overlapped joints

The current density in the direction perpendicular to the bar, i.e. as current transfers from one bar to the other, is highly non-uniform and is concentrated around the edges.

The resistance ratio *e* in Figure 66 is the ratio of the resistance of a joint due to streamline effect R_S, to the resistance of an equal length of single conductor R_b, i.e.

$$e = \frac{R_s}{R_b} = \frac{ab}{\rho l} R_s$$

where:

- *a* is the width of bar, mm
- *b* is the thickness of bar, mm
- *l* is the length of overlap, mm
- ρ is the resistivity of the conductor, $\mu\Omega$ mm
- R_S is the resistance of overlap section in $\mu\Omega$ (to which contact resistance must be added)

hence:

$$R_s = \frac{e\rho l}{ab}$$

From the graph it can be seen that the streamline effect falls very rapidly for *l*/*b* ratios up to two, and then very much more slowly for values up to ten. This means that, in most cases, the streamline effect has a limited effect as the overlap is often much greater than five times the thickness in order to allow space for bolting or clamping. There is no advantage in allowing very long overlaps; it is only necessary to allow enough space to accommodate sufficient bolts to achieve the required contact pressure.

In the case of bolted joints, the bolt holes also reduce efficiency due to the streamline effect. The resistance ratio of a bolted overlap section can be estimated by:

$$R_{sb} = \frac{e\rho l}{(a - nd)b}$$

where:

d is the diameter of the holes
n is the number of holes across the width of the bars.

It follows that holes should be placed in-line along the length of the joint, as shown in Figure 67; offsetting the holes increases the resistance by increasing the disturbance of the current flow. In Figure 67a, the value of *n* is 2 while in Figure 67b the value of *n* is 4.

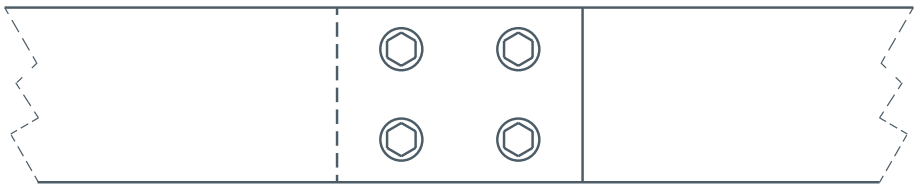

a) Correct bolt placement

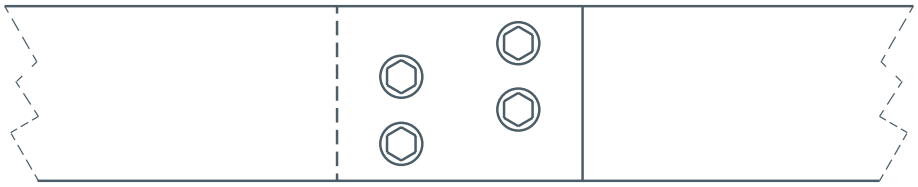

b) Incorrect bolt placement

Figure 67 – Bolt placement in overlapped joints

It has been found that the distortion effect in the tap-off of a T-joint is about the same as that in a straight joint. Note that the current flow in the straight bar is disturbed by the presence of bolt holes.

It has been shown that the current distortion is reduced if the ends of the bars are angled at less than 45 degrees, as shown in Figure 68. The initial joint resistance is reduced by 15%. Because the current flow is more uniform, the development of localised hot spots is reduced, leading to a factor of 1.3 to 1.5 reduction in the rate of increase in resistance under current cycling.

Figure 68 – Overlap joint between bars with angled ends

6.3.2 Contact Resistance

There are two main factors that affect the actual interface resistance of the surfaces:

1. The condition of the surfaces
2. The total applied pressure.

6.3.2.1 Condition of Contact Surfaces

In practice, an electrical contact between the solids is formed only at discrete areas within the contact interface and these areas (known as 'a-spots') are the only current conducting paths. The a-spots typically occupy an area of the order of 1% of the overlap area.

Obviously, the larger the number of a-spots, the more uniform the current distribution across the joint area will be. This can be encouraged by ensuring that the surfaces of the conductors are flat and roughened (which removes the oxide layer and produces a large number of asperities) immediately before assembly. As the contact pressure is increased, the higher peaks make contact, disrupt any remaining surface oxide and form metal to metal contact.

In some areas an oxide film may remain. Copper oxide films on copper form relatively slowly and are semiconducting because copper ions diffuse into the oxide layer. When copper oxide films are compressed between two copper surfaces, diffusion can take place in both directions so conduction takes place in both directions. This is very different from aluminium, where the oxide is a very good insulator and forms within microseconds of exposure to air.

Since the area of each a-spot contact is small, the current density is high, leading to higher voltage drop and local heating. In a well-made joint this heat is quickly dissipated into the mass of the conductor and the temperature of the interface will be only slightly above that of the bulk material. However, if the contact pressure is too low and the joint has deteriorated, local over-heating may be enough to induce basic metallurgical changes including softening and melting of the material at the a-spot. At first sight this may appear to be advantageous, however, as the joint cools the material contracts and fractures and is subsequently liable to oxidise.

Since elevated temperature is the first symptom of joint failure, maintenance procedures should be established to monitor the temperature of joints with respect to that of nearby bar using thermal imaging. If, under similar load conditions, the differential temperature increases, it may be a sign of early joint degradation. As a first step, more intensive monitoring should be undertaken and, if the trend continues, remedial action taken.

It is not normally recommended that the surfaces of copper-to-copper joints are plated unless required by environmental considerations. In fact, plating may reduce the stability of the joint because, as soft materials, the plating may flow at elevated temperatures leading to reduced contact pressure.

However, to ensure a long service life, a contact aid compound is recommended to fill the voids in the contact area and prevent oxidation or corrosion. Many proprietary compounds are available or, if none are available, petroleum jelly or, for higher temperatures, silicone vacuum grease may be used.

6.3.2.2 Effect of Pressure on Contact Resistance

Joint resistance normally decreases with an increase in the size and number of bolts used. Bolt sizes usually vary from M6 to M20 with either four or six bolts being used. The appropriate torque for each bolt size depends on the bolt material and the maximum operating temperature expected.

Contact resistance falls rapidly with increasing pressure, as shown in Figure 69, but above a pressure of about 30 N/mm^2 there is little further improvement. In most cases it is not advisable to use contact pressures of less than 7 N/mm^2, with pressures above 10 N/mm^2 being preferred. The contact resistance for a joint of a particular overlap area is obtained from Figure 69 by dividing the contact resistance for 1 mm^2 by the overlap area in mm^2.

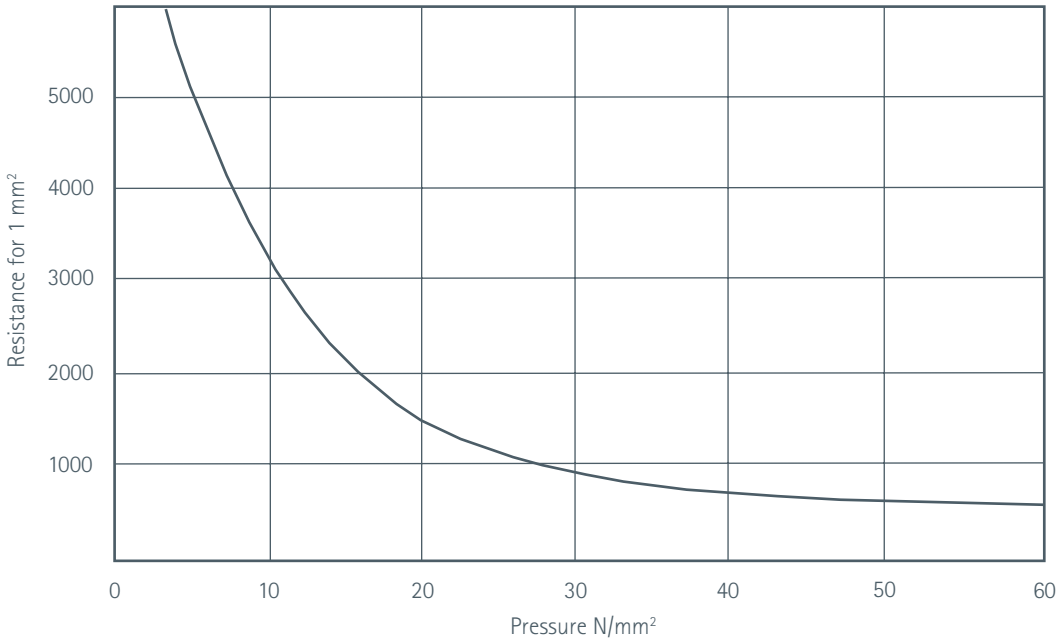

Figure 69 – The effect of pressure on the contact resistance of a joint

Contact pressure for both bolted and clamped joints is normally applied by tensioning one or more bolts. For bolted joints, the pressure is applied around the bolt holes, so using more bolts will result in a more even pressure distribution. Large, thick washers can be used to spread the load. For clamped joints, the load transferred from the bolts, which are outside the width of the conductors, depends on the rigidity of the clamps. Where the clamps are narrow, the pressure distribution provided by clamps can be quite uniform but, for wider conductors, the very rigid clamps required may be impractically large.

In everyday practice, contact pressure is impossible to measure and has to be inferred from the torque applied to the bolts from the following equation:

$$T = KFD$$

where:

- T is the tightening torque (Nm)
- K is a constant, often referred to as the 'nut factor' – see Table 19
- F is the force (kN)
- D is the nominal bolt diameter (mm) - see Table 21.

The 'nut factor' depends on a number of factors including the coefficient of friction, the surface finish and state of lubrication of the threads and other bearing surfaces. Table 19 gives typical nut factors for different states of lubrication.

Table 19 – Nut Factors for Different States of Lubrication

Bolt Lubrication	Nut Factor
Dry	0.20 – 0.22
Contact aid compound	0.19 – 0.21
Boundary lubricant (Mo_2S)	0.15 – 0.16

It is important to control the rate of applying the torque as well as the final value; bolts should be gradually tightened in rotation.

The correct tightening torque must be carefully determined to provide sufficient initial contact pressure at ambient temperature while not exceeding the proof or yield stress of the bolt material over the working temperature range of the joint. Differential expansion between the bolt and bar materials results in an increase or decrease in bolt tension (and therefore contact pressure) as temperature changes. Galvanised steel bolts are often used with copper busbars but copper alloy bolts, e.g. aluminium bronze (CW307G), are preferred because their coefficients of expansion closely match that of copper, resulting in a more stable contact pressure. Copper alloy bolts also have the advantage that the possibility of dissimilar metal corrosion is avoided and are also to be preferred where high magnetic fields are expected. Because these alloys do not have an easily discernible yield stress, however, care has to be taken not to exceed the correct tightening torque and the bolt stress over the working temperature range should not exceed 95% of proof strength.

Because of the strength of copper, deformation of the conductor under the pressure of the joint is not normally a consideration.

Table 20 shows the proof strength and coefficient of thermal expansion of some typical bolt materials compared to copper. It is clear from this table that the choice of bolt material will determine the thermal stability of the joint.

Table 20 – Proof Strength and Coefficient of Thermal Expansion for Copper and Typical Bolt Materials

Material	Proof Strength MPa	Coefficient of Expansion Per Degree C
Copper (reference)	Fully annealed - 50 Full temper - 340	16.5×10^{-6}
High tensile steel	700	11.1×10^{-6}
Stainless steel 316	414	15.9×10^{-6}
Aluminium bronze CW307G	400	16.2×10^{-6}
Stainless steel 304	207	$17.2 \cdot \times 10^{-6}$
Silicon bronze C651000	365	$17.8 \cdot \times 10^{-6}$

The increase in force (F_{Supp}) due to an increase in temperature (ΔT)is given by:

$$F_{supp} = \frac{(\alpha_a - \alpha_b)A_b E_b}{1 + \frac{t}{a}\left(1 + \frac{A_b}{A_w}\right) + \frac{A_b E_b}{A_a E_a}} \Delta T$$

where:

α_a is the coefficient of expansion of the busbar conductor
α_b is the coefficient of expansion of the bolt
A_b is the bolt cross-sectional area
E_b is the elastic modulus of the bolt
E_a is the elastic modulus of the busbar
t is the thickness of the washer
a is the thickness of the busbar
A_w is the apparent area under the washer
A_a is the apparent area of the joint overlap.

The change in bolt stress is proportional to $(\alpha_a - \alpha_b)$ so, for a joint made with high tensile steel bolt, the tension will increase considerably ($\Delta\alpha$ = 5.5 x 10^{-6}) while, if the joint were made with CW307G bolts, the tension will reduce only slightly ($\Delta\alpha$ = -0.3 x 10^{-6}).

In any case, the joint must be designed so that the maximum tension in the bolts, at any temperature within the working range, must be less than 95% of yield stress to avoid the risk of plastic deformation which would ultimately lead to loosening of the joint and failure.

The stress in the bolt is calculated using the Tensile Stress Area (see Table 21), not the nominal area.

Table 21 – Typical Thread Characteristics

Size Designation	Nominal (Major) Diameter D_n	Nominal Shank Area A_n	Pitch (mm per thread) p	Pitch Diameter d_p	Minor Diameter Area A_s	Tensile Stress Area A_{ts}
M6	6.00	28.274	1.000	5.3505	17.894	20.123
M8	8.00	50.265	1.250	7.1881	32.841	36.609
M10	10.00	78.540	1.500	9.0257	52.292	57.990
M12	12.00	113.10	1.750	10.863	76.247	84.267
M14	14.00	153.94	2.000	12.701	104.71	115.44
M16	16.00	201.06	2.000	14.701	144.12	156.67
M20	20.00	314.16	2.500	18.376	225.19	244.79
M22	22.00	380.13	2.500	20.376	281.53	303.40
M24	24.00	452.39	3.000	22.051	324.27	352.50
M27	27.00	572.56	3.000	25.051	427.09	459.41
M30	30.00	706.86	3.500	27.727	518.99	560.59
M33	33.00	855.30	3.500	30.727	647.19	693.55
M36	36.00	1017.9	4.000	33.402	759.28	816.72

If the design requirement is such that high tensile steel bolts must be used, the incremental force, F_{supp}, may be so high as to exceed 95% of the proof stress of the bolts. In these cases, disc-spring, or Belleville, washers must be used, as shown in Figure 70. The height and the spring rate of the washer are selected to reduce the value of F_{supp} according to the following equation:

$$F_{supp} = \frac{(\alpha_a - \alpha_b)A_b E_b}{1 + \frac{h}{a} + \frac{t}{a}\left(1 + \frac{A_b}{A_w}\right) + \frac{A_b E_b}{A_a E_a} + \frac{A_b E_b}{aK}}\Delta T$$

where:

h is the overall height of the disc-spring washer
K is the spring rate of the disc-spring washer.

In practice, the joint would be assembled normally with the required torque for the required contact pressure. In service, as the joint temperature rises, the spring is compressed, limiting the increase in bolt tension to a safe value.

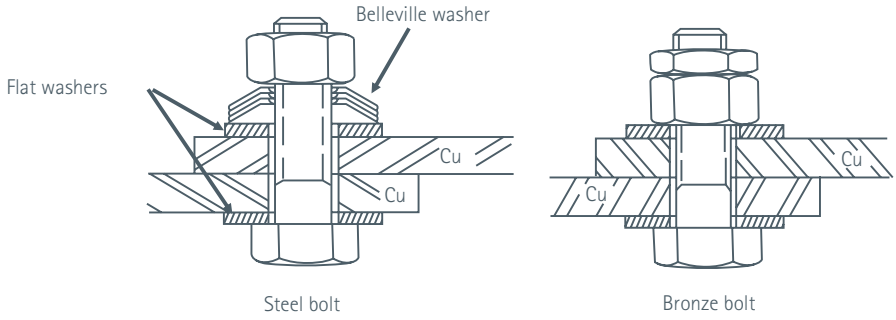

Figure 70 – Possible bolting techniques for copper busbars

Changing the design of a bolted joint, for example by introducing a longitudinal slot (see Figure 71), can reduce the contact resistance by 30 to 40%. The reduction in resistance is attributed to an improvement in the uniformity of contact pressure in each 'leg' of the joint leading to increased contact area.

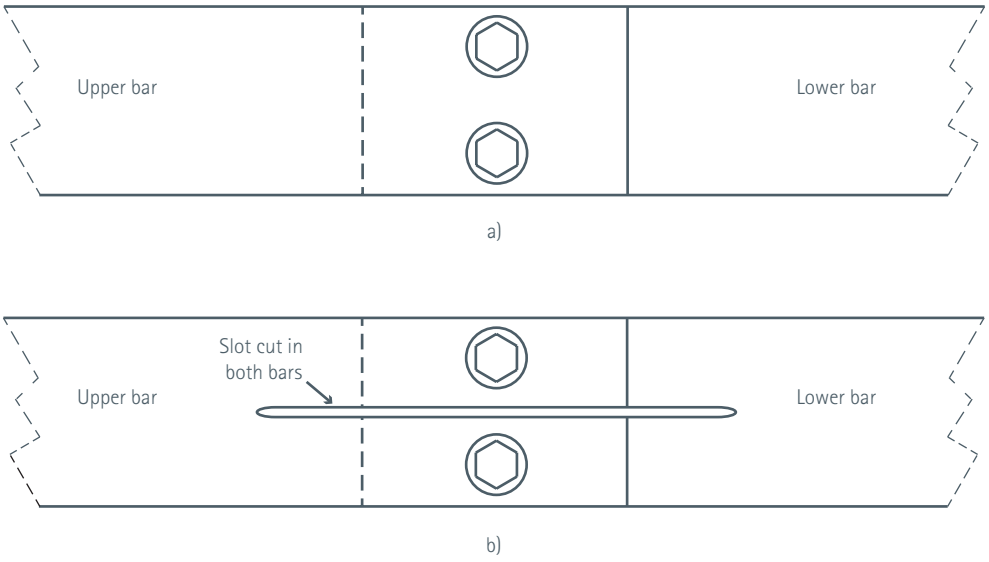

Figure 71 – Joint with a longitudinal slot

6.4 Bolting Arrangements

Although the required bolting arrangements should always be calculated for the circumstances of the installation, many sources give recommendations. Those given in Table 22 have been used for many years and are given here as a rough guide.

The recommended torque settings may be used for high-tensile steel (8.8) or aluminium bronze (CW307G, formerly C104) fasteners with unlubricated threads of normal surface finish.

Table 22 – Typical Busbar Bolting Arrangements (Single Face Overlap)

Bar Width mm	Joint Overlap mm	Joint Area mm²	Number of Bolts	Metric Bolt (Coarse Thread)	Bolt Torque Nm	Hole Size mm	Washer Diameter mm	Washer Thickness mm
16	32	512	2	M6	7.2	7	14	1.8
20	40	800	2	M6	7.2	7	14	1.8
25	60	1500	2	M8	17	10	21	2.0
30	60	1800	2	M8	17	10	21	2.0
40	70	2800	2	M10	28	11.5	24	2.2
50	70	3500	2	M12	45	14	28	2.7
60	60	3600	4	M10	28	11.5	24	2.2
80	80	6400	4	M12	45	14	28	2.7
100	100	10000	5	M12	45	15	28	2.7
120	120	14400	5	M12	45	15	28	2.7
160	160	25600	6	M16	91	20	28	2.7
200	200	40000	8	M16	91	20	28	2.7

6.4.1 Joint Efficiency

The efficiency of a joint may be measured in terms of the ratio of the resistance of the portion of the conductor comprising the joint to that of an equal length of straight conductor. It is possible to make joints with an efficiency of greater than 100% - i.e. the resistance of the joint is lower than that of an equivalent section of bar.

In terms of a complete busbar system, the proportion affected by joints is relatively small so that any inefficiency of the joints has only a small impact on the overall performance. However, joint inefficiency is important in two respects:

1. A joint with an efficiency of less than 100%, having a higher resistance, will run at a higher working temperature and experience greater temperature excursions than the normal bar. This could have an effect on the longevity of the joint and require more frequent maintenance.
2. In switchgear cabinets there will be many joints close together; less efficient joints will lead to excess heating and higher voltage drops.

The resistance of a joint, as already mentioned, is made up of two parts, one due to the distortion of lines of current flow and the other to contact resistance. The resistance due to the streamline effect at an overlapped joint is given by:

$$R_{sb} = \frac{e\rho l}{(a - nd)b}$$

where:

- e is the resistance ratio obtained from Figure 69
- a is the width of bar, mm
- b is the thickness of bar, mm
- l is the length of overlap, mm
- ρ is the resistivity of the conductor, $\mu\Omega$ mm (17.24 for 100% IACS copper)
- d is the diameter of the bolt holes, mm
- n is the number of holes across the width of the bars. For clamped joints, the value of n is zero.

The contact resistance, R_i, of the joint is:

$$R_i = \frac{Y}{al}$$

where Y is the contact resistance of a unit area, obtained from Figure 69.

The total joint resistance, R_j, is:

$$R_j = \frac{e\rho l}{(a - nd)b} + \frac{Y}{al}$$

Since the resistance, R_b, of an equal length of straight conductor is given by:

$$R_b = \frac{\rho l}{ab}$$

the efficiency of the joint is:

$$\frac{R_j}{R_b} = \varepsilon = \frac{ea}{a - nd} + \frac{Yb}{l^2\rho}$$

From this equation it is apparent that the most important factor is the reduction in cross-section due to the bolt holes, i.e. the term *nd*.

Taking the parameters for a 50 mm wide busbar from Table 22, the contact force, *F*, is given by (noting that there are two 12 mm bolts):

$$F = \frac{2T}{KD}$$

$$F = \frac{2 * 45}{0.2 * 12}$$

$$F = \frac{90}{2.4}$$

$$F = 37.5\ kN$$

The area of the joint is 3500 mm^2, so the pressure is:

$$P = \frac{F}{3500}$$

$$P = 10.7\ N/mm^2$$

From Figure 69, a Y value of 3000 $\mu\Omega$ is obtained.

For 10mm thick bar, the overlap to thickness ratio is 7 so that, from Figure 66, e = 0.55.

Substituting,

$$\varepsilon = \frac{0.55 \times 50}{50 - 14} + \frac{3000 \times 10}{70^2 \times 17.24}$$

$$\varepsilon = \frac{27.5}{36} + \frac{30000}{84476}$$

$$\varepsilon = 0.764 + 0.355 = 1.12$$

This joint has a resistance of 1.12 times that of a 70 mm length of 50 mm x 10 mm copper bar, i.e. equivalent to 78.4 mm of bar. The joint temperature will be slightly higher than that of the surrounding bar.

If the joint were redesigned with an overlap of 90 mm, using three in-line bolts at the same torque, the joint efficiency becomes:

$$F = 56.25\ kN$$

The area of the joint is 4500 mm^2, so the pressure is:

$$P = \frac{F}{4500}$$

$$P = 12.5\ N/mm^2$$

From Figure 69, a Y value of 2600 $\mu\Omega$ is obtained.

For 10 mm thick bar, the overlap to thickness ratio is 9 so that, from Figure 66, e = 0.55.

Substituting,

$$\varepsilon = \frac{0.52 \times 50}{50 - 14} + \frac{2600 \times 10}{90^2 \times 17.24}$$

$$\varepsilon = \frac{26}{36} + \frac{26000}{139644}$$

$$\varepsilon = 0.722 + 0.186 = 0.91$$

In this case, the joint has a resistance of 0.91 times that of a 90 mm length of 50 mm x 10 mm copper bar, i.e. equivalent to 82 mm of the bar. This joint will run at a slightly lower temperature than the surrounding bar.

6.5 Clamped Joints

The design criteria for bolted joints apply in principle also to clamped joints. However, some aspects require particular attention:

- The clamping plates must be designed to be rigid enough to transfer the pressure without flexing. Often, ribbed castings are used for this purpose.
- The bolts which provide the joint pressure are at the periphery of the joint and will run at a temperature somewhat below that of the bar. In some 'wrap around' lamp designs, the bolts will also be physically shorter than the thickness of the stacked bars. The bolts will therefore expand less, and joint pressure may rise excessively.

6.6 Degradation Mechanisms

The deterioration of a connector proceeds slowly at a rate determined by the nature of different processes operating in the contact zone and in the environment. This initial stage persists for a long time without causing any noticeable changes because it is an intrinsic property of clusters of a-spots that their overall constriction resistance is not sensitive to small changes in their size. However, when the contact resistance increases sufficiently to raise the local temperature, a self-accelerating deterioration resulting from the interaction of thermal, chemical, mechanical and electrical processes will be triggered, and the contact resistance will rise abruptly. Hence, no deterioration will be noticeable until the final stages of the connector life.

6.6.1 Oxidation

Oxidation of the metal–metal contacts within the contact interface is widely accepted as the most serious degradation mechanism occurring in mechanical connectors. Copper is not very active chemically and oxidises very slowly in air at ordinary temperatures. As mentioned earlier (see '6.3.2.1 Condition of Contact Surfaces'), cleaning and roughening the joint surfaces prior to assembly and the use of a contact aid will prevent oxidation.

6.6.2 Corrosion

Corrosion is a chemical or electrochemical reaction between a metallic component and the surrounding environment. It begins at an exposed metal surface with the formation of a corrosion product layer and continues as long as reactants can diffuse through the layer and sustain the reaction. The composition and characteristics of the corrosion product layer can significantly influence the corrosion rate.

Busbars are potentially affected by atmospheric, localised, crevice, pitting and galvanic corrosion. The most important factor in all these corrosion mechanisms is the presence of water. In the presence of a sulphur-bearing atmosphere, tarnishing of the copper surface occurs because of sulphide formation from hydrogen sulphide in the atmosphere. The growth of tarnished film is strongly dependent on the humidity, which can reduce it if a low sulphide concentration prevails or increase it if sulphide concentration is high.

6.6.3 Fretting

Fretting is the accelerated surface damage occurring at the interface of contacting materials subjected to small oscillatory movements. Experimental evidence shows that amplitudes of <100 nm are sufficient to produce fretting.

There is still no complete unanimity on the mechanisms of fretting, specifically with regard to the relative importance of the processes involved. Nevertheless, based on the existing knowledge of the phenomenon, it can be safely assumed that the following processes are present:

1. Disruption of oxide film on the surface by the mechanical action exposes clean and strained metal which will react with the environment and rapidly oxidise
2. The removal of material from the surfaces by adhesion wear, delamination or by shearing the microwelds formed between the asperities of the contacting surfaces when the contact was made
3. Oxidation of the wear debris and formation of hard abrasive particles that will continue to damage the surfaces by plowing
4. Formation of a thick insulating layer of oxides and wear debris (a third body) between the contacting surfaces.

The oscillatory movement of the contacting members can be produced by mechanical vibrations, differential thermal expansion, load relaxation, and by junction heating as the load is cycled. Because fretting is concerned with slip amplitudes not greater than 125 µm movement, it is ineffective in clearing away the wear debris and accumulated oxides, and a highly localised, thick insulating layer is formed in the contact zone, leading to a dramatic increase in contact resistance and, subsequently, to virtual open circuits.

6.6.4 Creep and Stress Relaxation

Creep, or cold flow, occurs when metal is subjected to a constant external force over a period of time. The rate of creep depends on stress and temperature and is higher for aluminum than for copper. Stress relaxation also depends on time, temperature, and stress but, unlike creep, is not accompanied by dimensional changes. It occurs at high stress levels and is evidenced by a reduction in the contact pressure due to changes in metallurgical structure. The change from elastic to plastic strain has the effect of significantly reducing the residual contact pressure in the joints, resulting in increased contact resistance, possibly to the point of failure.

6.6.5 Thermal Expansion

The effect of temperature variation on contact pressure has already been discussed. Longitudinal expansion is also important since it can lead to slip in the joint followed by loosening. It is important that long bars are provided with a flexible element so that movement can take place elsewhere.

6.7 Conclusion

The quality of busbar joints is crucial to the long term reliability of a busbar system. It is important to take care over the choice of joint design, the tightening torques, bolt types and the effect of temperature to ensure reliability. In-service maintenance should ideally include thermal imaging of joints so that any problems can be found before failure occurs.

Annex: Coatings

David Chapman

A1.0 Introduction

Although coatings have been applied to busbars for several perceived reasons, there are in reality few genuine engineering needs to do so. Since coatings are expensive to apply and may require additional maintenance, they should be applied only when truly necessary.

A2.0 Reasons for Coating

A2.1 Coating to Provide Electrical Insulation

The primary reason to insulate busbars is to provide protection against electric shock in the event of direct contact.

Two significant problems arise. Firstly, the electrical insulating material is also a thermal insulator, so the bars will run at a higher temperature or will be limited to a lower working current. As a result, bars with a larger cross-sectional area will be needed. Although coating can reduce the current-carrying capacity, the short circuit capacity is not affected because the SCC is always calculated assuming that no heat is lost.
Secondly, it is difficult to apply insulation to the required degree of integrity during installation. Even when using pre-insulated bars, additional insulation has to be applied at joints and connections, requiring clean working conditions and skilled operatives.

It is preferable to avoid the need for direct insulation, ensuring safety by mounting non-insulated bars out of reach or behind appropriate barriers, together with the provision of the appropriate fixed safety warning labels.

A2.2 Coating to Inhibit Corrosion

In most circumstances, copper is highly resistant to corrosion and does not normally need additional protection. However, in environments containing ammonia, sulphur and chlorine compounds, especially where the humidity may be high, protection is required.

A2.2.1 Metal Coatings

Historically, tin, tin-lead alloys, nickel or silver coatings have been used.

- Tin and tin-lead alloys: Pure tin coatings should be avoided because they tend to form whiskers, which can cause transient short circuits. Tin-lead alloys are rarely used now due to environmental concerns. Tin-containing coatings are relatively expensive.
- Nickel is the preferred material since it is relatively cheap, is durable (except at high humidity) and provides a harder surface than the alternatives. Nickel oxide is tough, so high pressure is required at joints to ensure reliability. Nickel may corrode significantly in contact with more noble metals such as gold.
- Silver is expensive but is very effective, except where sulphur compounds are present.

Protection will only be effective if it is continuous over the whole surface, including joints and connections. This means that metal coatings, which are always relatively thin (2 to 5 µm), are free of pinholes and other defects which would allow corrosion of the conductor material. Plated bars must be carefully protected before and during installation to avoid damage.

Metal coatings will not significantly affect the current rating or working temperature of the busbars.

A2.2.2 Non-Metallic Coatings

In very corrosive environments, busbars may need additional protection, using similar materials and techniques as would be used for electrical insulation. Obviously, the current rating of the busbars will be reduced due to the additional thermal insulation.

A2.3 Coating to Increase Current Rating

Matt black surfaces have higher emissivity than light-coloured polished surfaces, so it has often been suggested that matt black paint should be applied to busbars to improve cooling by radiation.

In practice, the potential improvement is small and sometimes negative. The natural emissivity of a copper bar that has been in use for even a short time will be above 0.5 and will rise over time to 0.7 or above, while a well applied matt black paint will have an emissivity of 0.9 to 0.95. As a result, an increase of about 30-35% in cooling by radiation may be expected. Even at a temperature rise of 60°C, this corresponds to an overall

increase in cooling of barely 12% and an increase in current-carrying capacity of less than 6%. At lower temperature rises, or where bars are facing each other, the radiation loss is lower and the 'gain' due to painting is much lower.

On the negative side, the paint layer acts as an insulator, reducing the efficiency of the convection process, perhaps by as much or more than the increase in radiation efficiency. In general, painting will give little increase, and quite possibly a reduction, in the current-carrying capacity of a busbar for a given working temperature.

Painting may be worthwhile for very wide bars (where convection is less effective) operating with high temperature rises (where radiation is more effective).

A2.4 Coating for Cosmetic Purposes

It is inevitable that fingermarks will occur on busbars during assembly and, in the first few weeks of operation, the natural grease in the marks darkens much more quickly than the surrounding copper. In some countries this is thought to be unsightly and the busbars are painted in order to hide the marks. There is no technical merit in painting busbars – it is an additional cost, increases the working temperature and makes maintenance more difficult. On the other hand, painting may be required to meet the demands of the local market.

A2.5 Coating to Improve Joint Performance

Plating of the contact area of joints is not recommended unless it is really necessary to combat corrosion.

As described in Section 6.0 'Jointing of Copper Busbars', a contact is formed by a large number of cold welds between the surfaces of the two conductors. If plated conductors are used, these cold welds cannot form and the softer plating material tends to flow, reducing contact pressure and reducing joint reliability.

A3.0 Methods of Coating

Coating of high conductivity copper is normally limited to the application of insulation to conductors in very long lengths, a method not well suited to the relatively short lengths used for busbars. In other, non-electrical applications, protection is usually achieved by the choice of a copper alloy with intrinsic resistance to the application environment, so there is a limited requirement for other types of coating. As a result, most direct experience with local coatings is with steel, primarily in the oil, gas and chemical industries. For use with HC copper, it is important to establish that the chosen coating will be compatible in the long-term. Many coatings methods will require some form of pre-treatment to ensure good adhesion and this should also be included in the compatibility assessment.

Whatever type of coating is used, it is important that the coating is continuous and free of pinholes and voids. To avoid thinning of coatings at edges, conductors with rounded, rather than sharp, edges should be used to reduce mechanical and electrical stresses.

Coatings can be applied either during manufacture of the conductors or during on-site assembly. In practice, there will probably always be a need to apply at least some coating on-site at joints and connection points, requiring an assessment of the mutual compatibility with the factory-applied coating. The following sections give some examples, but many other techniques are available.

A3.1 Factory Application Methods

Factory application of coatings during manufacture of the conductor allows a much greater choice of materials and processes and should ensure a more consistent quality of coating at lower cost than on-site coating. However, it is necessary to locally coat the busbar joints in a compatible manner during on-site installation.

A3.1.1 Extrusion

Extrusion is viable only for bars supplied in very long lengths, typically relatively small diameter round rods or tubes. It is cost-effective and is compatible with traditional electrical insulation materials such as PVC and XLPE.

A3.1.2 Powder Coating

As the name suggests, these coatings are applied in powder form, by electrostatic spraying or in a fluidised bed, and then cured either by heat, UV light or some other means. Nylon and epoxy powders are often used. For many materials, the heat curing temperature and time requirements will not result in the annealing of the copper conductor and will tolerate temperatures of 150°C.

A3.2 On-Site Application Methods

A3.2.1 Heat-Shrinkable Sleeve

Heat-shrinkable sleeve is normally made from cross-linked polyolefin. It will shrink to about 50% of the supplied perimeter temperatures above about 70°C, with a consequent increase in thickness. It is easy to apply on-site using an adequately powered hot air gun but can be time consuming. It can typically tolerate working temperatures up to 90°C.

A3.2.2 Painting

Painting, by brush or spray usually requires a primer coat. Note that paint cannot be expected to provide adequate shock protection because the integrity of the coating cannot be guaranteed.

A3.2.2.1 Alkyd Paints

Alkyd paints are traditional oil-based paints and are suitable for use at temperatures up to about 120°C. They have a limited lifetime of a few years.

A3.2.2.2 Two-Part Epoxy

Two-part epoxy paints are applied immediately after mixing and cure at normal ambient temperatures. The cured paint has good abrasion resistance with a lifetime of over ten years but it is not resistant to UV. It is typically suitable for use at temperatures up to about 150°C.

A4.0 Inspection and Maintenance

As with uncoated bars, routine inspection and maintenance is required. The biggest potential problem is the loosening of joints, which is normally detected as a local rise in temperature, detected during regular inspection with a thermal imaging camera.

In the case of coated bars, the presence of a coating on the nuts and bolts may initially prevent loosening but, once loosening has occurred, will certainly make it more difficult for the joint to be correctly re-tensioned. Because the coating thicknesses may vary, especially in the areas of the joints, it is important to establish the temperature profile in the early life of the installation for future comparison.

It is also necessary to visually inspect the coating for integrity, looking for cracking, especially at joints where different coatings meet or the size changes, and for disturbance of the surface that might indicate underlying corrosion.

Notes

Notes

Copper Development Association
5 Grovelands Business Centre
Boundary Way
Hemel Hempstead, HP2 7TE
UK

info@copperalliance.org.uk
www.copperalliance.org.uk

Cu

Copper Development Association

Copper Alliance